Royal HaskoningDHV
Enhancing Society Together

Section 5 Appendix 5.1 Hydraulic Studies to Support EIA

[Blank Page]

HR Wallingford
Working with water

York Potash Project
Harbour Facilities

Hydraulic Studies to Support the EIA

DDR5252-RT001-R03-00 March 2015

Document information

Document permissions	Confidential - client
Project number	DDR5252
Project name	York Potash Project Harbour Facilities
Report title	Hydraulic Studies to Support the EIA
Report number	RT001
Release number	R03-00
Report date	March 2015
Client	Royal HaskoningDHV
Client representative	Matt Simpson
Project manager	Jenny Semmence
Project director	John Baugh

Document history

Date	Release	Prepared	Approved	Authorised	Notes
19 Mar 2015	03-00	WJF	JVB	JVB	Release 1 for YPL
28 Nov 2014	02-00	WJF	JVB	JVB	Revision 0 for YPL
03 Jul 2014	01-00	WJF	JSE	JVB	

Document authorisation

Prepared	Approved	Authorised
[redacted]	[redacted]	[redacted]

Summary

York Potash Limited (YPL) is focussed on the development of the world's largest polyhalite resource situated in North Yorkshire. Polyhalite would be extracted from an underground mining operation and transported via conveyor to processing facilities at Wilton, Teesside. Once processed, the product would be distributed in bulk by sea from a port terminal to world markets and via road to UK customers.

A site for the export of processed polyhalite has been identified on the Tees Estuary adjacent to Bran Sands lagoon and a preliminary concept development study has been completed by Royal HaskoningDHV (RHDHV, 2014). The proposal is now being taken through an Environmental Impact Assessment (EIA) and the hydraulic studies described in this report support the EIA by predicting the effects of the development in its construction and operational phases on the physical process regimes of the Tees Estuary, i.e. tides, waves, suspended sediment concentration and morphology including infill in dredged areas.

A set of established modelling tools have been used to predict the effects of the construction and operation of two options for the harbour facilities on flows, waves and sediment transport.

During the construction phase

The plume dispersion simulations show the following key features:

- The effects of backhoe dredging are relatively small compared to those of a cutter suction dredger (CSD) and barge or trailing suction hopper dredger (TSHD).
- The CSD and barge overflowing produce considerable deposition of fine sediment locally on the bed while the TSHD dredging results in the release of more sediment into the water column.
- The CSD footprint of effect is smaller than that of TSHD dredging.
- Predicted mean concentration increases in suspended sediment outside of the dredging area are a few tens of mg/l at most. Peak predicted concentration increases are larger possibly rising to 100 or 200 mg/l outside of the dredging area for short periods.
- The footprint of effects of dredging for high river flow and neap tide conditions is considerably smaller than that for low river flow and spring tide conditions which extends past South Gare and Tees Dock.
- The predicted deposition is typically of the order of a few millimetres, except in the vicinity of the dredging itself where much higher rates of deposition are predicted. In practice the sediment depositing in the vicinity of the dredging will be re-dredged. During the period of the dredging operation a one off increase of up to 10% to the annual maintenance requirement in the Tees is predicted.

During the operational phase

Wave conditions are increased by the reflection effects of the solid quay. For representative waves (0.1 year return period) wave height increase by up to 0.1 m in the vicinity of the quay. For larger waves with a 5 year return the predicted increases in wave height are in the range 0.1 – 0.15 m in the vicinity of the quay and some changes in the range 0.03 – 0.05 m can occur at the opposite coastline. For the open quay case no effect in changing the distribution of wave energy is predicted.

Currents are predicted to decrease in the dredged areas for both options. The solid quay is shown to have a larger footprint of effect with some speed increase predicted at the Redcar Bulk Terminal quay during the

ebb tide and at the mouth of Dabholm Gut during the flood tide. Neither development option results in widespread changes in hydrodynamics.

Both development options show a negligible effect on the overall import of fine sediment into the estuary – less than 0.5 %. The predicted very small change in overall fine sediment regime in the Tees will not alter the present maintenance dredging frequency or methodology.

At the study site in Chart area 8, the predicted infill rate is reduced by 2-3% for the two development options compared to baseline conditions. In the berth pocket and approaches for the proposed facility the medium term average infill rates are predicted to be 5,100 m^3 per year for the reclaimed quay case and 5,900 m^3 per year for the open quay case.

Contents

Figures

Tables

1. Introduction

York Potash Limited (YPL) is focussed on the development of the world's largest polyhalite resource situated in North Yorkshire. Polyhalite would be extracted from an underground mining operation and transported via conveyor to processing facilities at Wilton, Teesside. Once processed, the product would be distributed in bulk by sea from a port terminal to world markets and via road to UK customers.

1.1. Background

A site for the export of processed polyhalite has been identified on the Tees Estuary adjacent to Bran Sands lagoon and a preliminary concept development study has been completed by Royal HaskoningDHV (RHDHV, 2014). The proposal is now being taken through an Environmental Impact Assessment (EIA) and the hydraulic studies described in this report support the EIA by predicting the effects of the development in its construction and operational phases on the physical process regimes of the Tees Estuary, i.e. tides, waves, suspended sediment concentration and morphology including infill in dredged areas.

The elements of the proposed export facility under consideration are:

- Extension of the area with channel depth of -14. 1 mCD to include the approaches to the new facility;
- Dredging of the approaches to the new berth to -14.1 mCD;
- Dredging of the berth pocket to -16 mCD, and either;
- A new vertical wall quay made up by a solid reclamation; or
- A new open piled quay fronting a 1:2 rock armour slope bank line.

1.2. Structure of this report

This report contains 5 further sections. Section 2 describes the effects of the works in their construction phase by modelling the release of fine sediment during the dredging process. Sections 3, 4 and 5 describe the effects of the development in its operational phase on waves (Section 3), tides (Section 4) and sediment transport and morphology (Section 5). Section 6 draws together the conclusions of the studies.

Figure 1.1: Study area

Source: Google Earth

2. Sediment plume modelling of construction phase impacts

To model the effects of the construction phase of the project, an analysis of the proposed capital dredging is required leading to the generation of sources terms for the sediment release rates from the dredger and from any barges used. The starting point for the overall dredging task has been taken from the preliminary concept development report (RHDHV, 2014). From this report, a set of representative dredging scenarios have been developed with the aim of presenting a reasonable "worst case" for the impact of the sediment release.

2.1. Background

2.1.1. Bed material types

Information on bed material types were provided by a set of boreholes along the length of the proposed facility. The cross section extends either side of the works area to show the overall variation in the geology of the surroundings (Figure 2.1).

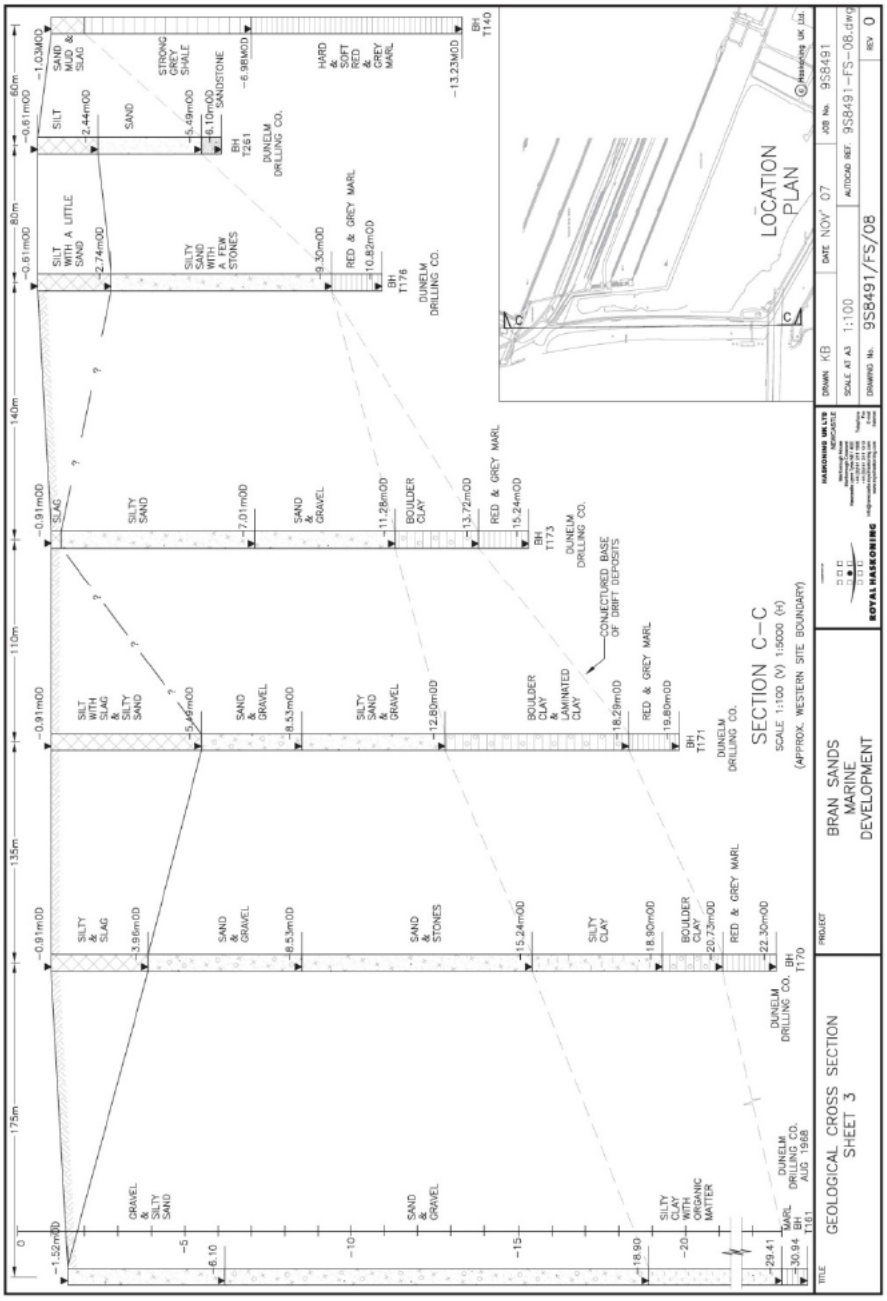

Figure 2.1: Geological cross section at proposed berth site

Source: Royal HaskoningDHV

Two material types were assessed to provide a precautionary view of sediment release, namely silty sand/gravel with a 10% fine sediment content (corresponding to the sediment which will be dredged by the trailing suction hopper dredger (TSHD)) and silt/sand with a 30% fine sediment content. The plume modelling was of the fine sediment fraction of the material so understanding the variation in fine sediment content was important in defining the source term. The particle size distributions for the two representative material types are shown in Table 2.1 below.

Table 2.1: Particle size distribution for representative sediment types

Particle size (microns)	Silty sand/gravel (%)	Silt/sand (%)
Less than 20	7	25
20 to 60	3	5
60 to 80	1	2
80 to 100	1.5	3
100 to 150	5	5
150 to 200	7.5	5
200 to 300	8	12
300 to 400	7	7
400 to 600	10	5
600 to 1000	10	5
1000 to 2000	10	5
2000 to 4000	10	5
4000 to 6000	10	8
>6000	10	8

2.1.2. Dredging task

The dredging is anticipated to be undertaken in two phases with the proposed dredge plant and material types assumed to be as described in Section 2.1.1. The total quantity of material to be dredged as part of the open quay option would be approximately 1,122,000 m^3. The construction of the closed (reclamation) option would involve capital dredging of approximately 814,000 m^3.

Definition of the dredgers has been undertaken noting the following factors which are used to help define a reasonable worst case for sediment release:

- Operations not restricted due to tides (water depths), port traffic, etc.;
- Overflow of material from hoppers/barges is not restricted and therefore maximum economical loads are achievable.

From the available bathymetry data it should be noted that there are potential tidal restrictions (i.e. depth limitations) of deepening within the berth area, particularly at the beginning of works before the dredge(s) create sufficient water depth for their unrestricted operation. In general a fully laden, a 6,000 m^3 TSHD could require 8-10 m of water for safe navigation (depending upon vessel design). For the present sediment release modelling the dredging is assumed to be unrestricted leading to a reasonable worst case for rate of sediment released into the water column.

Details of the dredgers considered in the generation of sediment release source terms are below.

- TSHD
  - Hopper capacity 6,000 m^3;
  - 144 operational hours per week;
  - The dredge site (i.e. trail length) is 500 m;
  - Offshore disposal time assumed to be 10 minutes plus travel time.
- CSD
  - Total installed power 10,000 kW – cutter power 1,300 kW, pump power 5,300 kW;
  - Discharge pipe diameter 800 mm;
  - 144 operational hours per week;
  - Pumping dredged materials directly to barges with hopper capacity 4,000 m^3;
  - Dual-sided barge loading is undertaken to permit continuous pumping of dredged material from the CSD.
- BHD
  - The source term for BHD operations were not modelled as it is not expected to be a source of significant sediment plumes. A constant release rate from literature was used for the sediment release rate from a BHD.

2.2. Sediment plume modelling method

The assessment of dispersion of the plume requires an assessment of the rates of release or "source terms" arising from dredging activities (see Section 2.2.1) which forms an input, together with the flow model results (see Section 4), to the plume dispersion modelling. The plume dispersion model itself is described in Section 2.2.2 and the results of the plume dispersion modelling are presented in Section 2.2.3.

2.2.1. Source terms

The dredge plant identified above was combined with the chosen particle size distributions using HR Wallingford dredger production models to develop a set of sediment release source terms for use by the SEDPLUME-RW model. The results of the production modelling provide a summary of the dredger activities and loss terms as summarised below.

BHD

For the backhoe dredger a typical source term of 3 kg/s of fine material is assumed. This is the loss of sediment as the bucket is raised through and out of the water column before being deposited in the barge.

TSHD

Using typical parameters of the type and size of dredger considered a production rate of 107,500 m^3/week is estimated. This is achieved at a rate of 32.5 dredge cycles/week. The elements of each dredge cycle are estimated as presented in Table 2.2.

Table 2.2: Modelled TSHD cycle

Cycle segment	Duration (mins)
Dredging, pre-overflow	63
Dredging, overflow	101
Sailing to offshore disposal area	47
Disposal	10
Sailing to dredge area	43
TOTAL	264

The sediment losses associated with this cycle are:

- 5 kg/s at the drag head during the dredging period(s);
- 88 kg/s during the hopper overflow period.

The hopper load of dredged material which would be taken to the disposal site is 7,850 Tonnes Dry Solids (TDS) with a 5% fines content suggesting each disposal operation would involve placement of 390 TDS.

CSD

The production rate for the CSD considered would be approximately 276,700 m^3/week and is estimated to be made up of 44.5 barge cycles/week. To maintain efficiency continuous operation of the CSD is required suggesting at least two barges will be needed. The barge cycle is described in Table 2.3.

Table 2.3: Modelled CSD barge cycle

Cycle segment	Duration (mins)
Loading, pre-overflow	30
Loading, overflow	70
Sailing to offshore disposal area	45
Disposal	10
Sailing to dredge area	40
TOTAL	195

The sediment losses associated with these activities are:

- 102 kg/s at the cutter head for the entire dredging duration of the CSD (i.e. 144 hours per week). 50% of this material is expected to be released into the water column. The remainder falls to the sea bed to be re-dredged almost immediately;
- 379 kg/s during the barge overflow period.

The barge load of material which would be taken to the disposal site under these conditions would comprise 5,430 TDS with 12% of the barge estimated to be fine material, equating to 650 TDS.

2.2.2. SEDPLUME-RW model

The plume dispersion model used in this study is a version of the SEDPLUME-3D lagrangian plume dispersion model (developed by HR Wallingford) which has been specifically modified to reproduce the complex releases of sediment that result from dredging. In particular the model incorporates the near-field mixing of the overflow from TSHD and barges.

The dispersion of sediment plumes is represented as discharge of large numbers (millions) of discrete particles. The horizontal and vertical components of velocity of each sediment particle are interpolated in space and time from the TELEMAC-2D flow model results, assuming a logarithmic vertical velocity profile. Each particle is advected at each time step by these local computed flow conditions. The effects of turbulent eddies on suspended sediment are represented by subjecting each particle to random displacements in addition to the advection by the mean current motion. The lengths of these random turbulent displacements are chosen based on the calculated turbulent diffusivity.

The deposition and resuspension of particles are modelled by establishing critical shear stresses for erosion and deposition. Erosion of deposited material occurs when the bed shear stress exceeds the critical shear stress for erosion while deposition of suspended material occurs when the bed shear stress falls below the critical shear stress for deposition.

The SEDPLUME-3D model predicts the increase in suspended sediment concentrations and fine sediment deposition over and above that over the background conditions.

2.2.3. Modelled scenarios

A total of six scenarios were modelled as set out in Table 2.4. Each simulation modelled a period of 3 tides.

Table 2.4: Modelled scenarios

Scenario	Hydrodynamic conditions	Dredging operation
1	Low river flow, spring tide	Backhoe dredging in channel
2		TSHD dredging at berth/quay area
3		CSD dredging at berth/quay area and pumping into a barge
4	High river flow, neap tide	Backhoe dredging in channel
5		TSHD dredging at berth/quay area
6		CSD dredging at berth/quay area and pumping into a barge

The locations of the simulated dredging operations are shown in Figure 2.2.

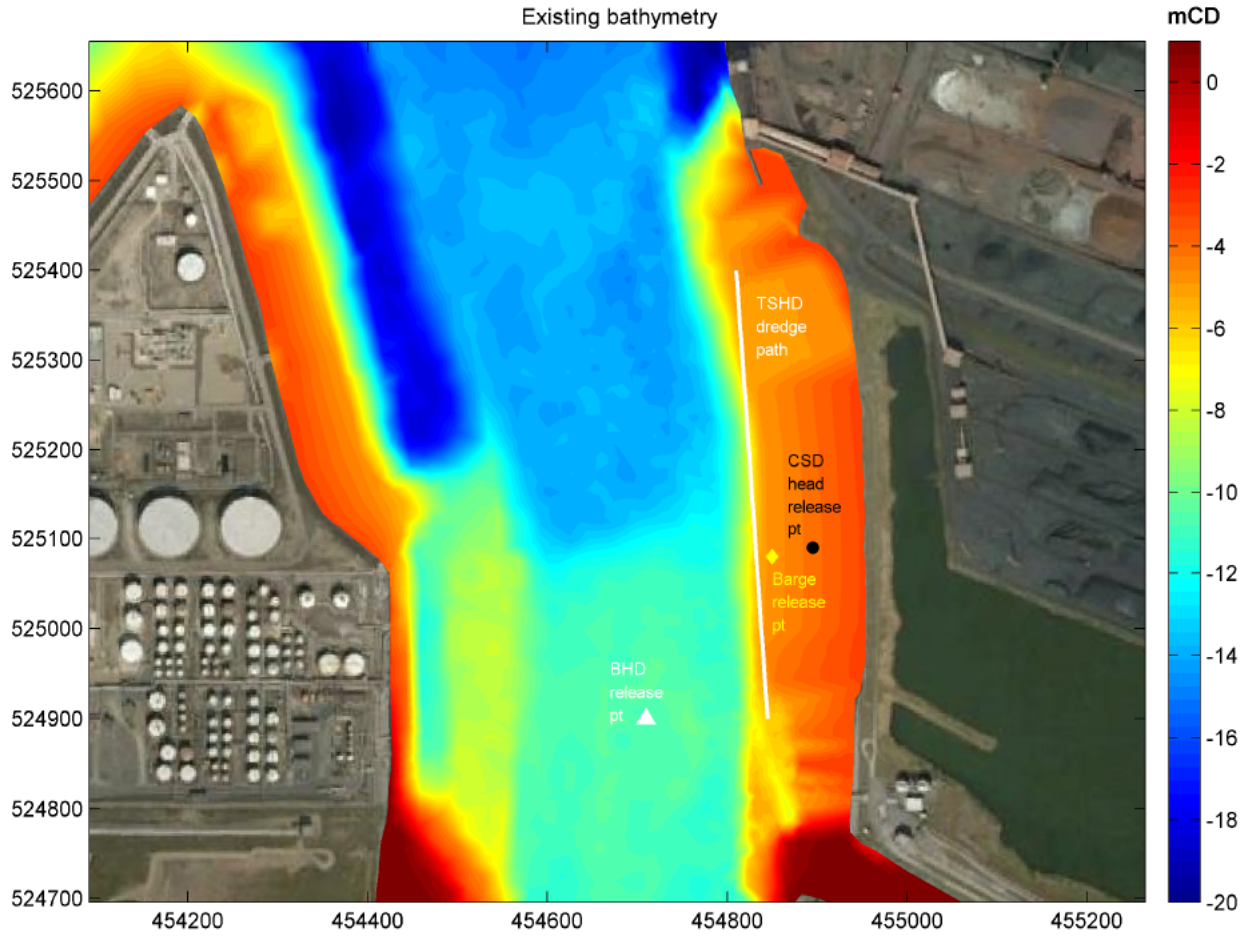

Figure 2.2: Simulated scenarios for BHD, TSHD and CSD dredging

2.2.4. Sediment parameters

The values of sediment parameters used in the plume dispersion modelling are presented in Table 2.5.

Table 2.5: Sediment parameter values

Parameter	Value
Critical shear stress for erosion	0.2 N/m^2
Critical shear stress for deposition	0.1 N/m^2
Erosion rate constant M_e $\left[\frac{\partial m}{\partial t} = M_e(\tau - \tau_e)\right]$	0.001 kg/Nsm^2
Settling velocity	0.001 m/s
Mass concentration of deposited fine sediment	500 kg/m^3

2.3. Sediment plume modelling results

The results of the sediment plume modelling are presented in Sections 2.3.1 to 2.3.6 using three different types of figure to illustrate the results:

- **Peak concentrations throughout the simulation**. These figures show the peak predicted values of the increase in depth-averaged suspended sediment concentration above background. Because the figure shows the maximum values attained this type of figure shows the envelope of the possible effects and is useful therefore for identifying the footprint of effect. However, this type of figure tends to over-emphasise the size of the plume to the reader as it does not show the plume at any given moment in time but rather a composite of all plumes at all times during the simulation.
- **Mean concentrations throughout the simulation**. These figures show the average increase in suspended sediment experienced over the course of the simulation. The footprint shown in these figures is generally much smaller than for the peak concentration figures and gives a better idea of the overall effect of sediment plume dispersion.
- **Predicted deposition at the end of the simulation**. These figures show the fine sediment deposition at the end of the simulation. It should be noted that the capital dredging will continue over a longer period than represented in the simulation.

2.3.1. Simulation 1: Backhoe dredging in low river flow, spring tide conditions

The predicted peak increase in depth-averaged suspended sediment concentration above background is shown in Figure 2.3. The figure shows that the predicted concentration increases are below 10 mg/l at a distance of more than 700 m upstream and downstream of the dredging and peak increases in concentrations are below 50 mg/l at all locations, except for within 30 m of the dredger.

The predicted mean increase in depth-averaged suspended sediment concentration above background over the simulation period is shown in Figure 2.4. The figure shows that predicted mean concentration increases above 10 mg/l are confined to the vicinity of the dredger.

The predicted fine sediment deposition is shown in Figure 2.5. The figure shows that the predicted fine sediment deposition over the simulation period is a few millimetres or less except at the position of the dredger itself.

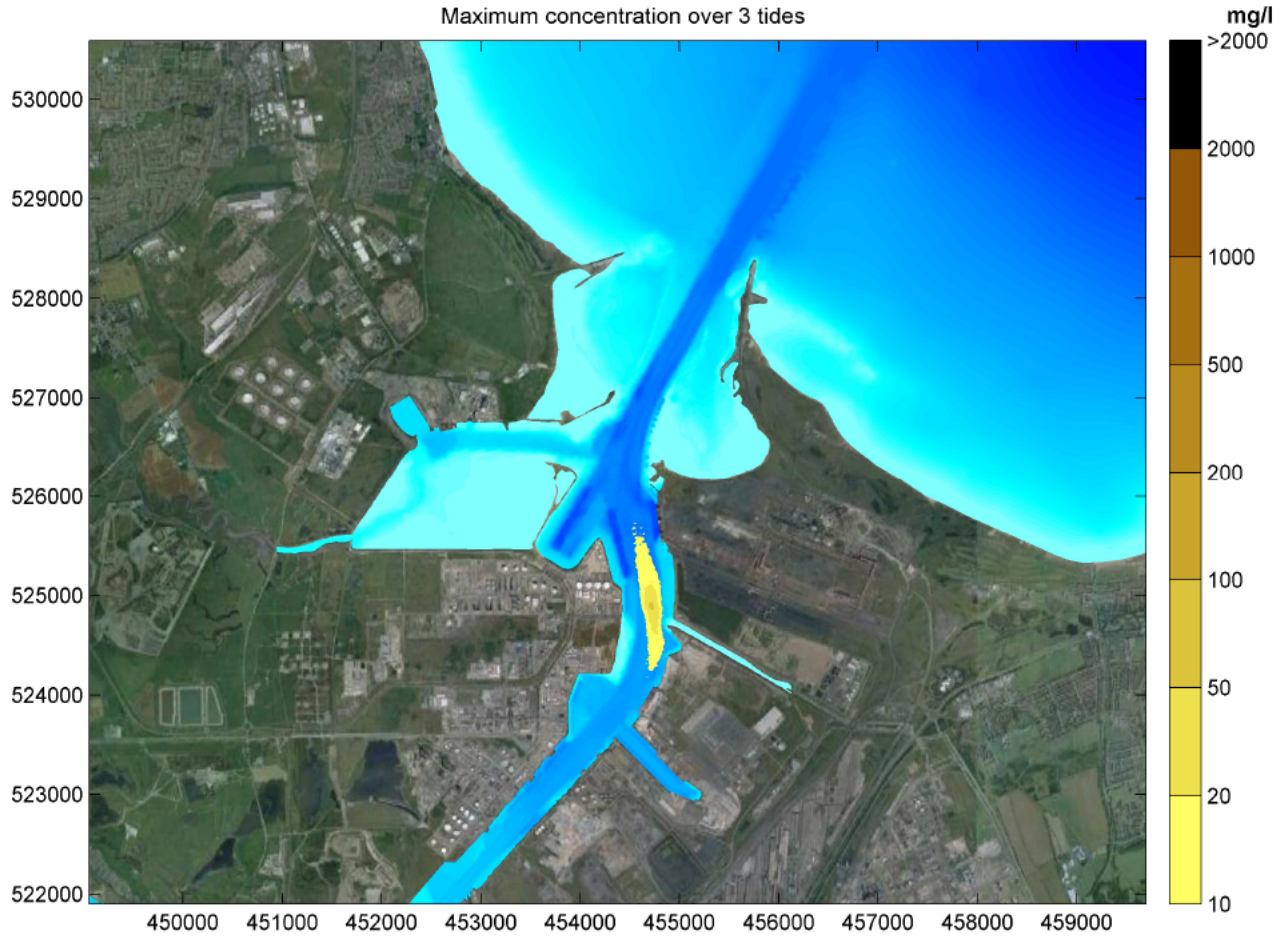

Figure 2.3: Peak predicted increase in depth-averaged suspended sediment concentration above background conditions, backhoe dredging in low river flow, spring tide conditions

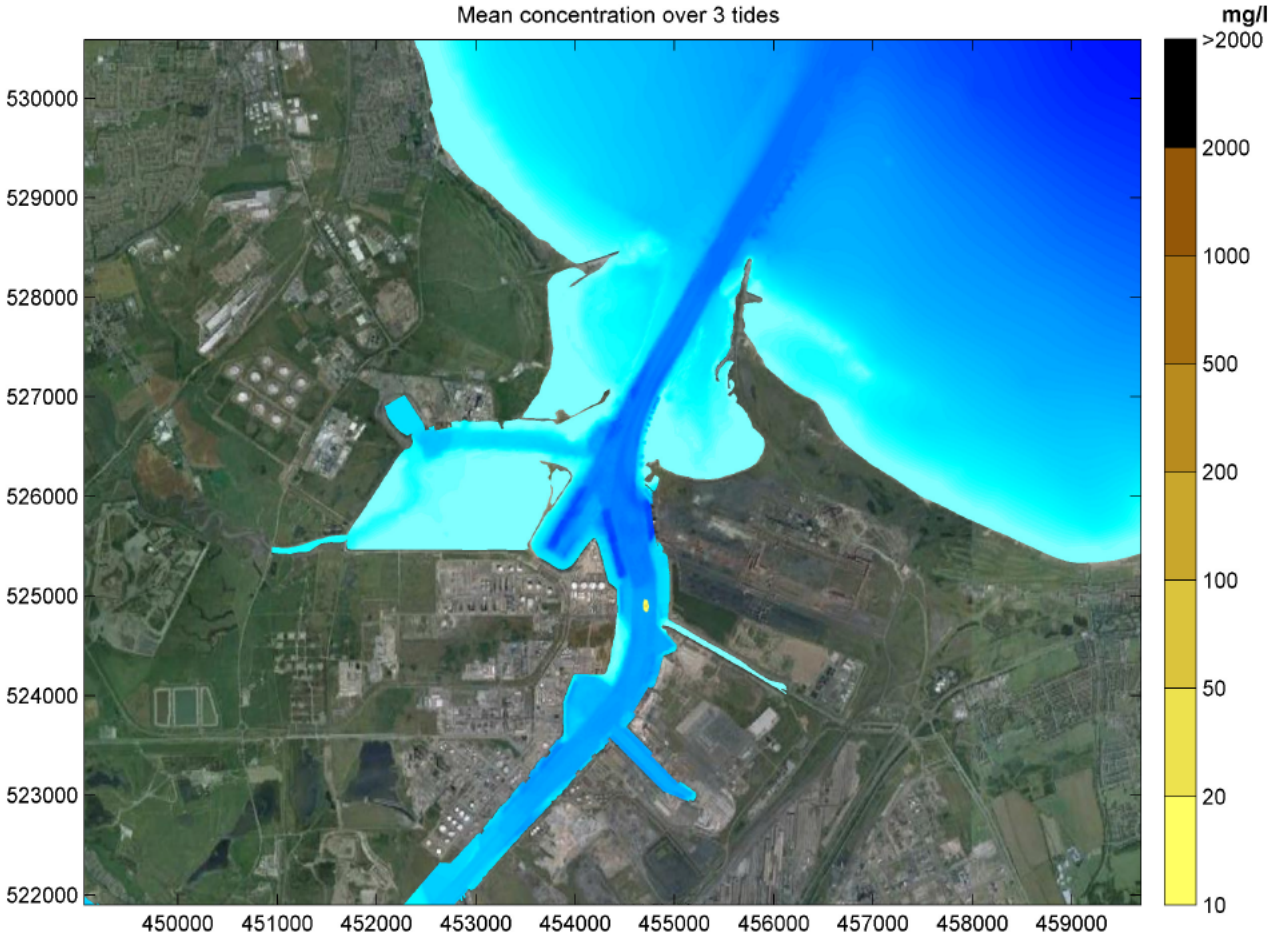

Figure 2.4: Predicted mean increase in depth-averaged suspended sediment concentration above background conditions, backhoe dredging in low river flow, spring tide conditions

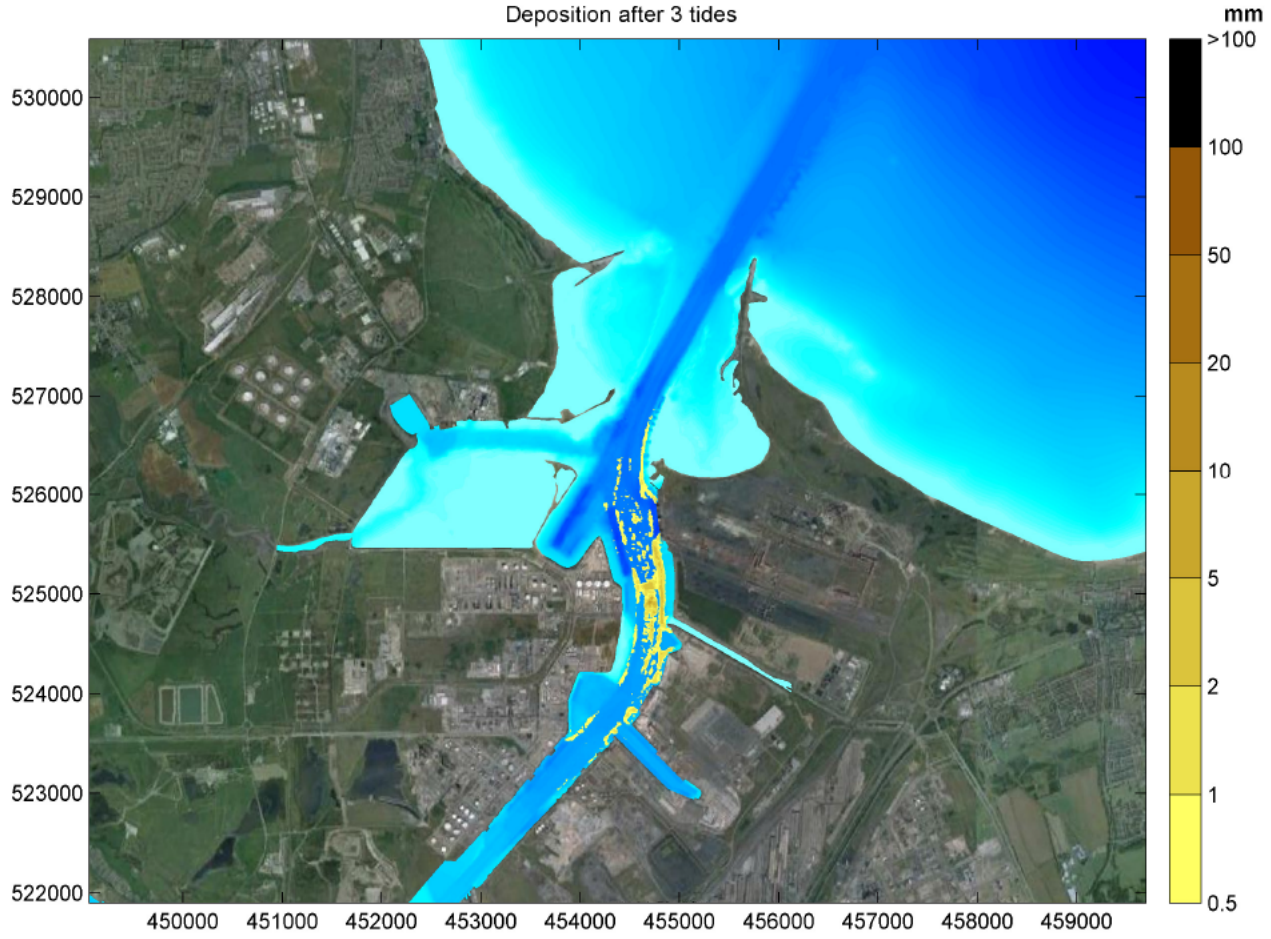

Figure 2.5: Predicted fine sediment deposition after 3 tides, backhoe dredging in low river flow, spring tide conditions

2.3.2. Simulation 2: TSHD dredging in low river flow, spring tide conditions

The predicted peak increase in depth-averaged suspended sediment concentration above background resulting from TSHD dredging in low river flow, spring tide conditions is shown in Figure 2.6. The figure shows that at times during the simulation concentration increases of more than 10 mg/l occurred up to 2.6 km upstream of the dredging and up to 1.5 km offshore of the South Gare breakwater. The largest predicted concentration increases are in the region of 1000 mg/l in the vicinity of the dredging itself.

The predicted mean increase in depth-averaged suspended sediment concentration above background over the simulation period is shown in Figure 2.7. The figure shows that predicted mean concentration increases above 10 mg/l extend up to 1 km upstream and downstream of the dredging with mean concentrations of around 200 mg/l at the dredging location itself.

The predicted fine sediment deposition is shown in Figure 2.8 The figure shows that the predicted fine sediment deposition over the simulation period is a few millimetres or less except at the dredging location,

where deposition of 10-20 mm occurred over the simulation, and in the downstream streamline of the dredging area where deposition of 5-10 mm was predicted to occur.

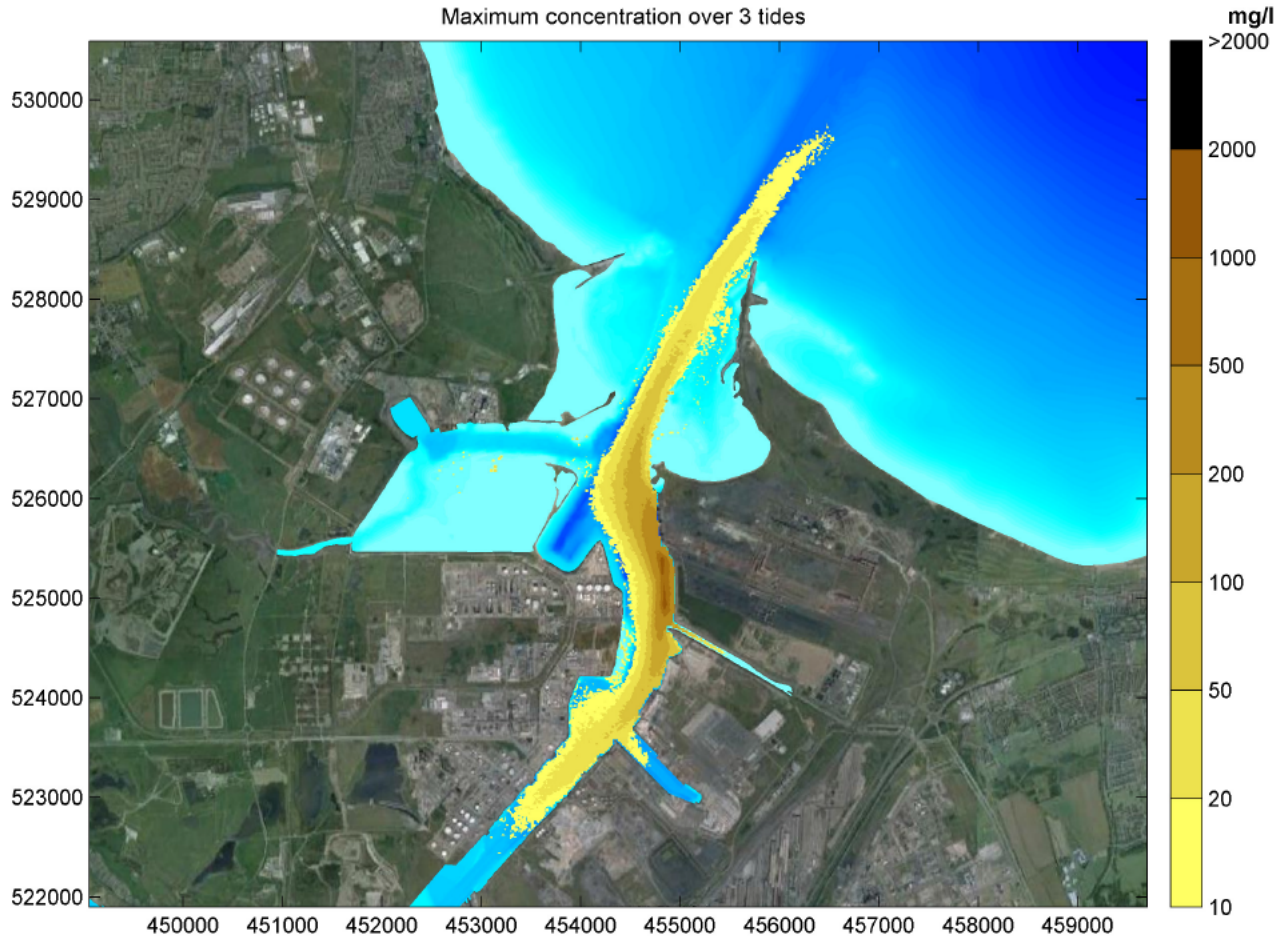

Figure 2.6: Peak predicted increase in depth-averaged suspended sediment concentration above background conditions, TSHD dredging in low river flow, spring tide conditions

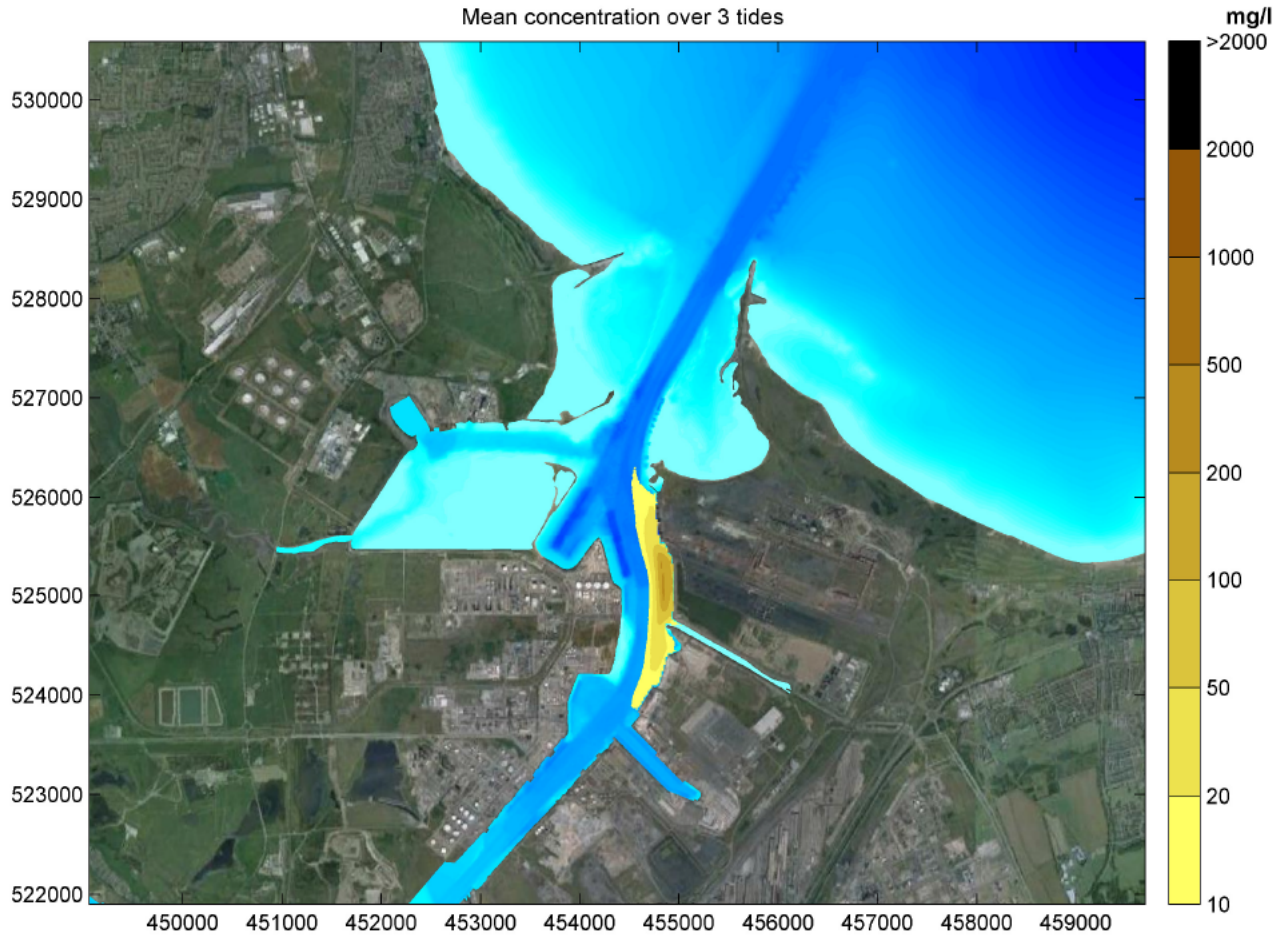

Figure 2.7: Predicted mean increase in depth-averaged suspended sediment concentration above background conditions, TSHD dredging in low river flow, spring tide conditions

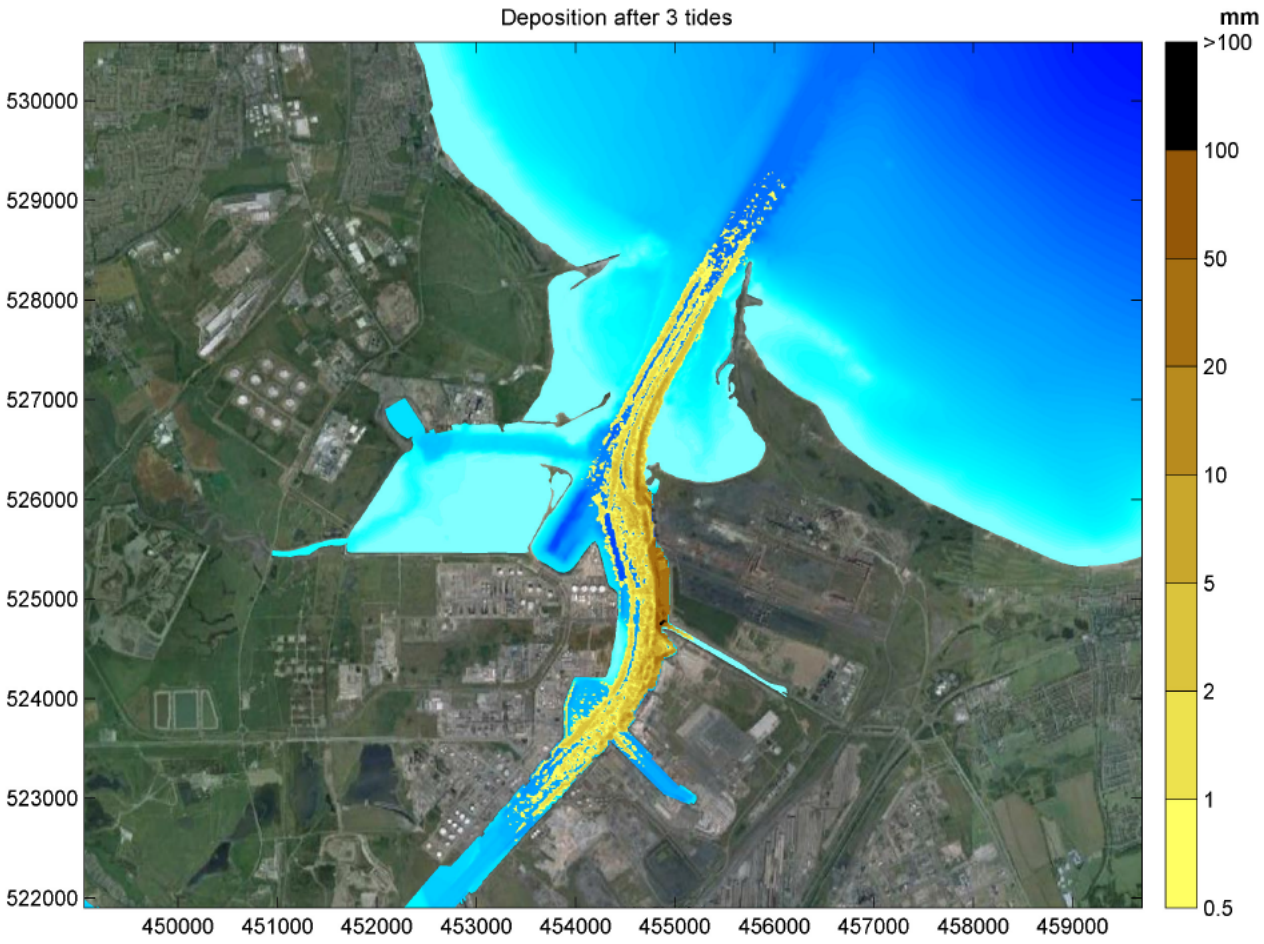

Figure 2.8: Predicted fine sediment deposition after 3 tides, TSHD dredging in low river flow, spring tide conditions

2.3.3. Simulation 3: CSD dredging in low river flow, spring tide conditions

The predicted peak increase in depth-averaged suspended sediment concentration above background is shown in Figure 2.9. The figure shows that the predicted concentration increases rise above 10 mg/l between the South Gare breakwater and 2.5 km upstream of the dredging at some point in the simulation. At the location of the dredging itself concentration increases of more than 500 mg/l are predicted in the shallow water.

The predicted mean increase in depth-averaged suspended sediment concentration above background over the simulation period is shown in Figure 2.10. The figure shows that predicted mean concentration increases above 10 mg/l are confined to 500 m upstream and downstream of the dredger. Mean concentrations of more than 500 mg/l are predicted at the location of the dredging itself.

The predicted fine sediment deposition at the end of the simulation period is shown in Figure 2.11. The figure shows that immediately upstream and downstream of the dredging and barge deposition of tens of millimetres is predicted while in the vicinity of the barge itself deposition of 100s of millimetres (tens of centimetres) is predicted. Elsewhere the predicted fine sediment deposition over the simulation period is a few millimetres or less.

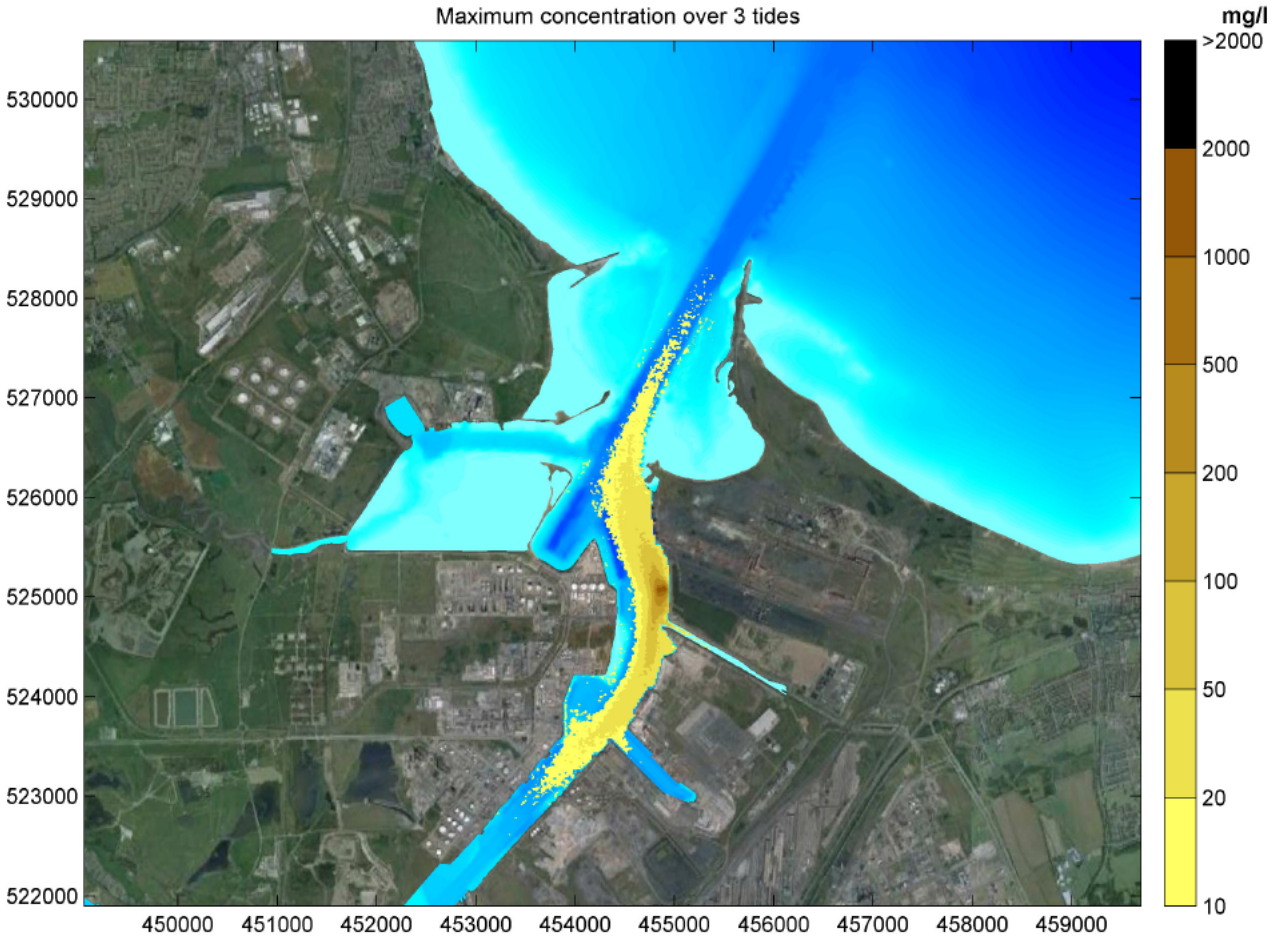

Figure 2.9: Peak predicted increase in depth-averaged suspended sediment concentration above background conditions, CSD dredging in low river flow, spring tide conditions

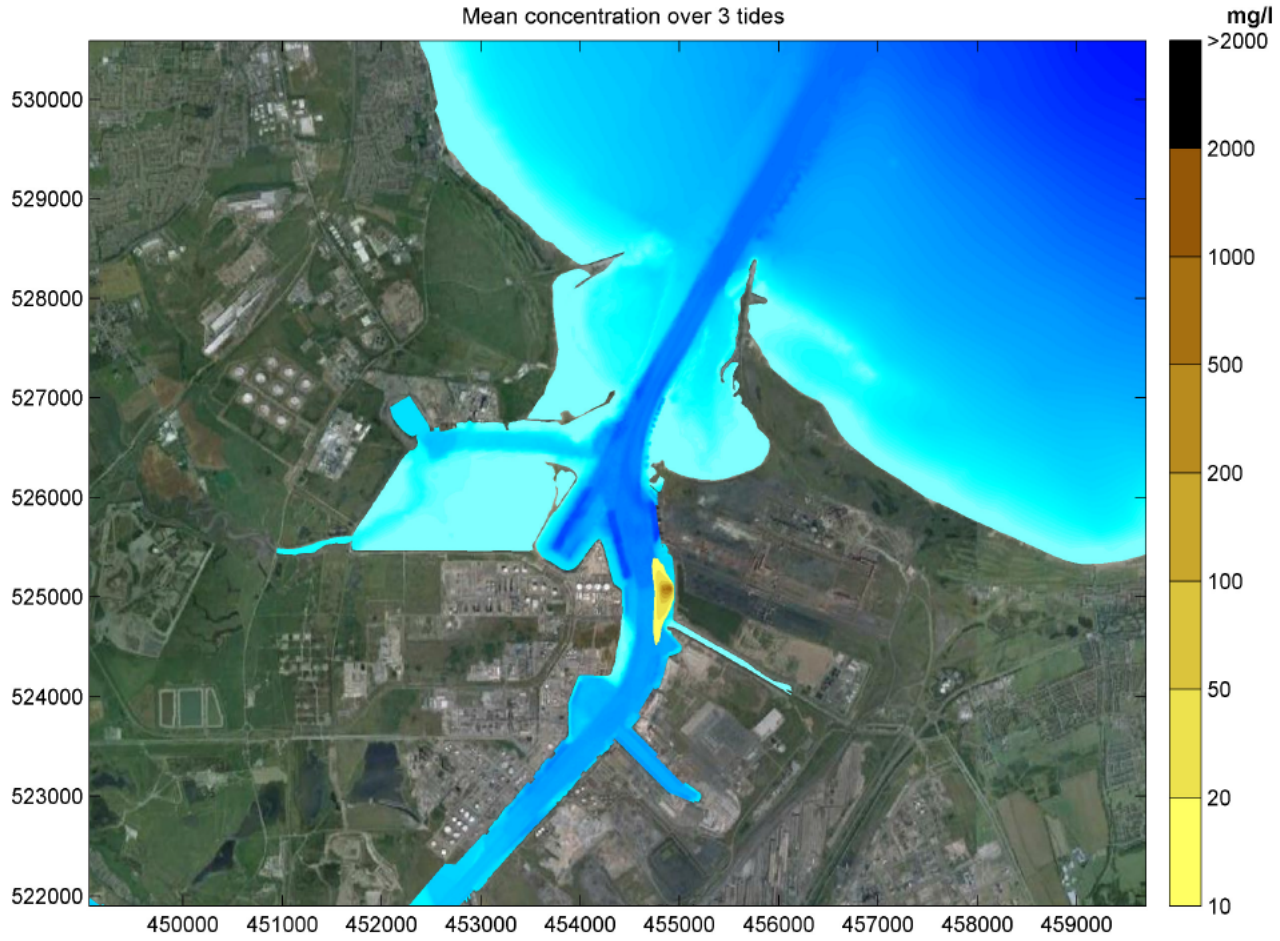

Figure 2.10: Predicted mean increase in depth-averaged suspended sediment concentration above background conditions, CSD dredging in low river flow, spring tide conditions

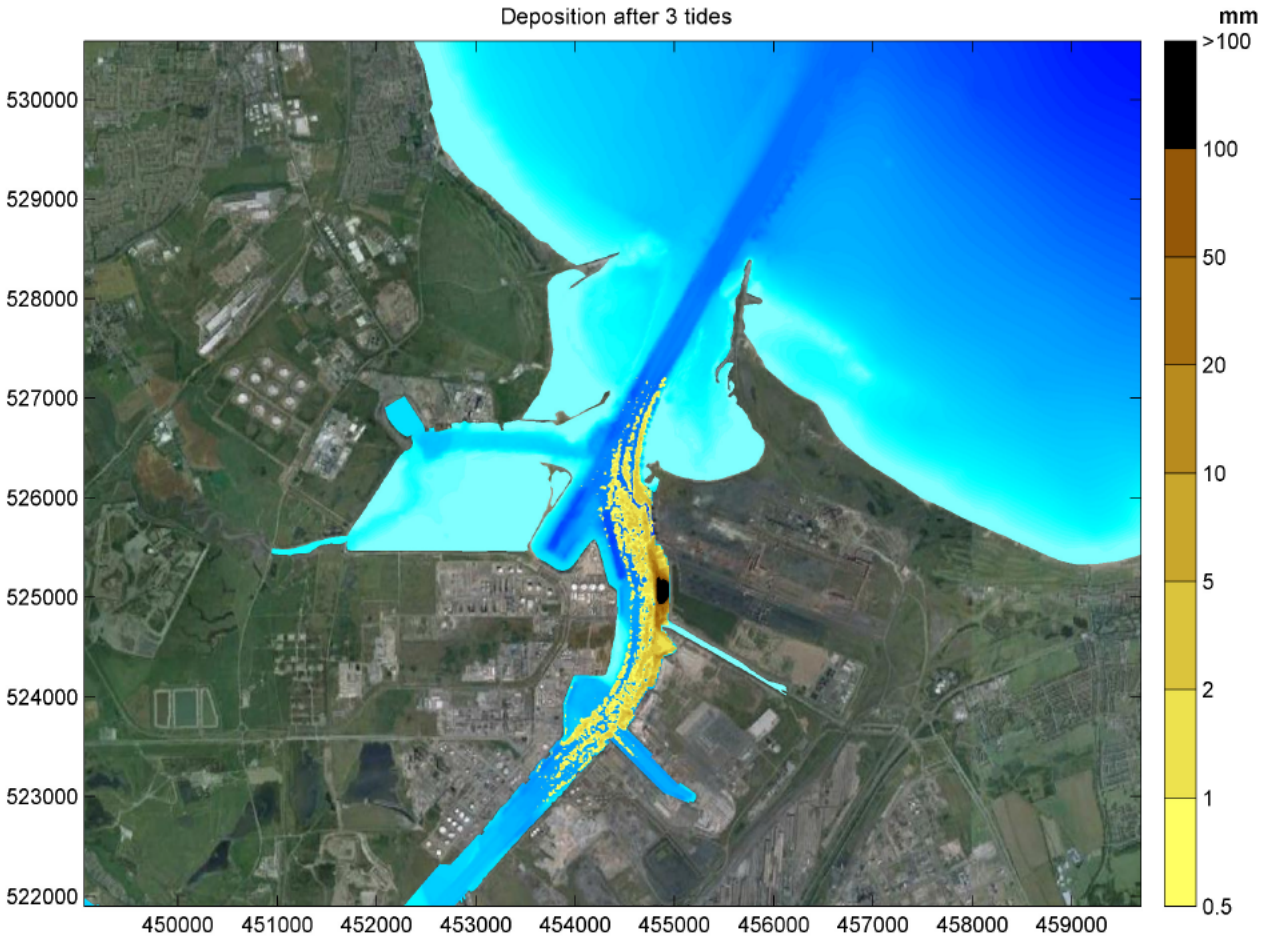

Figure 2.11: Predicted fine sediment deposition after 3 tides, CSD dredging in low river flow, spring tide conditions

2.3.4. Simulation 4 Backhoe dredging in high river flow, neap tide conditions

The predicted peak increase and mean increase in depth-averaged suspended sediment concentration above background for high river flow neap tide conditions are shown in Figure 2.12 and Figure 2.13. The figures show similar results to those for low river flow, spring tide conditions (see Section 2.3.1).

The predicted fine sediment deposition is shown in Figure 2.14. The figure shows that the distribution of fine sediment is more localised than for the low river flow, spring tide conditions. However, as before the predicted fine sediment deposition over the simulation period is a few millimetres or less except at the position of the dredger itself.

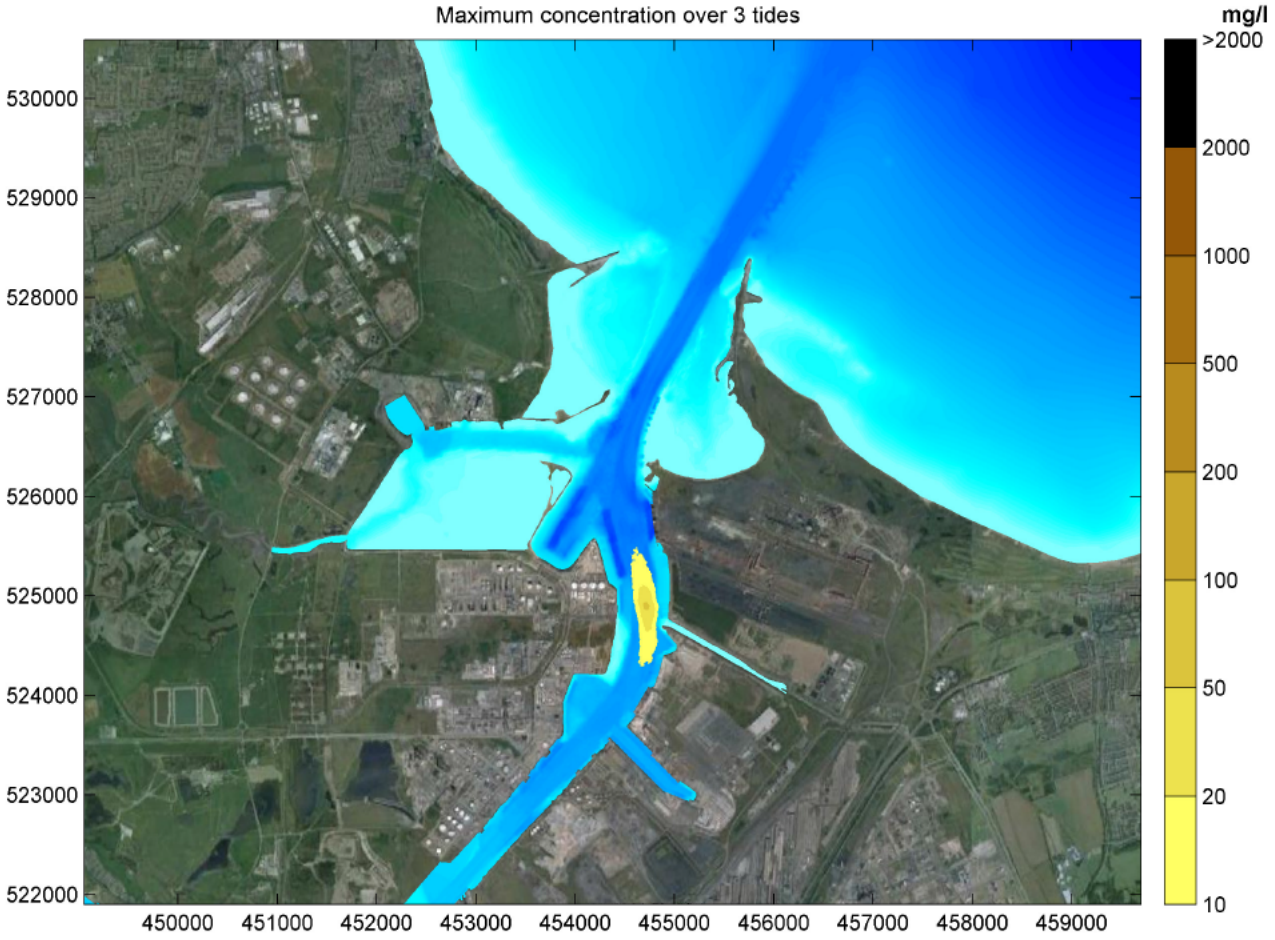

Figure 2.12: Peak predicted increase in depth-averaged suspended sediment concentration above background conditions, backhoe dredging in high river flow, neap tide conditions

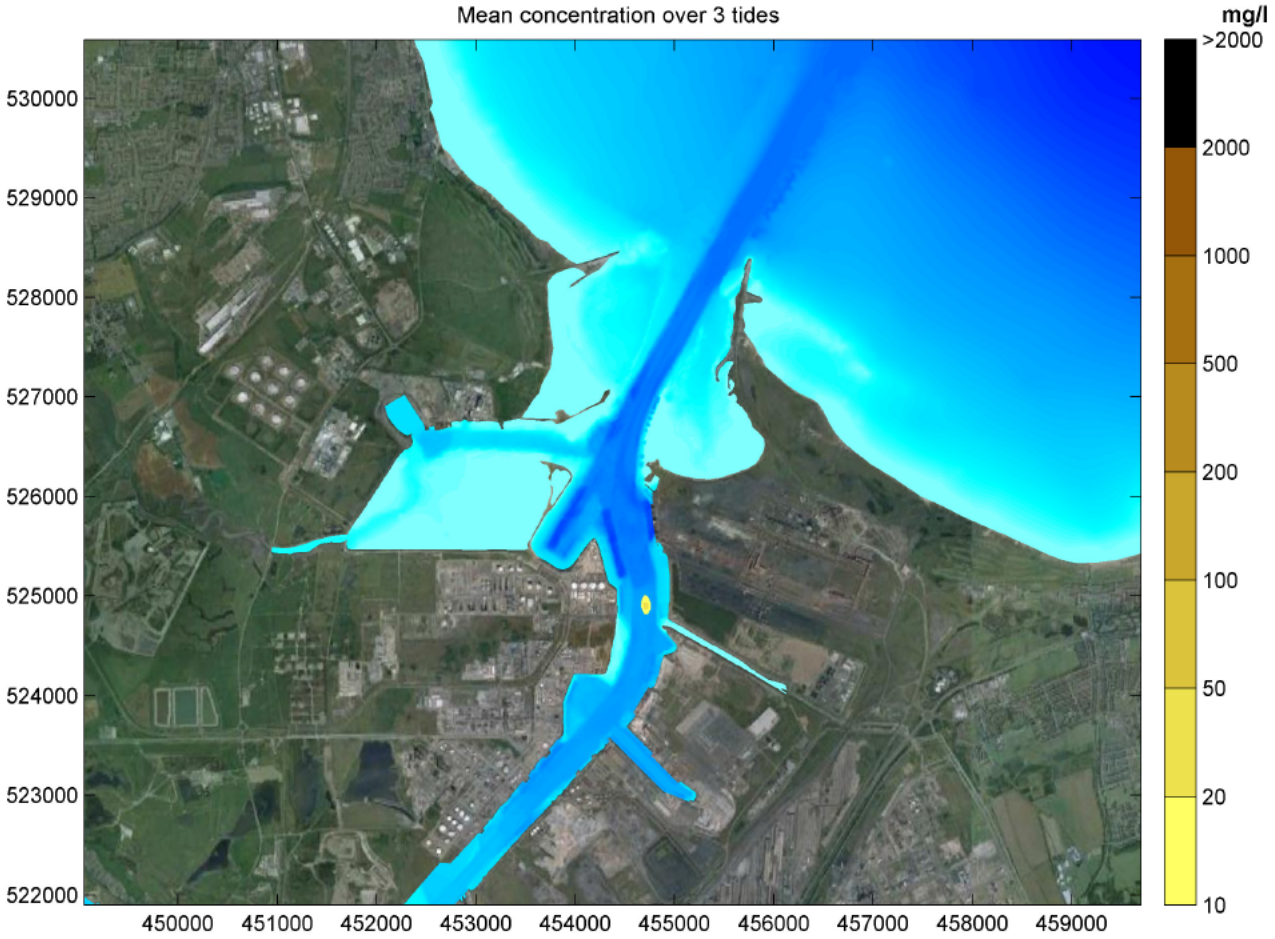

Figure 2.13: Predicted mean increase in depth-averaged suspended sediment concentration above background conditions, backhoe dredging in high river flow, neap tide conditions

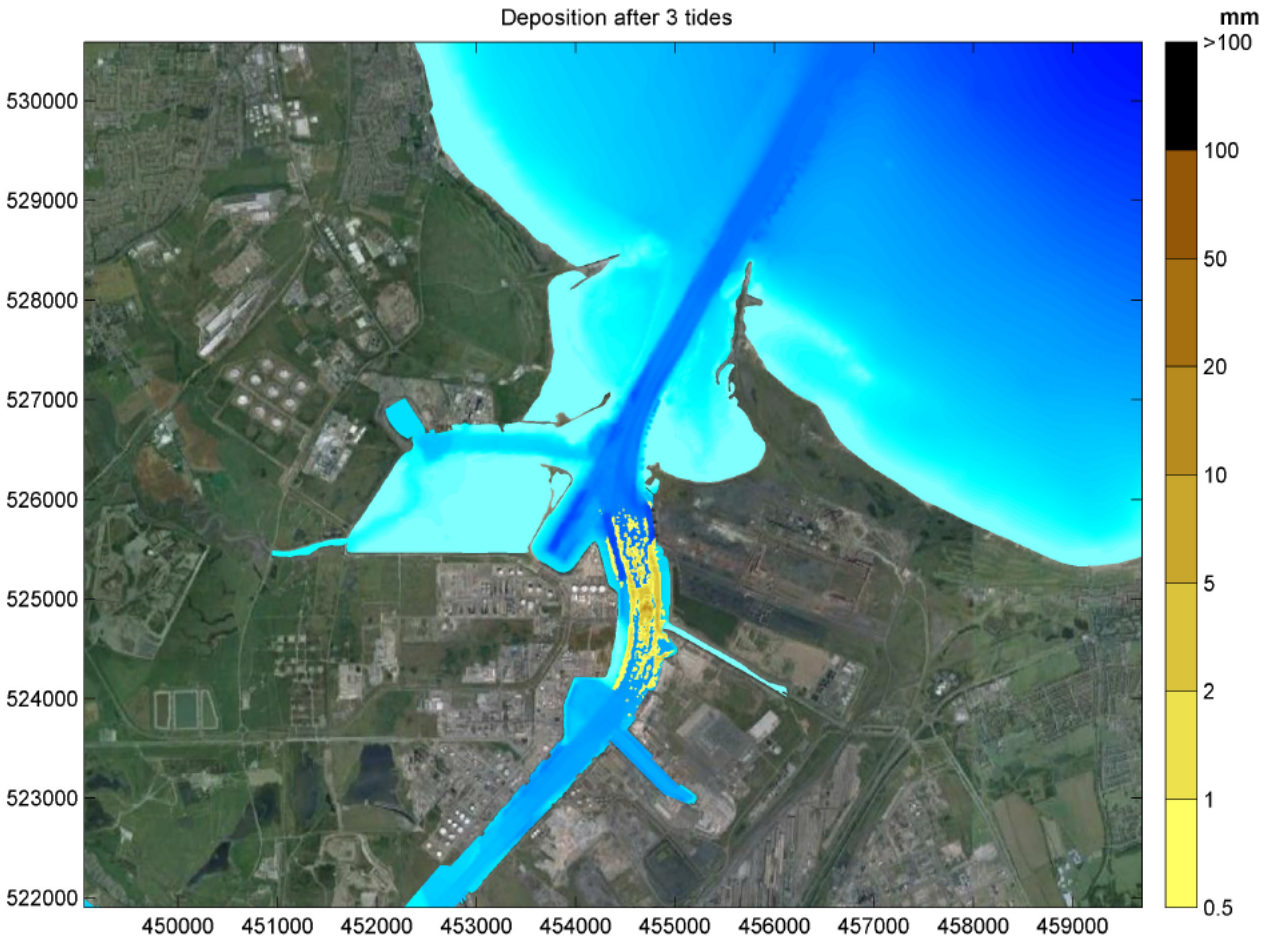

Figure 2.14: Predicted fine sediment deposition after 3 tides, backhoe dredging in high river flow, neap tide conditions

2.3.5. Simulation 5: TSHD dredging in high river flow, neap tide conditions

The predicted peak increase in depth-averaged suspended sediment concentration above background resulting from TSHD dredging in low river flow, spring tide conditions is shown in Figure 2.15. The figure shows that the footprint of TSHD plumes is less extensive for the high river flow, neap tide conditions than the low river flow, spring tide conditions of Section 2.3.2. The high river flow, neap tide footprint extends from Tees mouth to Tees Dock. The largest predicted concentration increases are in the region of 1000 mg/l in the vicinity of the dredging itself.

The predicted mean increase in depth-averaged suspended sediment concentration above background over the simulation period is shown in Figure 2.16. The figure shows that predicted mean concentration increases above 10 mg/l extend up to 1 km upstream and downstream of the dredging with mean concentrations of around 200 mg/l at the dredging location itself.

The predicted fine sediment deposition is shown in Figure 2.17. The figure shows that the predicted fine sediment deposition over the simulation period is a few millimetres or less except at the dredging location,

where deposition of 10-20 mm occurred over the simulation, and in the downstream streamline of the dredging area where deposition of 5-10 mm was predicted to occur.

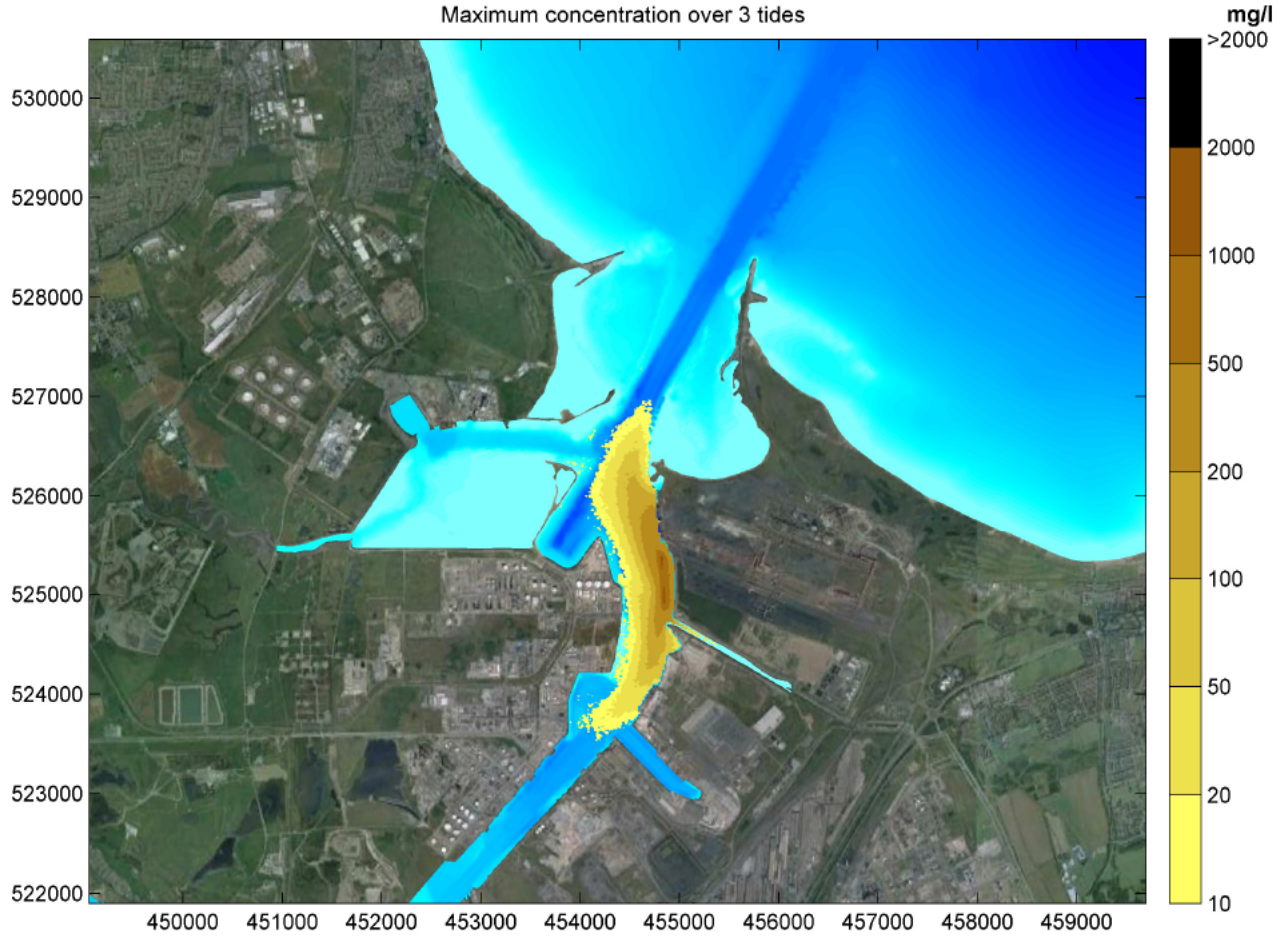

Figure 2.15: Peak predicted increase in depth-averaged suspended sediment concentration above background conditions, TSHD dredging in high river flow, neap tide conditions

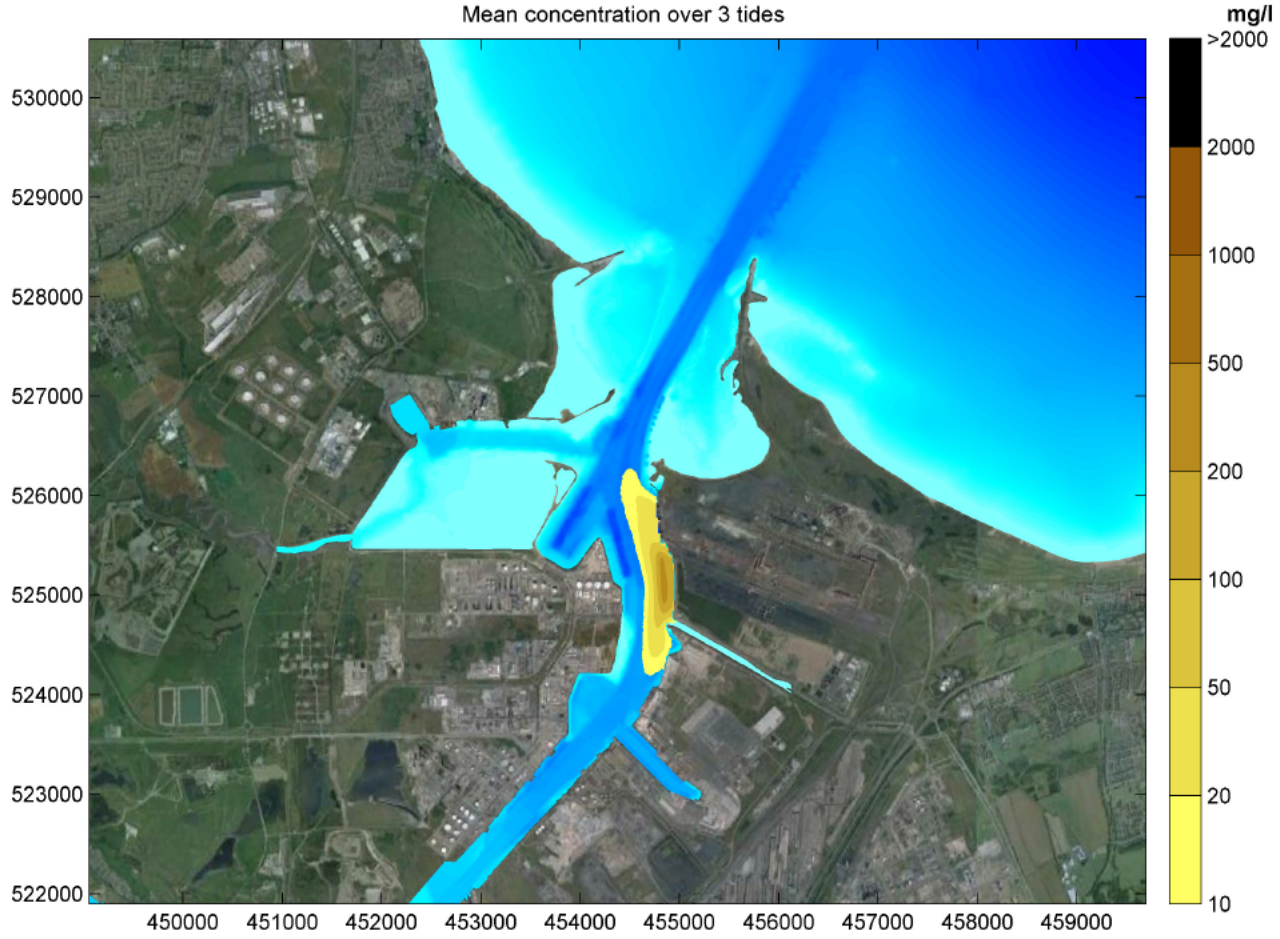

Figure 2.16: Predicted mean increase in depth-averaged suspended sediment concentration above background conditions, TSHD dredging in high river flow, neap tide conditions

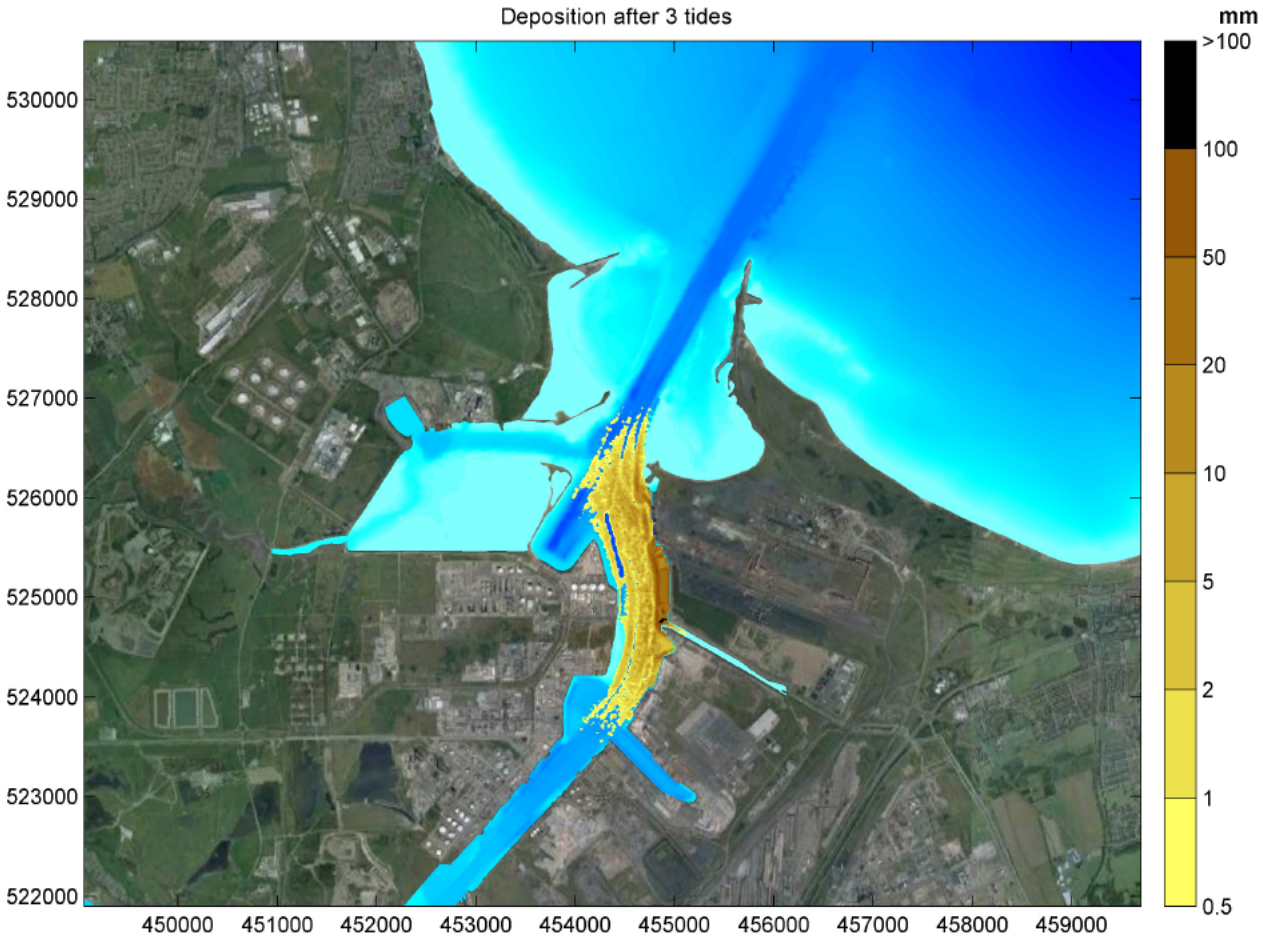

Figure 2.17: Predicted fine sediment deposition after 3 tides, TSHD dredging in high river flow, neap tide conditions

2.3.6. Simulation 6: CSD dredging in high river flow, neap tide conditions

The predicted peak increase in depth-averaged suspended sediment concentration above background is shown in Figure 2.18. The figure shows that the predicted concentration increases rise above 10 mg/l up to 1.5 km upstream and downstream of the dredging at some point in the simulation. At the location of the dredging itself concentration increases of more than 500 mg/l are predicted in the shallow water.

The predicted mean increase in depth-averaged suspended sediment concentration above background over the simulation period is shown in Figure 2.19. The figure shows that predicted mean concentration increases above 10 mg/l are confined to 250 m upstream and downstream of the dredger and barge. Mean concentrations of more than 250 mg/l are predicted at the location of the dredging itself.

The predicted fine sediment deposition at the end of the simulation period is shown in Figure 2.20. The figure shows that immediately upstream and downstream of the dredging and barge deposition of tens of millimetres is predicted while in the vicinity of the barge itself deposition of 100s of millimetres (tens of centimetres) is predicted. Elsewhere the predicted fine sediment deposition over the simulation period is a few millimetres or less.

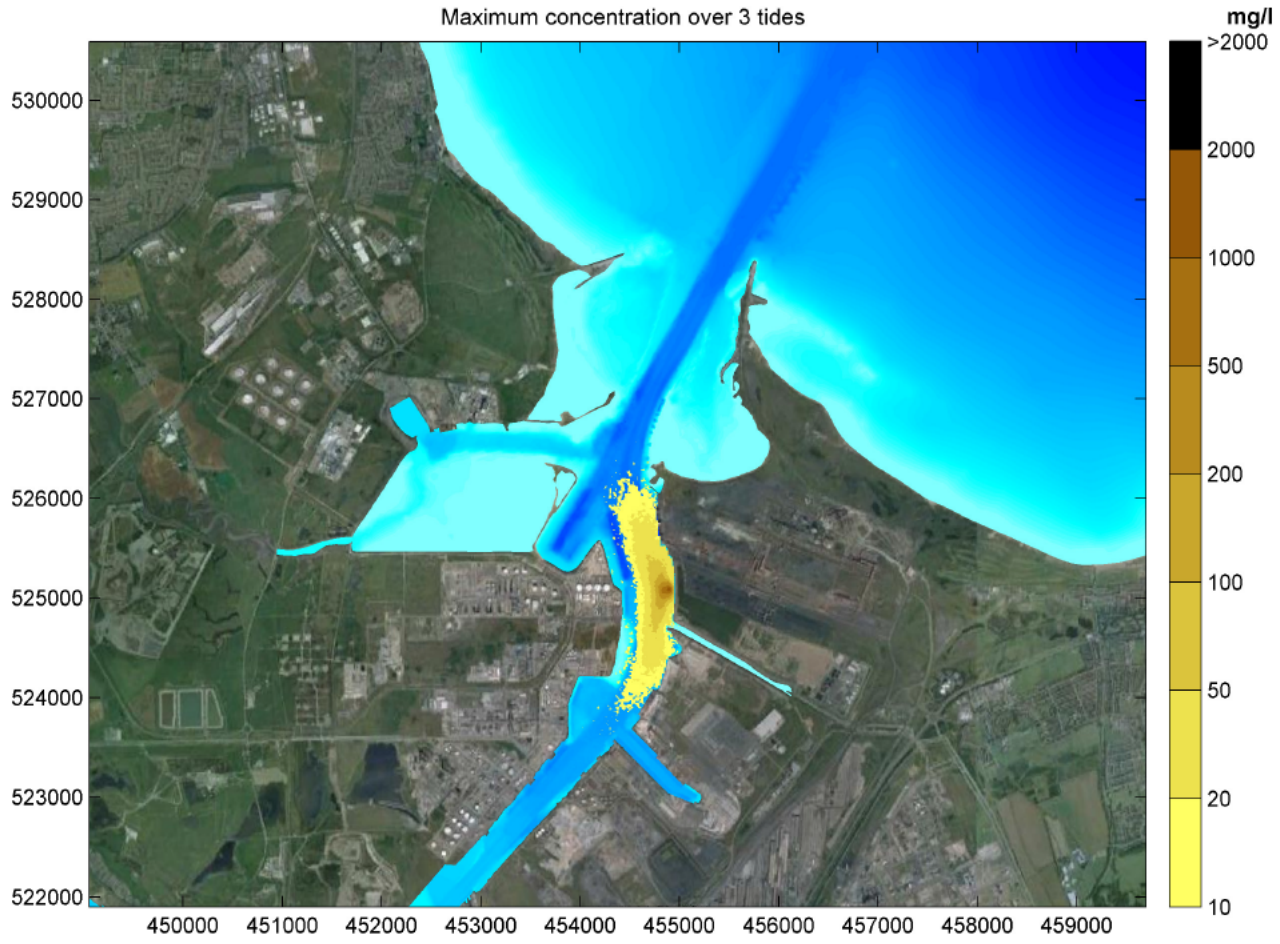

Figure 2.18: Peak predicted increase in depth-averaged suspended sediment concentration above background conditions, CSD dredging in high river flow, neap tide conditions

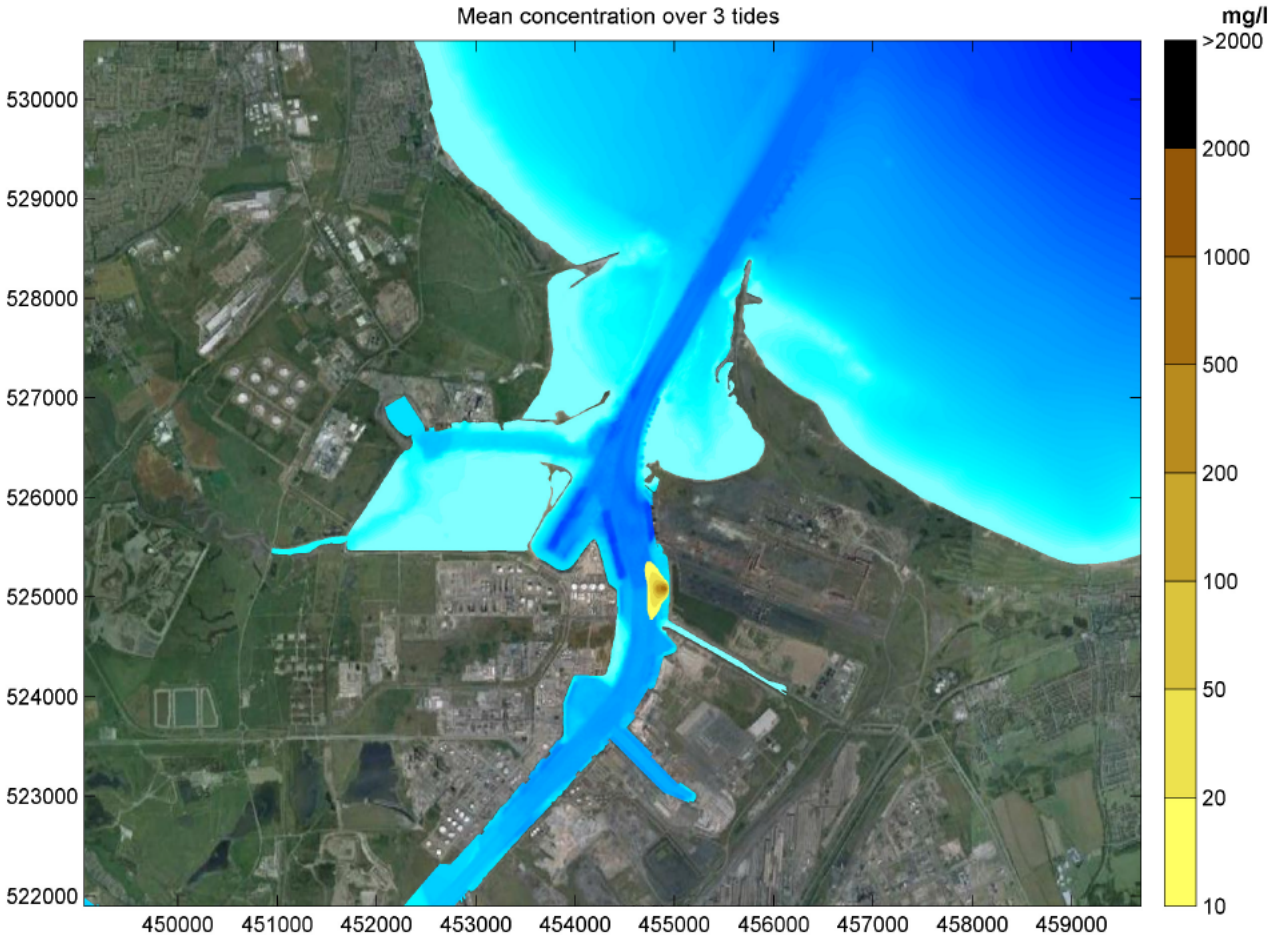

Figure 2.19: Predicted mean increase in depth-averaged suspended sediment concentration above background conditions, CSD dredging in high river flow, neap tide conditions

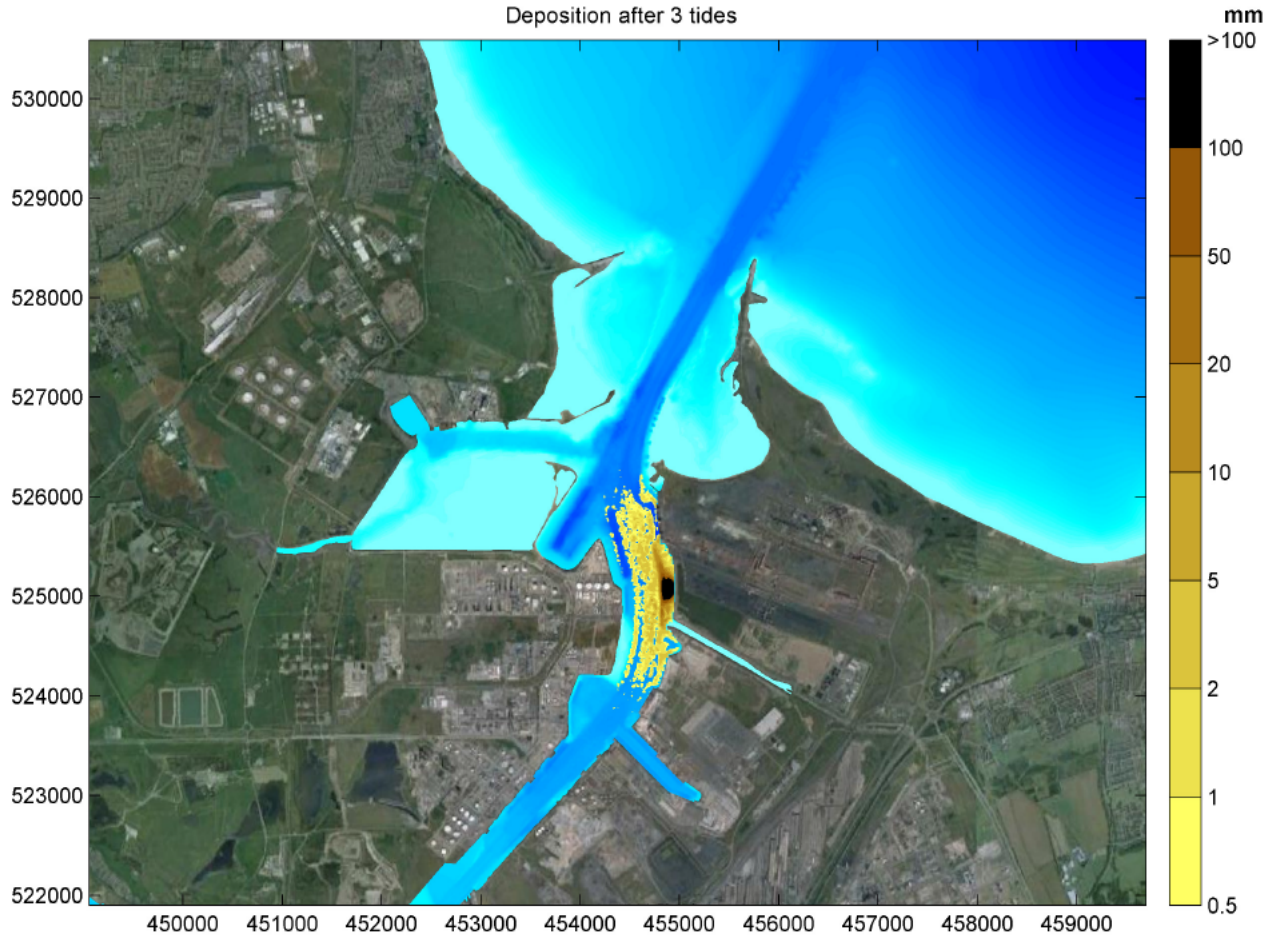

Figure 2.20: Predicted fine sediment deposition after 3 tides, CSD dredging in high river flow, neap tide conditions

2.3.7. Longer term deposition

The simulations undertaken above indicate that deposition of a millimetre per tide may occur between Teesmouth and Tees Dock, with patchier, lower rates of deposition further away and higher rates in the vicinity of the dredging. The higher rates of infill in the area of the dredging are assumed to be re-dredged.

These rates of deposition arise during the simulated periods of 3 tides. Accounting for the total dredge using the range of plant available suggests a one-off additional supply of deposited sediment to the areas presently maintained during the capital works. An initial view of the total depth of infill associated with the released material during the capital works suggests it may be up to 10% of the annual maintenance requirement for the Tees, but given that this is a one-off construction phase effect there is no longer term effect on maintenance dredging requirement related to sediment that is deposited during construction.

2.3.8. Summary

The simulations shown in Sections 2.3.1 to 2.3.6 show the following key features:

- The effects of backhoe dredging are relatively small compared to those of CSD and barge or TSHD.

- The CSD and barge overflowing produce considerable deposition of fine sediment locally on the bed while the TSHD dredging results in the release of more sediment into the water column.
- The CSD footprint of effect is smaller than that of TSHD dredging.
- On average predicted mean concentration increases outside of the dredging area are a few tens of mg/l at most. Peak predicted concentration increases are larger possibly rising to 100 or 200 mg/l outside of the dredging area for short periods.
- The footprint of effects of dredging for high river flow, neap tide conditions is considerably smaller than that for low river flow, spring tide conditions which extends past South Gare and Tees Dock.
- The predicted deposition is typically of the order of a few millimetres, except in the vicinity of the dredging itself where much higher rates of deposition are predicted. In practice the sediment depositing in the vicinity of the dredging will be re-dredged. During the period of the dredging operation a one off increase of up to 10% to the annual maintenance requirement in the Tees is predicted.

3. Wave modelling of operational phase impacts

3.1. Background

The proposed development involves the construction of a quay, a dredged pocket adjacent to the quay and dredging in the channel adjacent to the proposed berth. Wave conditions in the Tees Estuary are a combination of offshore swell and locally generated wind waves. The swell entering the estuary is limited in direction by the North Gare and South Gare Breakwaters.

The impact of the proposed development on wave conditions in the Tees Estuary was modelled using the SWAN wave model. Three configurations for the port terminal were tested:

1. The existing arrangement;
2. A solid, vertical sided quay;
3. A suspended jetty on piles over a 1:2 rock armour slope.

The proposed layouts also include a lowering of the estuary bed by dredging. The dredging plan is identical for the two proposed layouts. A berth pocket adjacent to the proposed quay would be dredged to -16.1 mCD and a section of the channel adjacent to the berth is to be dredged to -14.1 mCD.

3.2. Wave modelling method

3.2.1. The SWAN wave model

Wave conditions within the Tees Estuary were modelled using the SWAN wave model. SWAN is a 3rd generation spectral wave model which simulates the transformation of random directional waves considering the following processes:

- wave shoaling;
- wave refraction;
- partial and total reflection from structures and shorelines;
- depth-induced breaking, bottom friction and white-capping;
- wave growth due to the wind;

- wave-wave interactions.

The SWAN wave model is designed for modelling waves over coastal areas and is widely used in academia and industry. In this case it is used to model both the propagation of waves from offshore into the estuary and also the generation and propagation of waves within the estuary.

3.2.2. SWAN model area and bathymetry

The SWAN model was used in this study to transform refracted waves from the North Sea and those generated locally within the estuary, accounting for refraction, shoaling, seabed friction, breaking and reflections. The domain was chosen to include the fetch of all wind waves generated locally and incident upon the proposed quay, and extended offshore as far as the location of the wave rider buoy that is deployed by PD Teesport in Tees Bay.

The SWAN model area and bathymetry for the existing layout, solid quay layout and open quay layout is shown in Figure 3.1, Figure 3.2 and Figure 3.3 respectively.

The open quay is assumed to be transparent to waves so the quay itself is not included in the model, only the slope and shoreline below and behind the quay. The location of the quay is indicated on Figure 3.3 by a red outline.

The above figures also show 9 points along the estuary channel. At these points, the wave conditions predicted by SWAN are tabulated. Point 5 is directly in front of the proposed development.

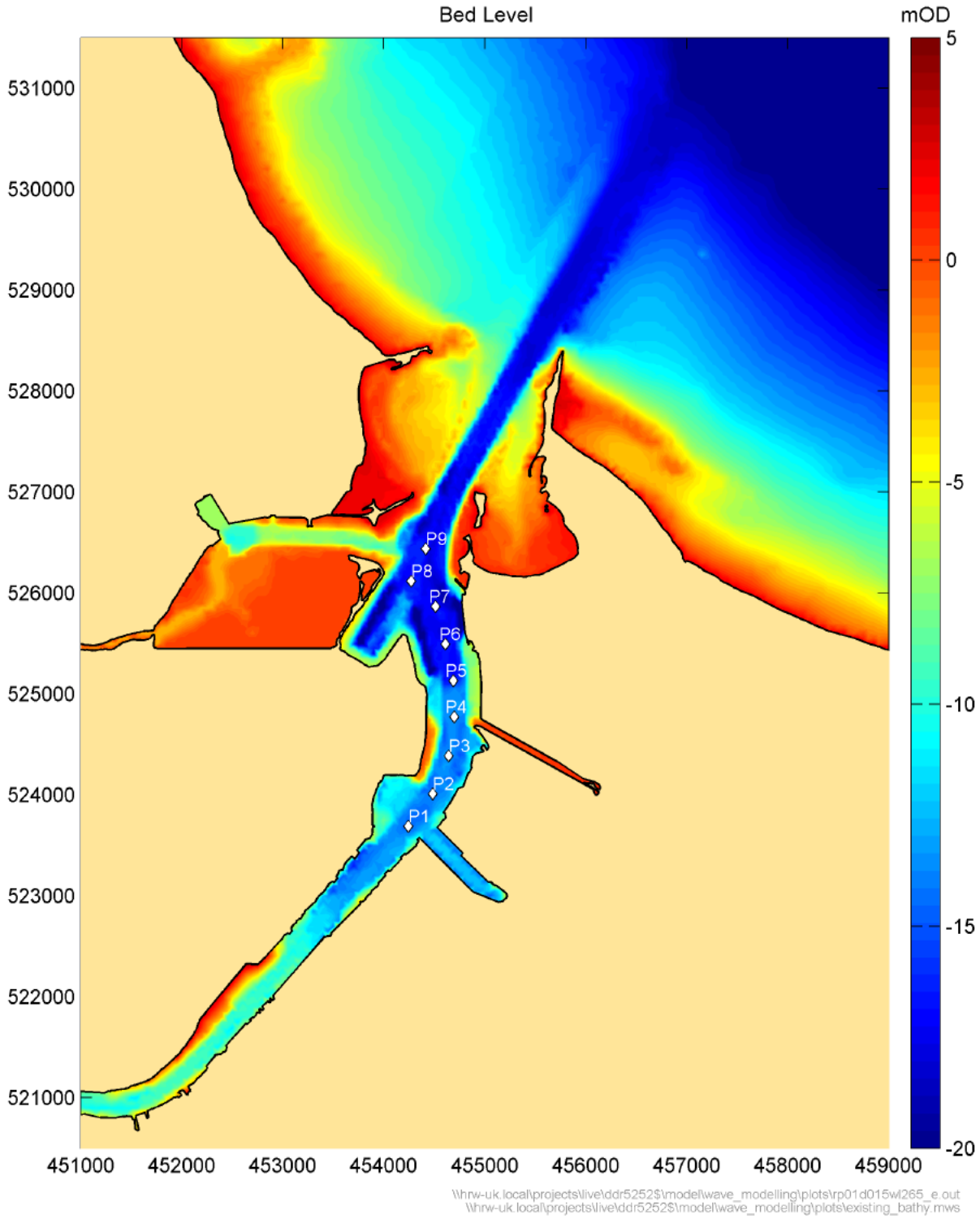

Figure 3.1: SWAN model area and bathymetry for the existing arrangement. Diamonds show the reporting locations for the tabulated results

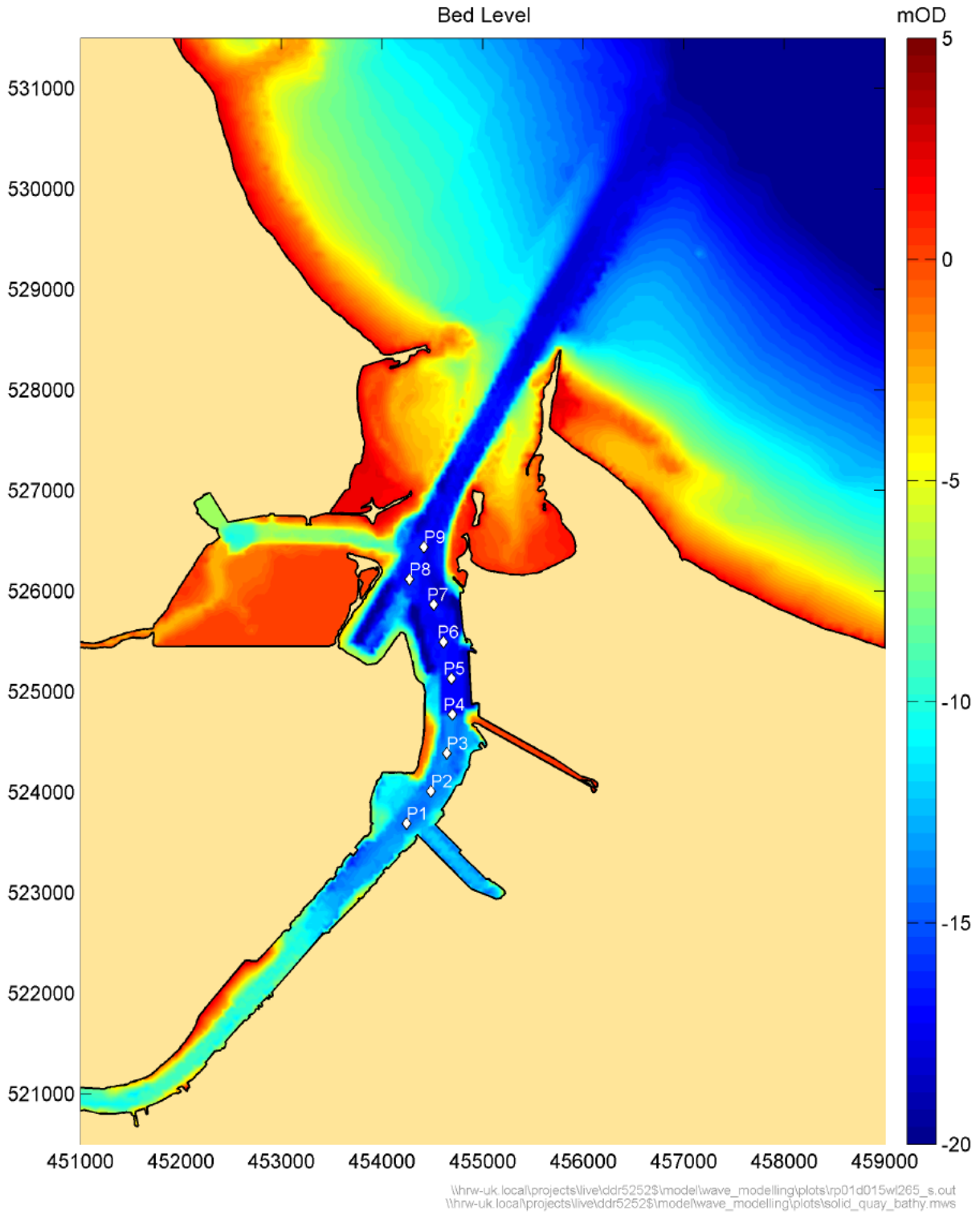

Figure 3.2: SWAN model area and bathymetry for the solid quay layout. Diamonds show the reporting locations for the tabulated results

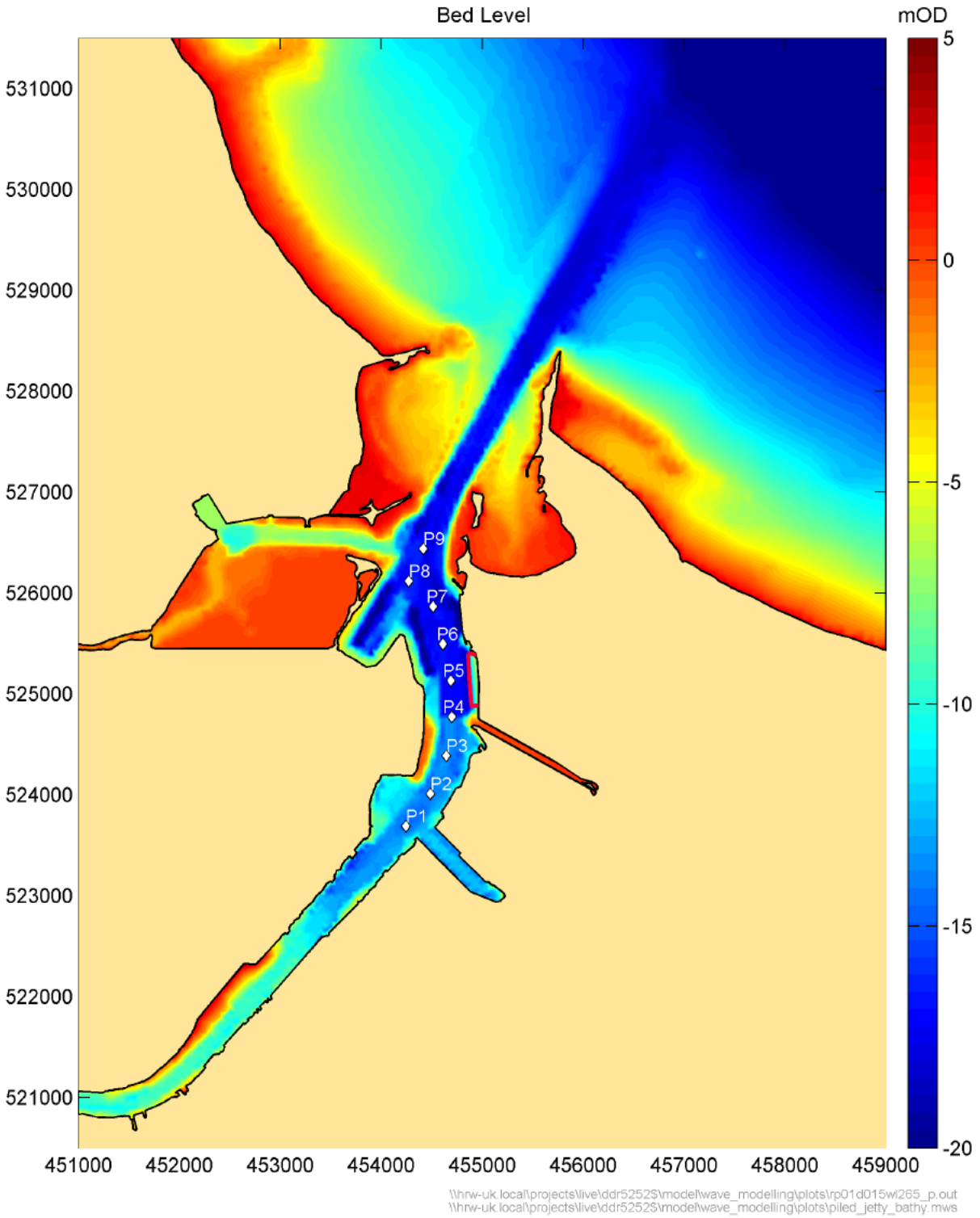

Figure 3.3: SWAN model area and bathymetry for the open quay layout. The location of the quay is outlined in red. Diamonds show the reporting locations for the tabulated results

3.2.3. Representation of reflection

The reflection properties of the boundaries of the estuary were represented in the SWAN model by assigning an appropriate reflection coefficient (k_r) to each of the boundary types. These reflection coefficients were calculated using a method developed at HR Wallingford, (Allsop (1990)), which takes into account the type of construction and slope of the boundary as well as the incident wave conditions. A reflection coefficient of 1.0 indicates that all the incident wave energy will be reflected, while a lower reflection coefficient indicates that some wave energy will be dissipated. The reflection boundaries were included in the SWAN model and the reflection coefficients assigned are shown in Table 3.1. The proposed extended quay is either an open structure above a slope faced with rock armour or a vertically sided solid quay face. Both options included some change to the reflectivity of the river frontage and so each required testing in the wave model. The reflection coefficients for the quay options described below correspond to locally generated wind waves, with short periods. It was found that longer period swell waves do not reach this upstream area with any significant strength.

Table 3.1: Reflection coefficients used in the SWAN model, derived from the formulation of Allsop (1990). The estimated reflection coefficients for the proposed quay options are shown in bold.

Description of region of coastline	Reflection Coefficient
Beach (e.g. Coatham Sands, Seaton Sands)	0.1
Small rock, steep slope (e.g. much of banks of Tees between jetties)	0.4
Small rock, shallow slope	0.2
Smooth concrete, steep slope	0.6
Smooth concrete, shallow slope	0.3
Vertical wall	0.95
Riverside Ro-Ro and region of Shell Jetty	0.4
Vertical side of solid quay	**0.95**
Small rock 1:2 slope under open quay	**0.3**

3.2.4. Wind and wave conditions

The scope of this study is to consider the impact of the proposed scheme under a representative range of realistic wind and wave conditions. The conditions selected drew on experience from previous studies in the area (e.g. HR Wallingford 2006) and more detailed wind data obtained from South Gare. Each layout was tested for a total of 8 conditions. Previous experience has shown that at the location of the proposed terminal, waves generated locally within the estuary are more severe than swell waves propagating through the estuary mouth. Therefore the test conditions include six local wind waves and two swell wave conditions.

Wind condition

The proposed port terminal is located on a bend of the Tees estuary and the longest fetches from the terminal are approximately in the north and southwest directions and it is from these directions that the locally generated waves are the largest at the site of the proposed terminal. A time series of wind conditions was obtained from the South Gare Met Station for April 1975 to December 1984. This wind data was used to select wind speeds from the southwest and north that correspond to return periods of 0.1, 1 and 5 years. A number of test model runs were carried out to determine the most suitable directions.

The selected test wind conditions are listed in Table 3.2.

Swell conditions

In addition to the six local wind conditions, two offshore wave conditions were selected from those used in the previous project reported in HR Wallingford (2006). A number of test model runs were carried out to determine the most suitable direction.

The selected test swell wave conditions are also listed in Table 3.2.

Test conditions

The full list of test conditions is reported in Table 3.2.

Table 3.2: Test conditions used in the wave modelling

Return period (years)	Wind speed (m/s)	Wind direction (°N)	Hs (m)	Tp (s)	Wave direction (°N)
0.1	0	0	3.9	9.0	15
1.0	0	0	6.0	12.2	15
0.1	16	215	0	0	0
1	22	215	0	0	0
5	30	215	0	0	0
0.1	16	350	0	0	0
1	22	350	0	0	0
5	30	350	0	0	0

Water levels

The SWAN model was run at two water levels – MHWS at 5.5 mCD and MLWS at 0.9 mCD.

3.3. Wave modelling results

The object of this exercise is to assess the impact on wave conditions in the Tees Estuary due to the presence of the proposed terminal. For this purpose, the SWAN model results are presented in two ways:

- 2-dimensional contour plots of significant wave height and direction;
- Tabulated results at reporting locations along the estuary, adjacent to the proposed terminal and both upstream and downstream. These points are shown on Figure 3.1, Figure 3.2 and Figure 3.3.

3.3.1. Solid Quay

The solid quay option involves a vertical sided solid quay, a berth pocket dredged to -16.1 mCD and channel adjacent to the berth dredged to -14.1 mCD. The predicted effects of these works on waves are shown in Figure 3.4 to Figure 3.11 for all wave conditions listed in Table 3.2 at MHWS. For each wave condition, three plots are shown: the predicted significant wave height and direction for the existing layout (left), the predicted significant wave height and direction for the solid quay option (centre) and the difference in significant wave height (right).

The wave modelling results are also tabulated (Tables 3.3 to 3.8) for all wave conditions at both MHWS and MLWS. The tables show the wave conditions at the analysis points for the existing layout, solid quay option

and open quay option. Significant wave height (Hs), Peak wave height (Tp) and wave direction are shown together with the difference in significant wave height between the proposed options and existing layout. Due to a large amount of data, the tables have been split according to wave condition and water level. Table 3.3 and Table 3.4 show the results for the swell wave conditions at MHWS and MLWS respectively. Table 3.5 and Table 3.6 show the results for winds from 215°N at MHWS and MLWS respectively. Table 3.7 and Table 3.8 show the results for winds from 350°N at MHWS and MLWS respectively.

The vertical face of the solid quay has higher reflection properties than the existing shoreline and less wave energy is absorbed. Hence it can be seen that wave energy is reflected off the quay and leads to localised areas of larger wave heights; for example Figure 3.8 for south-westerly wind generated waves and Figure 3.11 under northerly winds. The greatest increases under southwest winds occur at points P5 and P6 (Table 3.5) where Hs is predicted to increase by up to approximately 7%. For northerly winds, the largest increase is at point P4, also up to 7%.

3.3.2. Open Quay

The open quay option involves a suspended quay on open piles, a berth pocket dredged to -16.1 mCD and the channel adjacent to the berth dredged to -14.1 mCD. The dredged pocket necessitates a retreated shoreline protected by a 1:2 rock stabilised revetment.

The predicted effects of these works on waves are shown in Figure 3.12 to Figure 3.19 for all wave conditions listed in Table 3.2 at MHWS. For each wave condition, three plots are shown: the predicted significant wave height and direction for the existing layout (left), the predicted significant wave height and direction for the open quay option (centre) and the difference in significant wave height (right).

The wave modelling results are also tabulated (Tables 3.3 to 3.8) for all wave conditions at both MHWS and MLWS. The tables show the wave conditions at the points for the existing layout, solid quay options and open quay option. Significant wave height (Hs), Peak wave height (Tp) and wave direction are shown together with the difference in significant wave height between the proposed layouts and existing layout. Due to a large amount of data, the tables have been split according to wave direction and water level. Table 3.3 and Table 3.4 show the results for the swell wave conditions at MHWS and MLWS respectively. Table 3.5 and Table 3.6 show the results for winds from 215°N at MHWS and MLWS respectively. Table 3.7 and Table 3.8 show the results for winds from 350°N at MHWS and MLWS respectively.

The open piles fully transmit wave energy through to the shore protection behind the proposed quay. The shore protection has similar reflection characteristics to the existing shoreline and so there is no increase in wave energy in the estuary. The differences in the dredging do not change the overall pattern of wave conditions in the estuary. The only differences evident in the results are in Figure 3.19 where there is a strip of enhanced wave heights adjacent to the quay. This is due to deeper water due to dredging. In the existing layout, the water is shallow and depth-induced breaking reduces the wave heights. The deeper water allows higher wave heights.

In conclusion, there are predicted to be no significant effects on wave conditions in the Tees Estuary due to the open quay layout.

Table 3.3: Predicted wave conditions at reporting locations for swell waves from 15°N at MHWS.

Return period (years)	Point	Exiting Layout			Solid Quay layout				Open Quay layout			
		Hs (m)	Tp (s)	Dir (°N)	Hs (m)	Hs difference (m)	Tp (s)	Dir (°N)	Hs (m)	Hs difference (m)	Tp (s)	Dir (°N)
0.1	P1	0.04	9.0	54	0.05	0.01	8.9	50	0.04	0.00	9.0	56
0.1	P2	0.05	9.0	17	0.06	0.01	8.9	16	0.05	0.00	9.0	17
0.1	P3	0.09	8.9	357	0.10	0.01	8.9	357	0.09	0.00	8.9	356
0.1	P4	0.15	8.9	340	0.19	0.04	8.9	357	0.15	0.00	8.9	339
0.1	P5	0.19	8.9	319	0.21	0.02	8.9	329	0.19	0.00	8.9	318
0.1	P6	0.17	8.9	341	0.18	0.01	8.9	339	0.17	0.00	8.9	340
0.1	P7	0.27	8.9	321	0.27	0.00	8.9	319	0.27	0.00	8.9	320
0.1	P8	0.63	8.8	22	0.63	0.00	8.8	22	0.63	0.00	8.8	22
0.1	P9	0.68	8.8	24	0.68	0.00	8.9	24	0.68	0.00	8.8	24
1	P1	0.04	12.2	56	0.04	0.00	12.2	54	0.04	0.00	12.2	58
1	P2	0.05	12.2	19	0.06	0.01	12.2	17	0.05	0.00	12.2	18
1	P3	0.09	12.2	356	0.10	0.01	12.2	356	0.09	0.00	12.2	356
1	P4	0.14	12.2	345	0.16	0.02	12.2	356	0.13	-0.01	12.2	345
1	P5	0.16	12.1	325	0.19	0.03	12.1	340	0.16	0.00	12.1	323
1	P6	0.18	12.1	333	0.19	0.01	12.1	330	0.18	0.00	12.1	332
1	P7	0.25	12.2	305	0.26	0.01	12.2	301	0.25	0.00	12.2	304
1	P8	0.63	12.1	22	0.63	0.00	12.1	22	0.63	0.00	12.1	22
1	P9	0.69	12.1	25	0.69	0.00	12.1	25	0.69	0.00	12.1	25

Table 3.4: Predicted wave conditions at reporting locations for swell waves from 15°N at MLWS.

Return period (years)	Point	Exiting Layout			Solid Quay layout				Open Quay layout			
		Hs (m)	Tp (s)	Dir (°N)	Hs (m)	Hs difference (m)	Tp (s)	Dir (°N)	Hs (m)	Hs difference (m)	Tp (s)	Dir (°N)
0.1	P1	0.02	9.0	57	0.03	0.01	9.0	54	0.02	0.00	9.0	57
0.1	P2	0.03	8.8	27	0.03	0.00	8.8	25	0.03	0.00	8.8	26
0.1	P3	0.06	5.7	358	0.07	0.01	5.7	359	0.06	0.00	6.5	358
0.1	P4	0.09	8.9	350	0.11	0.02	8.9	1	0.09	0.00	8.9	350
0.1	P5	0.11	8.9	329	0.12	0.01	8.9	336	0.11	0.00	8.9	329
0.1	P6	0.11	8.9	355	0.11	0.00	8.9	353	0.11	0.00	8.9	354
0.1	P7	0.12	9.0	9	0.12	0.00	9.0	10	0.12	0.00	9.0	9
0.1	P8	0.37	8.9	25	0.37	0.00	8.9	25	0.37	0.00	8.9	25
0.1	P9	0.42	8.9	26	0.42	0.00	8.9	26	0.42	0.00	8.9	26
1	P1	0.02	12.2	56	0.02	0.00	12.2	55	0.02	0.00	12.2	56
1	P2	0.03	12.2	25	0.03	0.00	12.2	22	0.03	0.00	12.2	23
1	P3	0.06	12.2	357	0.06	0.00	12.2	359	0.06	0.00	12.2	358
1	P4	0.09	12.2	350	0.10	0.01	12.2	357	0.09	0.00	12.2	351
1	P5	0.10	12.2	334	0.11	0.01	12.2	343	0.10	0.00	12.2	334
1	P6	0.11	12.2	352	0.11	0.00	12.2	351	0.11	0.00	12.2	352
1	P7	0.12	12.2	4	0.12	0.00	12.2	5	0.12	0.00	12.2	4
1	P8	0.36	12.2	25	0.36	0.00	12.2	25	0.36	0.00	12.2	25
1	P9	0.41	12.2	25	0.41	0.00	12.2	25	0.41	0.00	12.2	25

Table 3.5: Predicted wave conditions at reporting locations for wind from 215°N at MHWS.

Return period (years)	Point	Exiting Layout			Solid Quay layout				Open Quay layout			
		Hs (m)	Tp (s)	Dir (°N)	Hs (m)	Hs difference (m)	Tp (s)	Dir (°N)	Hs (m)	Hs difference (m)	Tp (s)	Dir (°N)
0.1	P1	0.58	2.6	223	0.58	0.00	2.7	223	0.58	0.00	2.6	223
0.1	P2	0.59	2.7	221	0.59	0.00	2.7	221	0.59	0.00	2.7	221
0.1	P3	0.63	2.7	208	0.63	0.00	2.8	208	0.63	0.00	2.7	208
0.1	P4	0.61	2.8	201	0.61	0.00	2.8	201	0.61	0.00	2.8	201
0.1	P5	0.62	2.8	195	0.66	0.04	2.9	187	0.61	-0.01	2.8	195
0.1	P6	0.62	2.8	188	0.66	0.04	2.9	183	0.62	0.00	2.8	189
0.1	P7	0.64	2.9	187	0.67	0.03	2.9	186	0.64	0.00	2.9	186
0.1	P8	0.59	2.8	193	0.61	0.02	2.9	192	0.59	0.00	2.7	193
0.1	P9	0.64	2.8	198	0.65	0.01	2.9	197	0.64	0.00	2.8	198
1	P1	0.93	3.2	223	0.93	0.00	3.2	223	0.93	0.00	3.2	223
1	P2	0.95	3.2	220	0.95	0.00	3.2	221	0.95	0.00	3.2	221
1	P3	1.00	3.3	207	1.01	0.01	3.3	207	1.00	0.00	3.3	207
1	P4	0.96	3.3	200	0.97	0.01	3.3	200	0.96	0.00	3.3	200
1	P5	0.98	3.3	195	1.05	0.07	3.4	187	0.97	-0.01	3.3	195
1	P6	0.99	3.4	189	1.06	0.07	3.5	184	0.99	0.00	3.4	189
1	P7	1.03	3.4	188	1.08	0.05	3.5	186	1.02	-0.01	3.4	187
1	P8	0.95	3.3	194	0.99	0.04	3.5	193	0.95	0.00	3.3	193
1	P9	1.02	3.4	198	1.04	0.02	3.5	196	1.02	0.00	3.4	197
5	P1	1.44	3.8	223	1.44	0.00	3.8	223	1.44	0.00	3.8	223
5	P2	1.48	3.8	220	1.48	0.00	3.8	220	1.48	0.00	3.8	220
5	P3	1.55	3.9	206	1.55	0.00	3.9	206	1.55	0.00	3.9	206

Return	Point	Exiting Layout			Solid Quay layout				Open Quay layout			
5	P4	1.48	3.9	200	1.49	0.01	3.9	200	1.48	0.00	3.9	200
5	P5	1.52	3.9	196	1.63	0.11	4.0	187	1.51	-0.01	3.9	196
5	P6	1.55	4.0	190	1.66	0.11	4.2	185	1.54	-0.01	4.0	190
5	P7	1.61	4.1	190	1.70	0.09	4.2	188	1.60	-0.01	4.1	189
5	P8	1.51	3.9	196	1.56	0.05	4.2	194	1.51	0.00	3.9	195
5	P9	1.58	4.0	198	1.62	0.04	4.1	196	1.59	0.01	4.0	197

Table 3.6: Predicted wave conditions at reporting locations for wind from 215°N at MLWS.

Return period (years)	Point	Exiting Layout			Solid Quay layout				Open Quay layout			
		Hs (m)	Tp (s)	Dir (°N)	Hs (m)	Hs difference (m)	Tp (s)	Dir (°N)	Hs (m)	Hs difference (m)	Tp (s)	Dir (°N)
0.1	P1	0.56	2.6	223	0.56	0.00	2.6	223	0.56	0.00	2.6	223
0.1	P2	0.58	2.6	220	0.58	0.00	2.6	220	0.57	-0.01	2.6	220
0.1	P3	0.60	2.7	206	0.60	0.00	2.7	206	0.60	0.00	2.7	206
0.1	P4	0.57	2.7	198	0.57	0.00	2.7	198	0.57	0.00	2.7	198
0.1	P5	0.56	2.6	192	0.61	0.05	2.7	184	0.56	0.00	2.6	193
0.1	P6	0.57	2.7	187	0.61	0.04	2.8	182	0.57	0.00	2.7	187
0.1	P7	0.60	2.7	187	0.63	0.03	2.8	185	0.60	0.00	2.7	186
0.1	P8	0.56	2.6	193	0.58	0.02	2.8	191	0.57	0.01	2.6	192
0.1	P9	0.59	2.7	194	0.60	0.01	2.8	192	0.59	0.00	2.7	192
1	P1	0.89	3.1	223	0.89	0.00	3.1	223	0.89	0.00	3.1	223
1	P2	0.91	3.2	219	0.91	0.00	3.2	220	0.91	0.00	3.2	220
1	P3	0.94	3.2	205	0.94	0.00	3.2	205	0.94	0.00	3.2	205
1	P4	0.91	3.2	198	0.91	0.00	3.2	198	0.91	0.00	3.2	198
1	P5	0.90	3.2	193	0.97	0.07	3.3	185	0.90	0.00	3.2	193
1	P6	0.91	3.2	187	0.98	0.07	3.3	183	0.91	0.00	3.2	188
1	P7	0.95	3.2	190	1.02	0.07	3.4	186	0.96	0.01	3.3	188
1	P8	0.90	3.1	194	0.94	0.04	3.3	191	0.91	0.01	3.1	193
1	P9	0.94	3.2	193	0.96	0.02	3.3	191	0.94	0.00	3.3	193
5	P1	1.36	3.6	222	1.37	0.01	3.6	222	1.37	0.01	3.6	222
5	P2	1.40	3.6	219	1.40	0.00	3.6	219	1.40	0.00	3.6	219
5	P3	1.44	3.8	205	1.44	0.00	3.8	205	1.44	0.00	3.8	205

Return	Point	Exiting Layout			Solid Quay layout				Open Quay layout			
5	P4	1.38	3.8	197	1.39	0.01	3.8	197	1.38	0.00	3.8	197
5	P5	1.39	3.8	194	1.49	0.10	3.9	186	1.39	0.00	3.8	194
5	P6	1.43	3.8	189	1.53	0.10	3.9	184	1.42	-0.01	3.8	189
5	P7	1.50	3.8	193	1.60	0.10	4.0	188	1.53	0.03	3.8	190
5	P8	1.39	3.7	196	1.45	0.06	3.9	192	1.41	0.02	3.8	193
5	P9	1.45	3.8	194	1.49	0.04	3.9	192	1.46	0.01	3.8	193

Table 3.7: Predicted wave conditions at reporting locations for wind from 350°N at MHWS.

Return period (years)	Point	Exiting Layout			Solid Quay layout				Open Quay layout			
		Hs (m)	Tp (s)	Dir (°N)	Hs (m)	Hs difference (m)	Tp (s)	Dir (°N)	Hs (m)	Hs difference (m)	Tp (s)	Dir (°N)
0.1	P1	0.58	2.8	20	0.60	0.02	2.9	21	0.58	0.00	2.8	20
0.1	P2	0.63	2.9	11	0.64	0.01	2.9	12	0.63	0.00	2.9	11
0.1	P3	0.69	3.0	356	0.70	0.01	3.1	358	0.68	-0.01	3.0	356
0.1	P4	0.72	3.0	346	0.77	0.05	3.1	353	0.71	-0.01	3.0	345
0.1	P5	0.74	3.0	336	0.77	0.03	3.1	343	0.74	0.00	3.0	335
0.1	P6	0.66	2.9	355	0.67	0.01	2.9	355	0.66	0.00	2.9	355
0.1	P7	0.66	3.0	356	0.66	0.00	3.0	356	0.66	0.00	3.0	356
0.1	P8	0.71	3.1	9	0.71	0.00	3.1	10	0.71	0.00	3.1	9
0.1	P9	0.70	3.1	10	0.70	0.00	3.1	10	0.70	0.00	3.1	10
1	P1	0.92	3.3	19	0.95	0.03	3.5	20	0.92	0.00	3.3	19
1	P2	0.99	3.4	12	1.01	0.02	3.5	12	0.98	-0.01	3.4	11
1	P3	1.07	3.5	357	1.09	0.02	3.6	358	1.07	0.00	3.5	356
1	P4	1.12	3.6	347	1.20	0.08	3.7	354	1.11	-0.01	3.6	346
1	P5	1.14	3.5	336	1.19	0.05	3.6	343	1.14	0.00	3.5	336
1	P6	1.03	3.3	354	1.05	0.02	3.4	355	1.03	0.00	3.3	354
1	P7	1.00	3.4	354	1.01	0.01	3.5	354	1.00	0.00	3.4	354
1	P8	1.10	3.7	9	1.10	0.00	3.7	10	1.10	0.00	3.7	9
1	P9	1.08	3.6	11	1.08	0.00	3.6	11	1.08	0.00	3.6	11
5	P1	1.48	4.0	19	1.51	0.03	4.1	19	1.47	-0.01	3.9	19
5	P2	1.55	4.0	12	1.59	0.04	4.2	12	1.54	-0.01	4.0	12
5	P3	1.66	4.2	357	1.69	0.03	4.3	358	1.66	0.00	4.2	357

Return	Point	Exiting Layout			Solid Quay layout				Open Quay layout			
5	P4	1.76	4.2	348	1.89	0.13	4.3	355	1.75	-0.01	4.2	346
5	P5	1.77	4.2	338	1.85	0.08	4.2	345	1.77	0.00	4.2	338
5	P6	1.62	3.9	353	1.65	0.03	4.0	354	1.62	0.00	3.9	353
5	P7	1.54	3.9	353	1.55	0.01	4.0	353	1.54	0.00	3.9	353
5	P8	1.68	4.3	9	1.69	0.01	4.3	10	1.68	0.00	4.3	9
5	P9	1.64	4.3	12	1.64	0.00	4.3	12	1.64	0.00	4.3	12

Table 3.8: Predicted wave conditions at reporting locations for wind from 350°N at MLWS.

Return period (years)	Point	Exiting Layout			Solid Quay layout				Open Quay layout			
		Hs (m)	Tp (s)	Dir (°N)	Hs (m)	Hs difference (m)	Tp (s)	Dir (°N)	Hs (m)	Hs difference (m)	Tp (s)	Dir (°N)
0.1	P1	0.55	2.7	19	0.57	0.02	2.8	21	0.54	-0.01	2.6	19
0.1	P2	0.55	2.7	15	0.57	0.02	2.9	16	0.55	0.00	2.7	15
0.1	P3	0.63	2.9	358	0.64	0.01	2.9	1	0.63	0.00	2.9	357
0.1	P4	0.66	2.9	348	0.71	0.05	2.9	354	0.66	0.00	2.9	347
0.1	P5	0.66	2.8	338	0.69	0.03	2.9	344	0.66	0.00	2.8	338
0.1	P6	0.59	2.6	354	0.60	0.01	2.6	354	0.59	0.00	2.6	354
0.1	P7	0.55	2.6	359	0.56	0.01	2.6	359	0.55	0.00	2.6	359
0.1	P8	0.59	2.9	17	0.59	0.00	2.9	17	0.59	0.00	2.9	17
0.1	P9	0.58	2.9	18	0.58	0.00	2.9	18	0.58	0.00	2.9	18
1	P1	0.87	3.2	19	0.91	0.04	3.4	20	0.88	0.01	3.2	19
1	P2	0.89	3.3	15	0.93	0.04	3.5	15	0.89	0.00	3.3	15
1	P3	0.99	3.4	358	1.01	0.02	3.5	1	0.99	0.00	3.4	358
1	P4	1.06	3.4	348	1.13	0.07	3.5	355	1.05	-0.01	3.4	347
1	P5	1.05	3.4	339	1.09	0.04	3.4	345	1.05	0.00	3.4	339
1	P6	0.95	3.2	354	0.96	0.01	3.2	354	0.95	0.00	3.2	354
1	P7	0.88	3.1	358	0.88	0.00	3.1	358	0.88	0.00	3.1	358
1	P8	0.94	3.5	16	0.94	0.00	3.5	17	0.94	0.00	3.5	16
1	P9	0.92	3.4	18	0.93	0.01	3.4	18	0.92	0.00	3.4	18
5	P1	1.39	3.7	18	1.44	0.05	4.0	19	1.39	0.00	3.8	18
5	P2	1.39	3.8	15	1.48	0.09	4.1	15	1.41	0.02	3.9	15
5	P3	1.52	4.0	359	1.57	0.05	4.2	2	1.54	0.02	4.0	359

Return	Point	Exiting Layout			Solid Quay layout				Open Quay layout			
5	P4	1.67	4.1	349	1.77	0.10	4.2	355	1.66	-0.01	4.1	348
5	P5	1.66	4.1	341	1.73	0.07	4.1	347	1.67	0.01	4.1	341
5	P6	1.53	3.8	354	1.53	0.00	3.8	353	1.53	0.00	3.8	353
5	P7	1.41	3.7	358	1.41	0.00	3.7	358	1.41	0.00	3.7	358
5	P8	1.48	4.1	16	1.48	0.00	4.1	16	1.48	0.00	4.1	16
5	P9	1.45	4.0	18	1.45	0.00	4.0	18	1.45	0.00	4.0	18

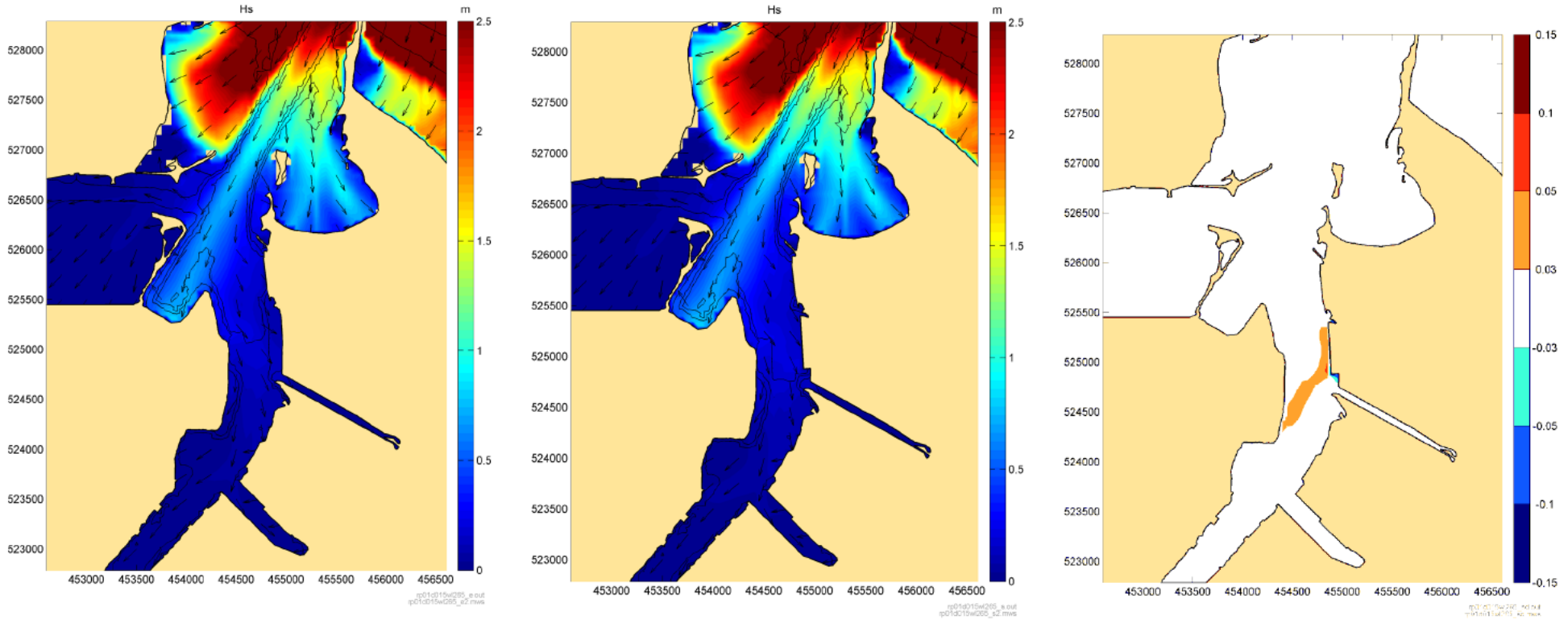

Figure 3.4: Significant wave height for 0.1 year swell wave from 15°N at MHWS. Left: existing layout; Centre: Solid Quay layout; Right: Solid Quay Hs – Existing Hs

Source: rp01d015wl265

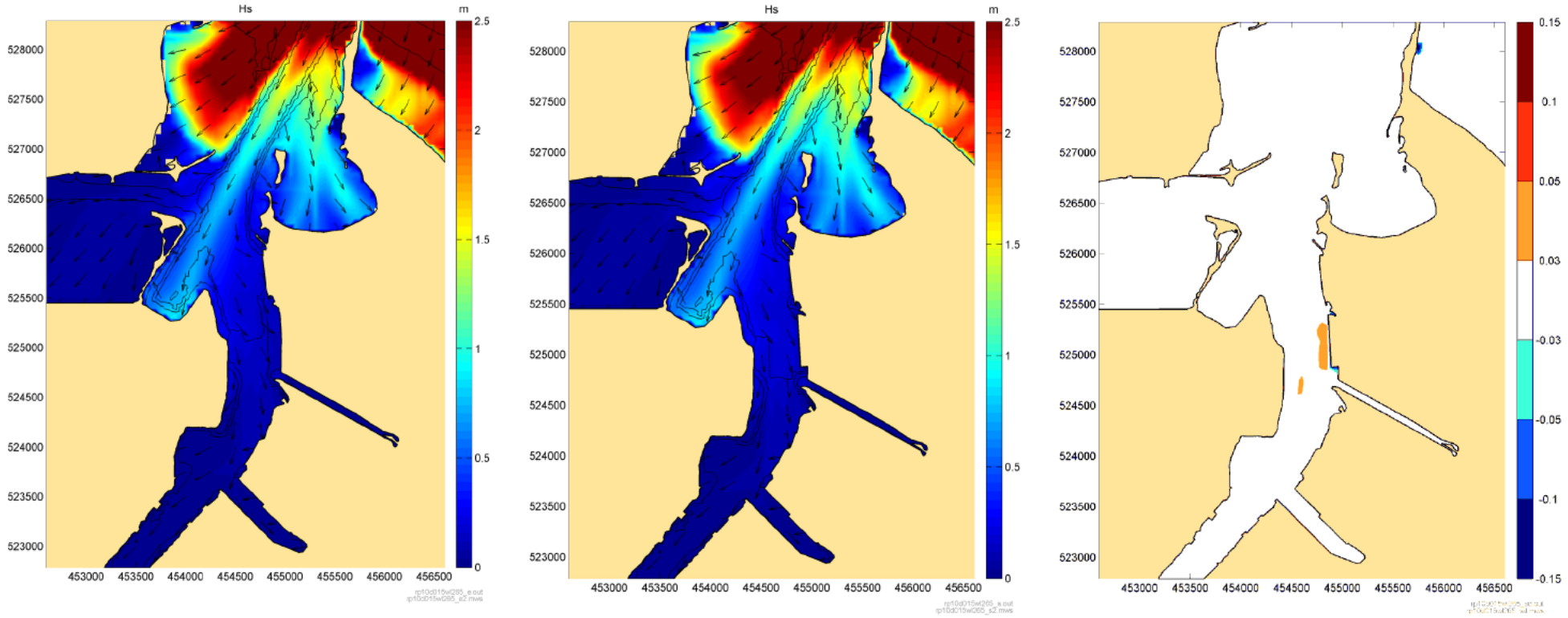

Figure 3.5: Significant wave height for 1 year swell wave from 15°N at MHWS. Left: existing layout; Centre: Solid Quay layout; Right: Solid Quay Hs – Existing Hs

Source: rp10d015wl265

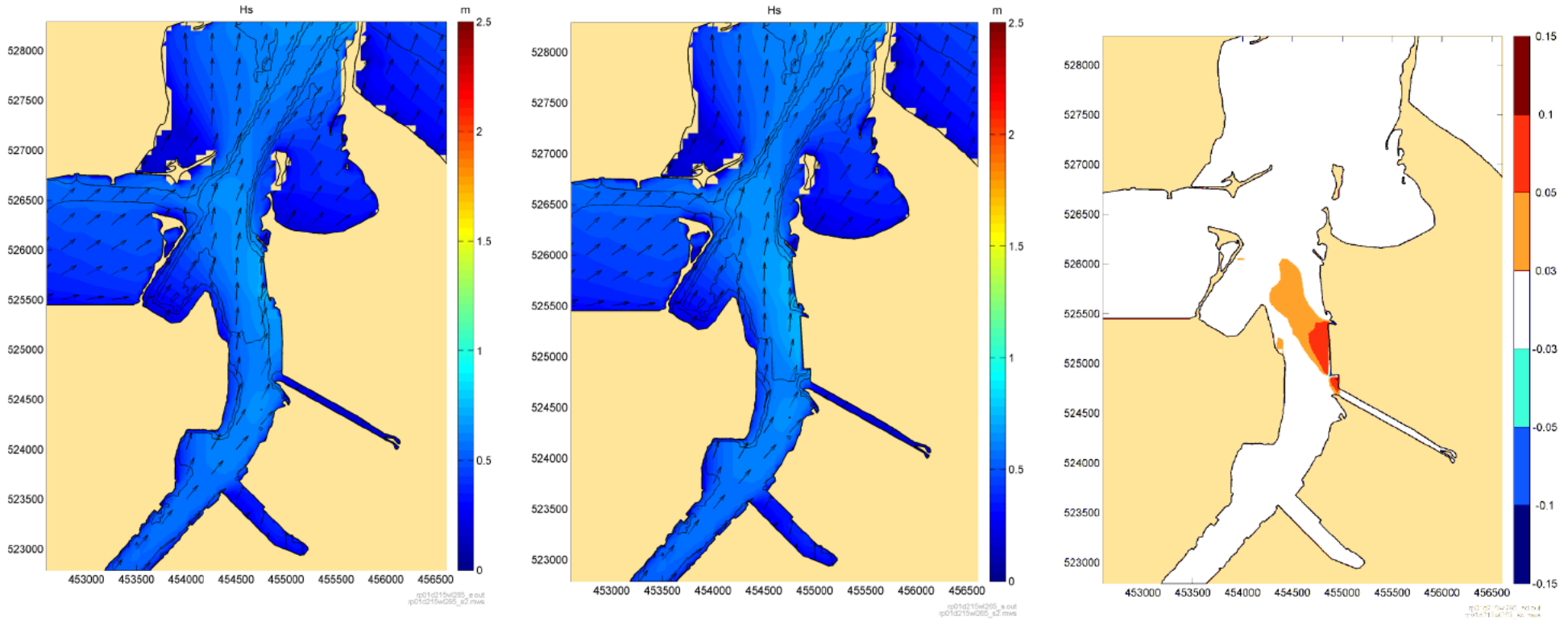

Figure 3.6: Significant wave height for 0.1 year wind from 215°N at MHWS. Left: existing layout; Centre: Solid Quay layout; Right: Solid Quay Hs – Existing Hs

Source: rp01d215wl265

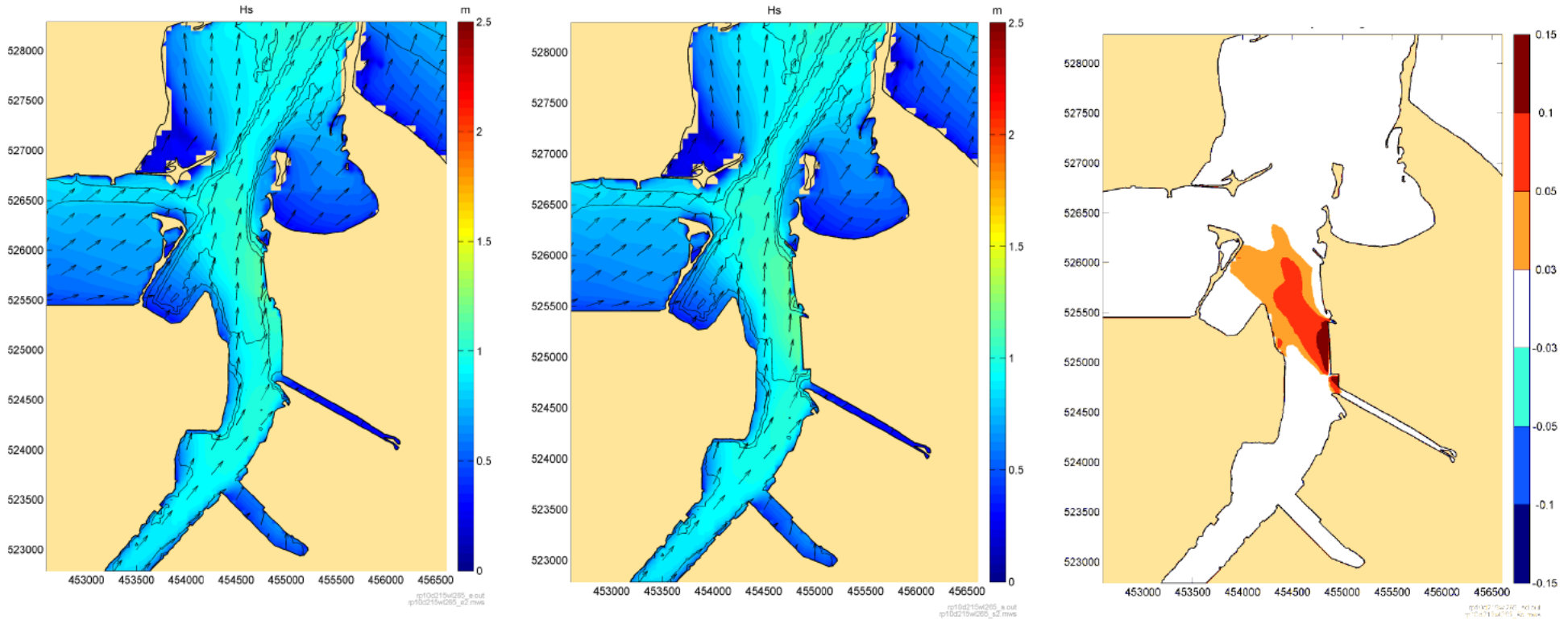

Figure 3.7: Significant wave height for 1 year wind from 215°N at MHWS. Left: existing layout; Centre: Solid Quay layout; Right: Solid Quay Hs – Existing Hs

Source: rp10d215wl265

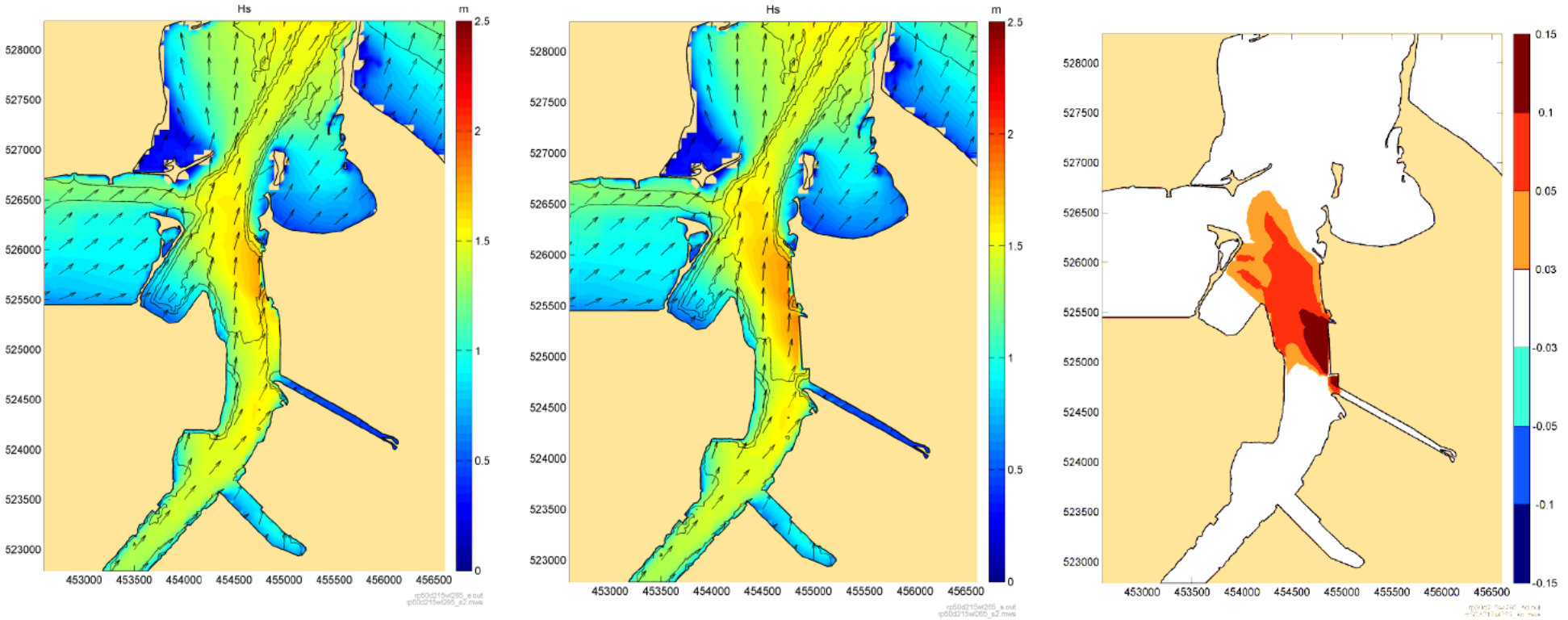

Figure 3.8: Significant wave height for 5 year wind from 215°N at MHWS. Left: existing layout; Centre: Solid Quay layout; Right: Solid Quay Hs – Existing Hs

Source: rp50d215wl265

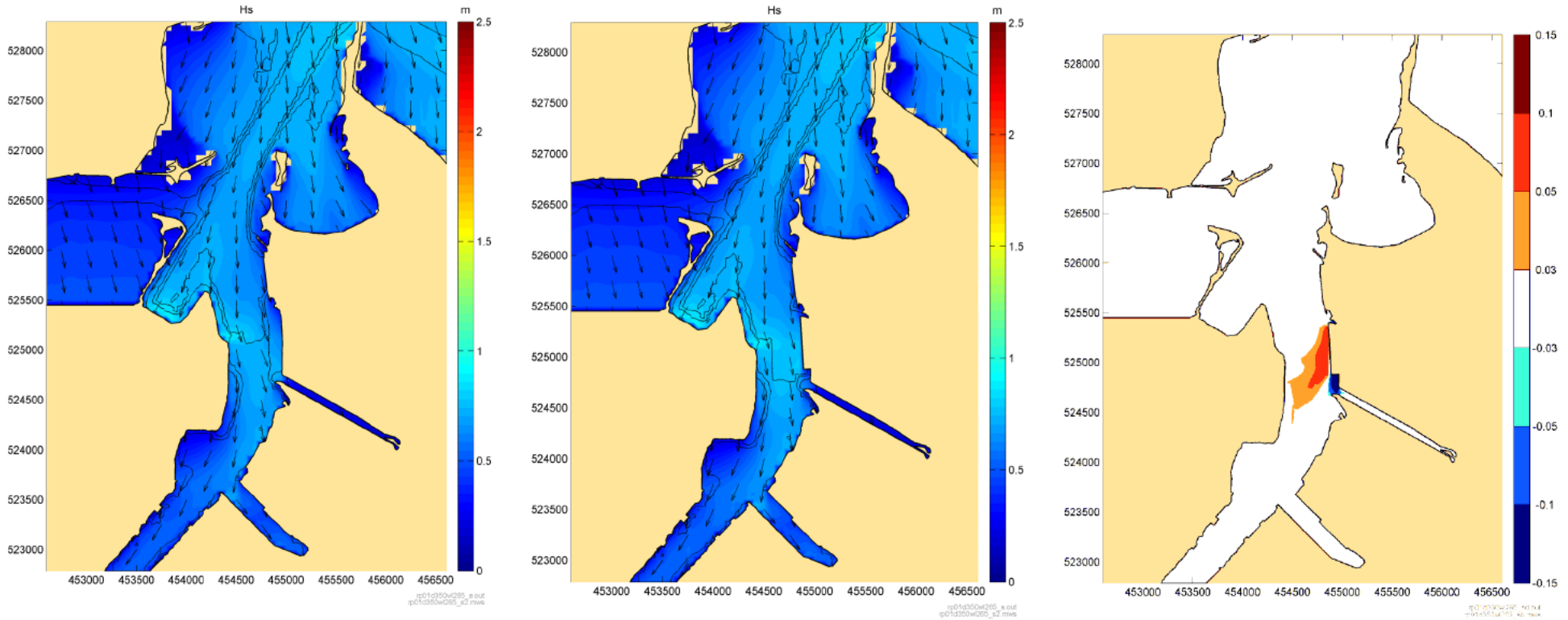

Figure 3.9: Significant wave height for 0.1 year wind from 350°N at MHWS. Left: existing layout; Centre: Solid Quay layout; Right: Solid Quay Hs – Existing Hs

Source: rp01d350wl265

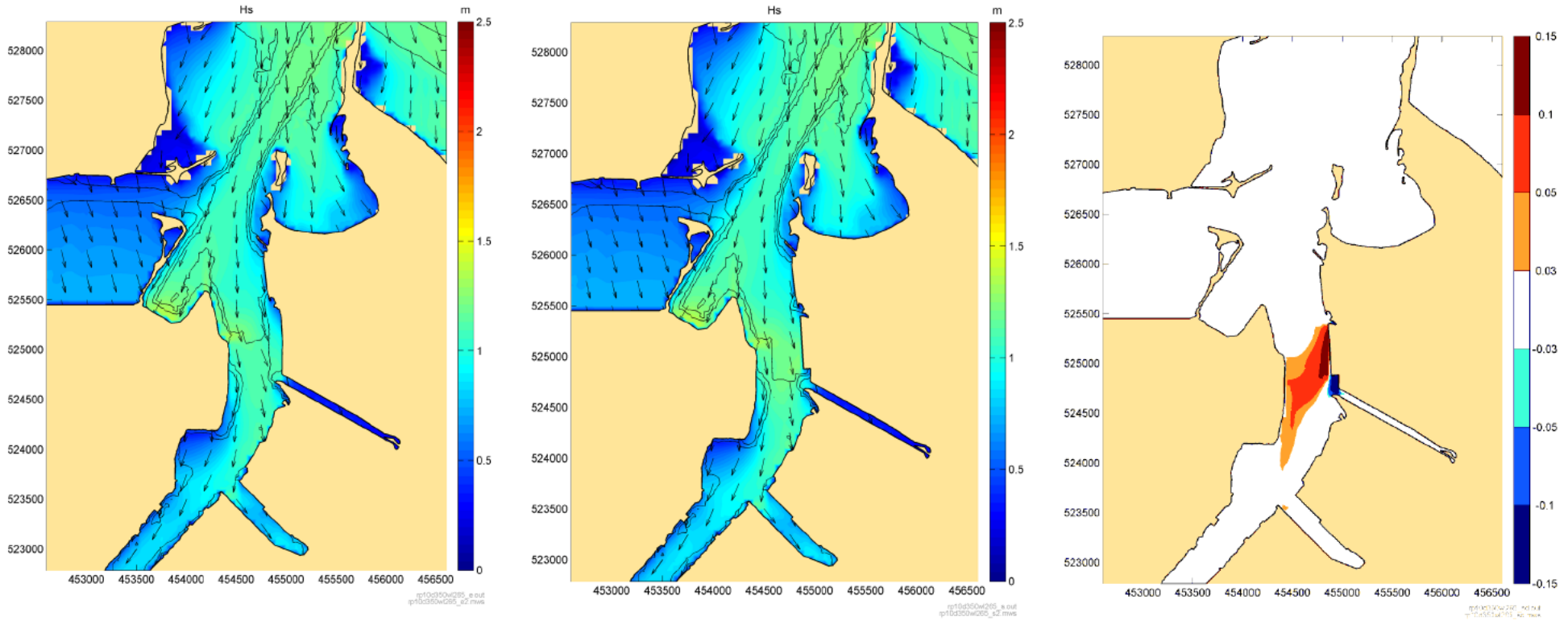

Figure 3.10: Significant wave height for 1 year wind from 350°N at MHWS. Left: existing layout; Centre: Solid Quay layout; Right: Solid Quay Hs – Existing Hs

Source: rp10d350wl265

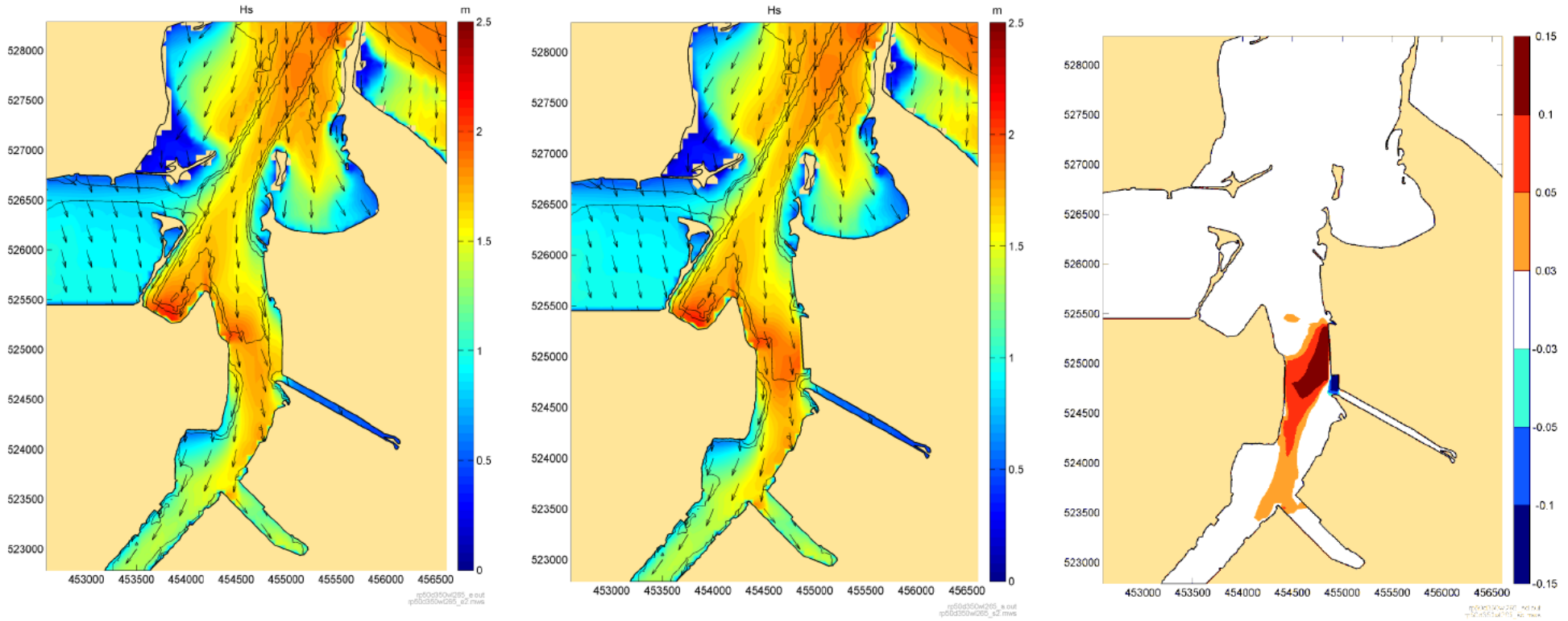

Figure 3.11: Significant wave height for 5 year wind from 350°N at MHWS. Left: existing layout; Centre: Solid Quay layout; Right: Solid Quay Hs – Existing Hs

Source: rp50d350wl265

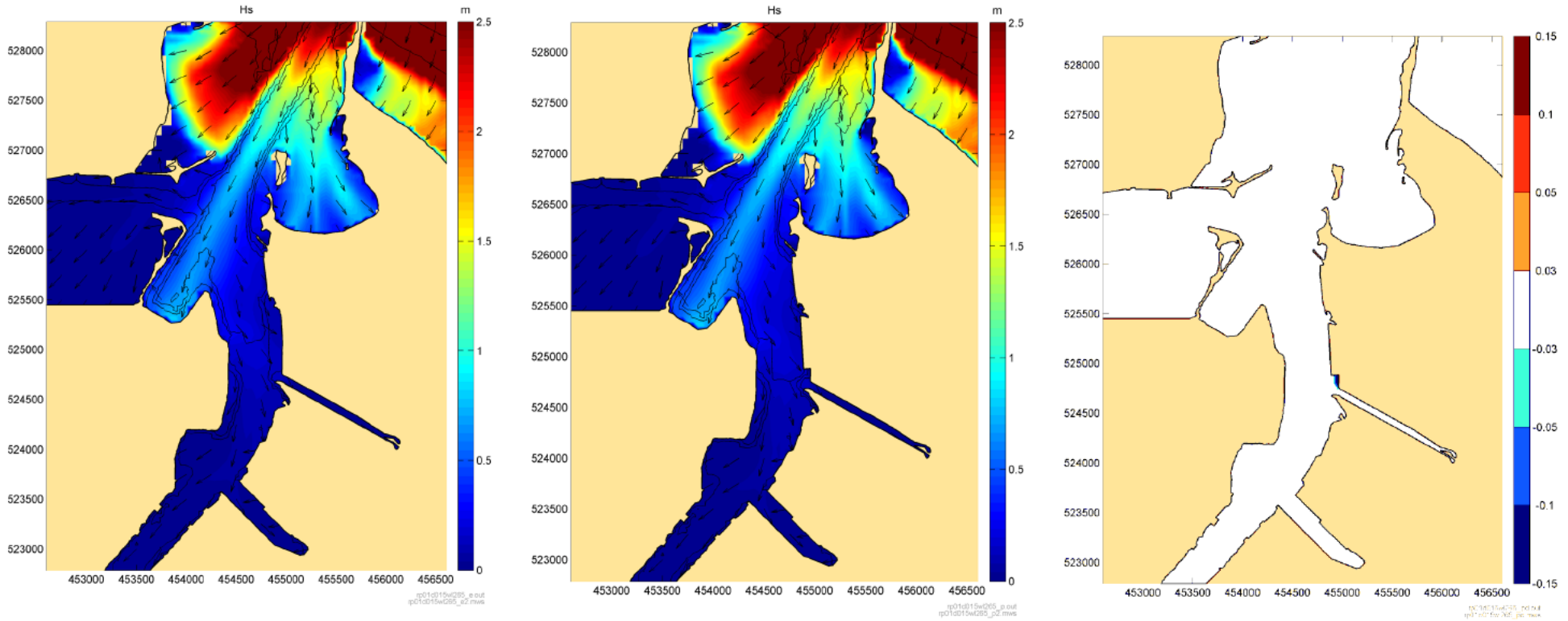

Figure 3.12: Significant wave height for 0.1 year swell wave from 15°N at MHWS. Left: existing layout; Centre: Open Quay layout; Right: Open Quay Hs – Existing Hs

Source: rp01d015wl265_p

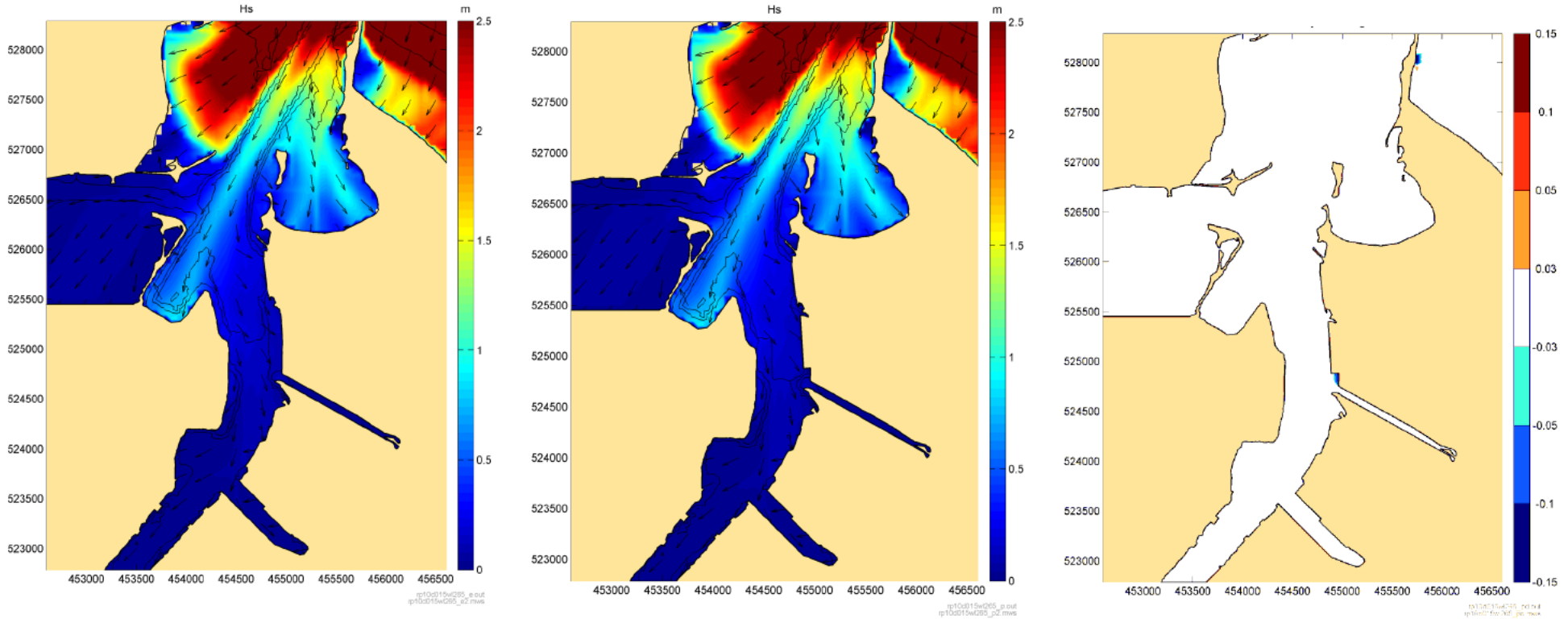

Figure 3.13: Significant wave height for 1 year swell wave from 15°N at MHWS. Left: existing layout; Centre: Open Quay layout; Right: Open Quay Hs – Existing Hs

Source: rp10d015wl265_p

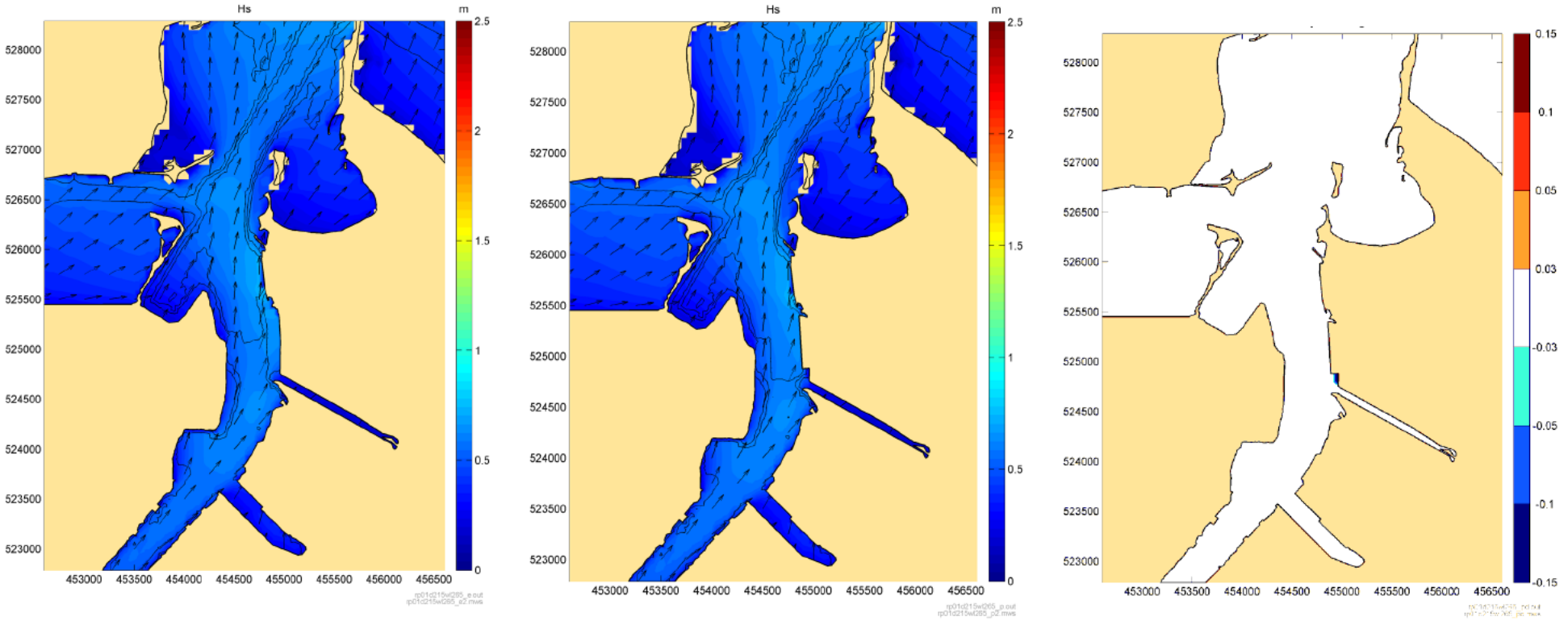

Figure 3.14: Significant wave height for 0.1 year wind from 215°N at MHWS. Left: existing layout; Centre: Open Quay layout; Right: Open Quay Hs – Existing Hs

Source: rp01d215wl265_p

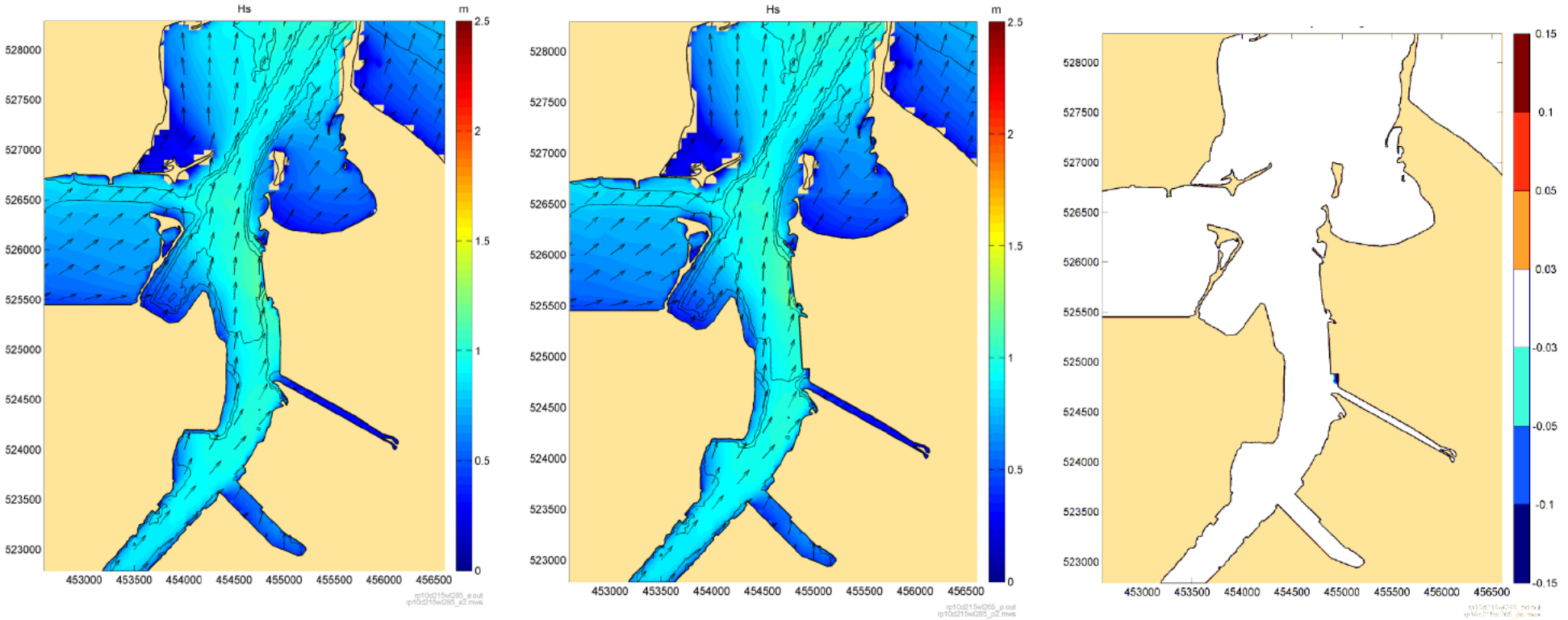

Figure 3.15: Significant wave height for 1 year wind from 215°N at MHWS. Left: existing layout; Centre: Open Quay layout; Right: Open Quay Hs – Existing Hs

Source: rp10d215wl265_p

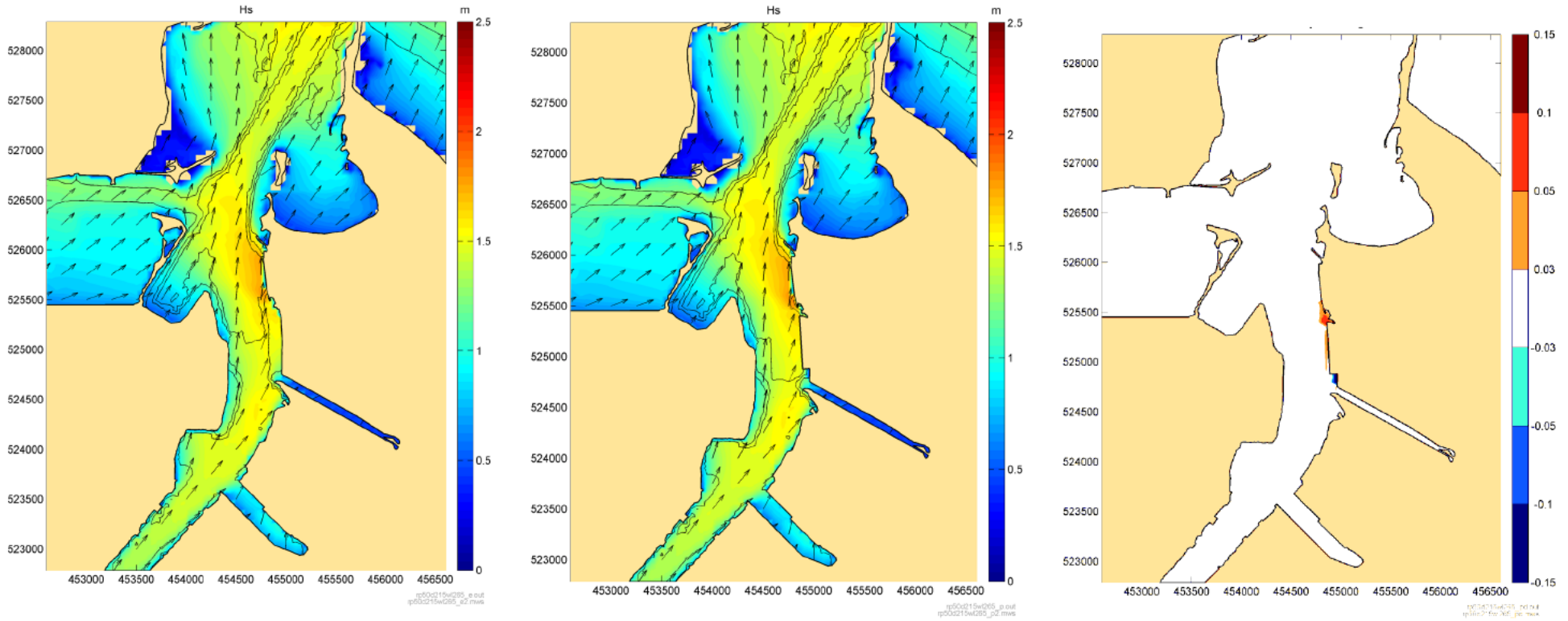

Figure 3.16: Significant wave height for 5 year wind from 215°N at MHWS. Left: existing layout; Centre: Open Quay layout; Right: Open Quay Hs – Existing Hs

Source: rp50d215wl265_p

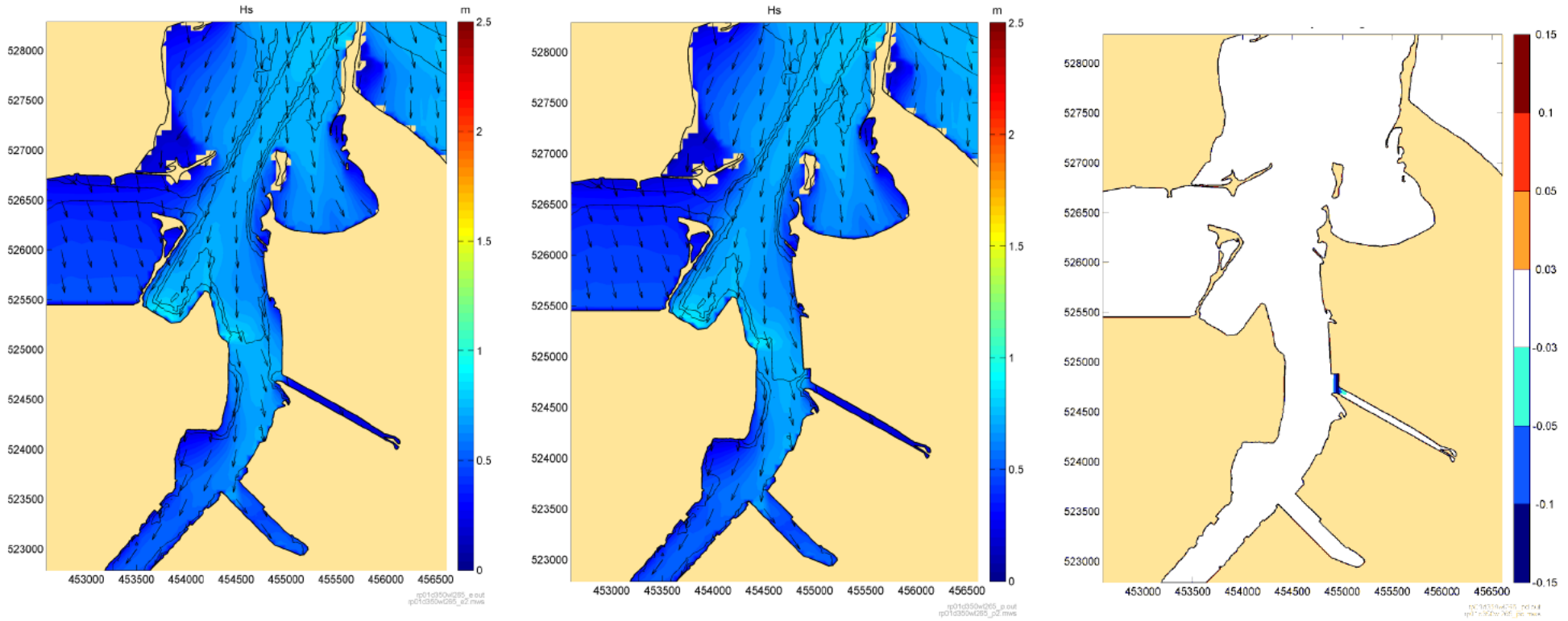

Figure 3.17: Significant wave height for 0.1 year wind from 350°N at MHWS. Left: existing layout; Centre: Open Quay layout; Right: Open Quay Hs – Existing Hs

Source: rp01d350wl265_p

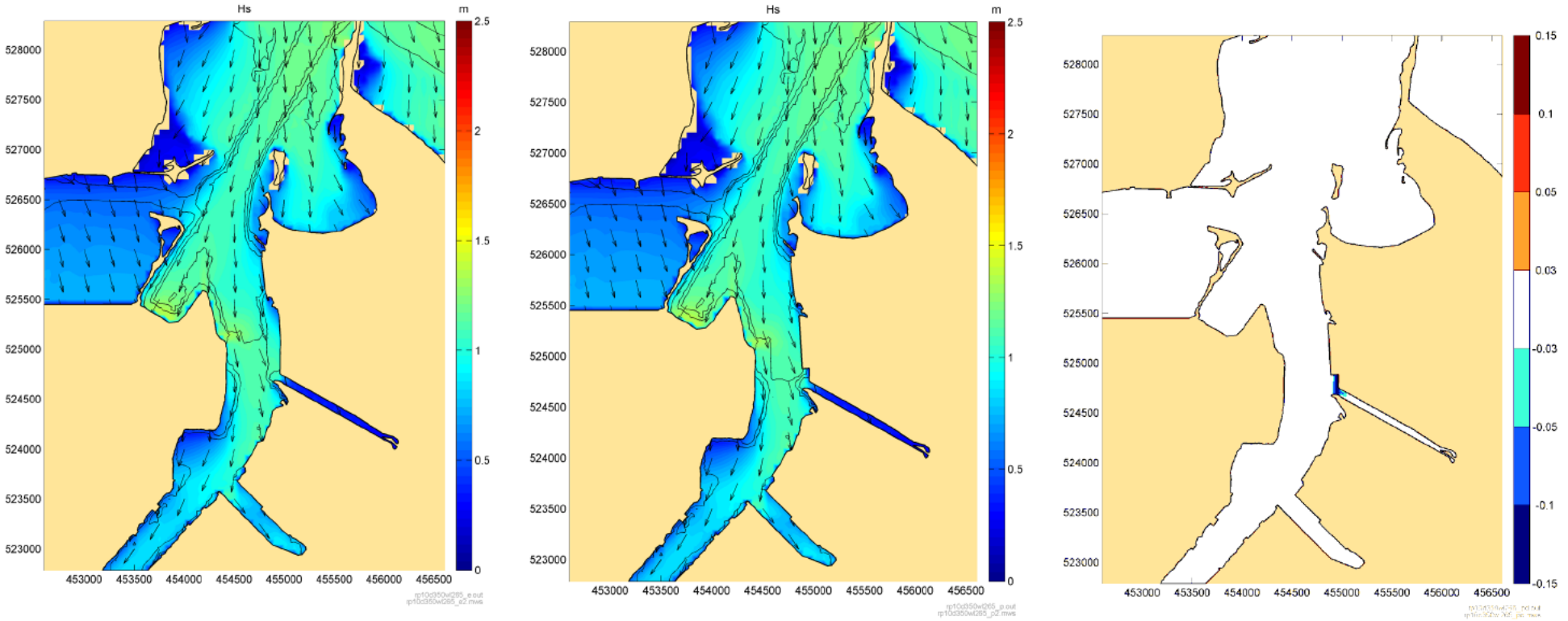

Figure 3.18: Significant wave height for 1 year wind from 350°N at MHWS. Left: existing layout; Centre: Open Quay layout; Right: Open Quay Hs – Existing Hs

Source: rp10d350wl265_p

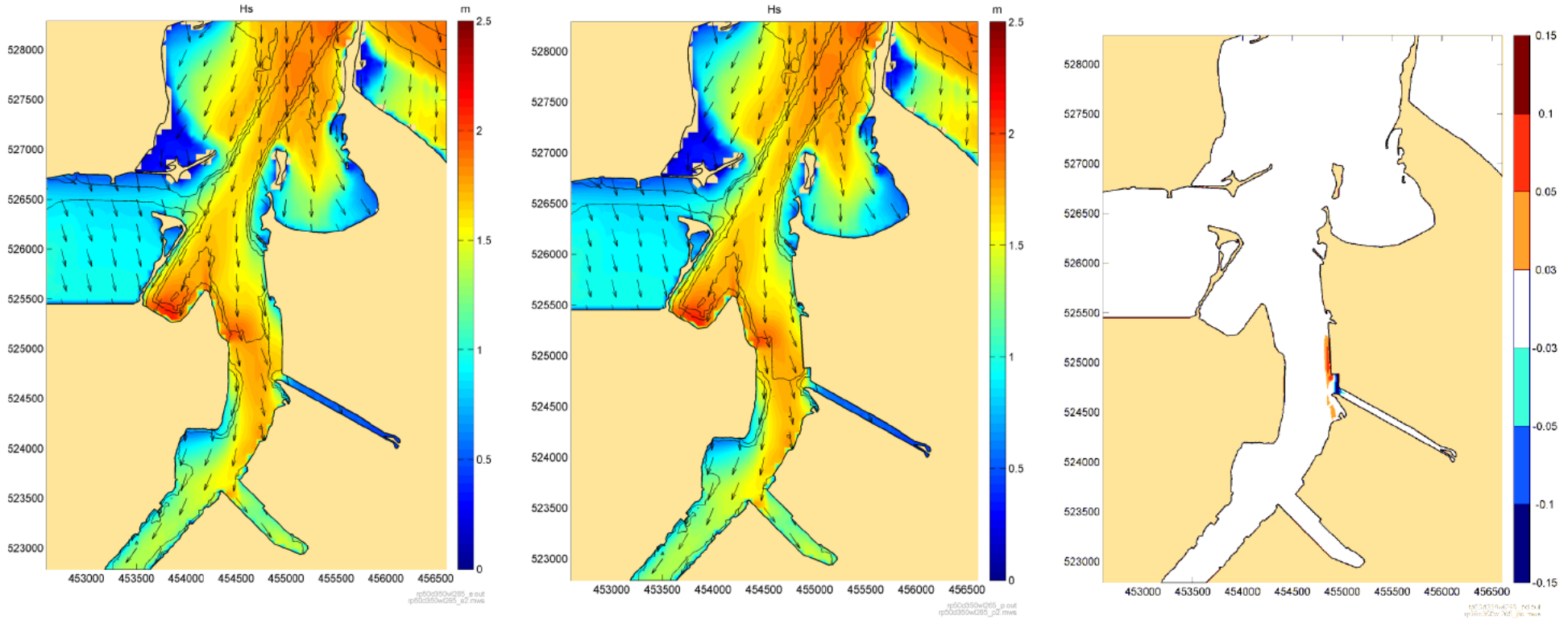

Figure 3.19: Significant wave height for 5 year wind from 350°N at MHWS. Left: existing layout; Centre: Open Quay layout; Right: Open Quay Hs – Existing Hs

Source: rp50d350wl265_p

4. Flow modelling of operational impacts

The scheme has the potential to influence the hydrodynamic regime of the estuary due to the dredging and, to a lesser extent, due to the construction of the solid (reclaimed) quay or open structure.

4.1. Background

To demonstrate the effects of the development on the hydrodynamics of the Tees Estuary a model based approach was used. In this case an existing TELEMAC-3D flow model set up to simulate currents in the Tees Estuary and Tees Bay for the Northern Gateway Container Terminal EIA studies (HR Wallingford, 2006) was available. TELEMAC-3D is a state-of-the-art finite element flow model, originally developed by EDF-LNHE Paris, which uses a completely unstructured grid enabling the accurate simulation of water movement in complex shaped areas. The unstructured mesh also allows an existing model to be locally refined to provide detailed current modelling in a new area of interest. TELEMAC-3D also includes vertical layers, enabling three-dimensional flow structures in the river to be accurately represented. Distribution of salinity, its evolution and its effect on modifying water flow can also be modelled.

During its establishment prior to the NGCT EIA studies the model's simulation of the tidal currents was compared to low river flow conditions measured by Acoustic Doppler Current Profiler (ADCP) undertaken on 15th and 16th June (HR Wallingford, 1995) and high river flow conditions measured between 22nd and 30th April 2005. A full description of the model's establishment is presented in HR Wallingford (2006).

4.2. Flow modelling method

The model's upstream limit is at the Tees Barrage, and extends to 6.5 km offshore in Tees Bay, covering an area of approximately 80 km^2. The mesh resolution varied from 800 m at the seaward model boundary, to 20 m over most of the estuary, and 10 m in the immediate area of the proposed works. Figure 4.1 shows the model mesh for the whole domain included in the modelling and with some detail at the study site.

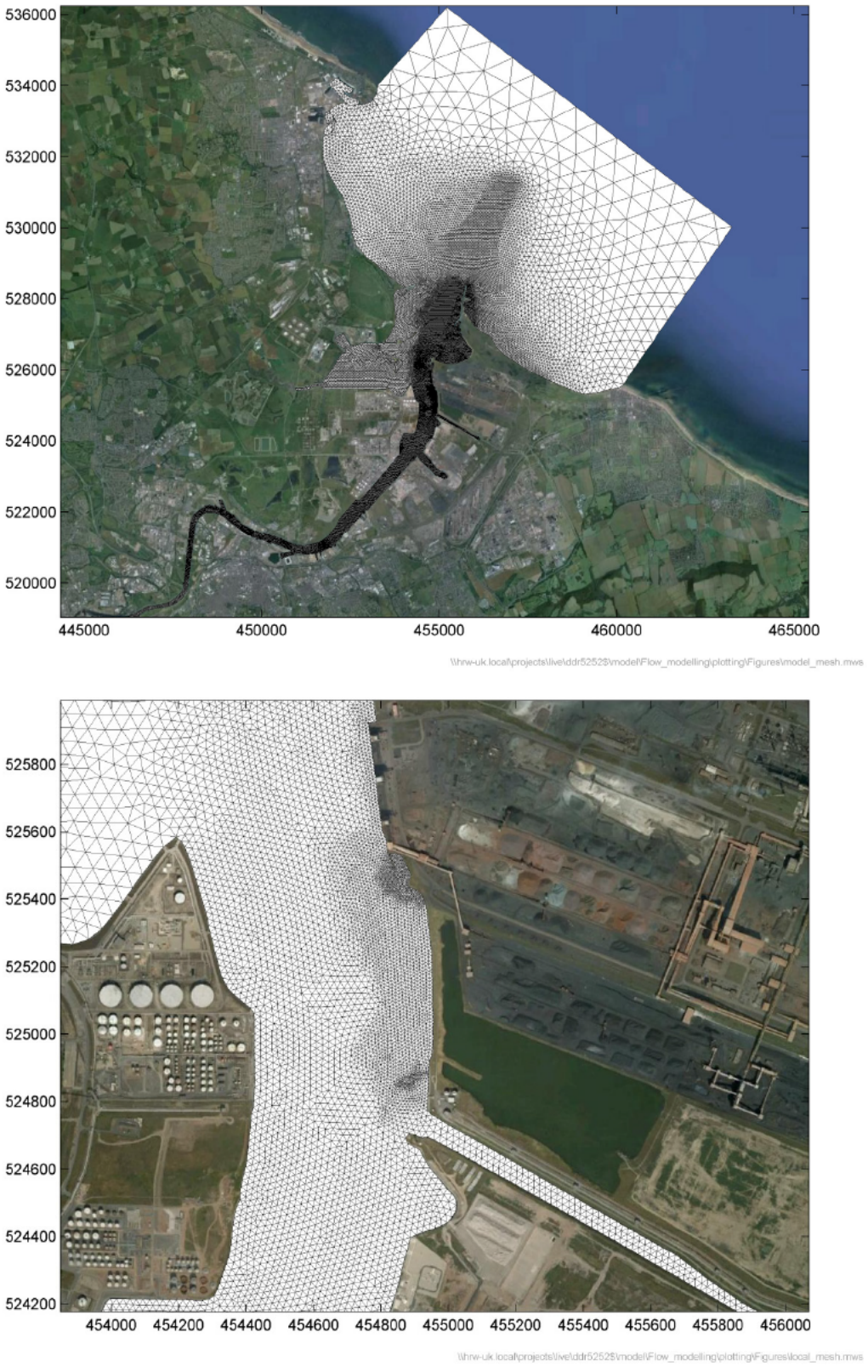

Figure 4.1: Model mesh used for the flow modelling study

The model was run to simulate baseline (pre works) and post works conditions for four tide/river flow conditions which encompassed a range of conditions which occur at the site – high river flows with spring and neap tides and low river flows with spring and neap tides. The high river flow cases had 60 m^3/s imposed at the Tees Barrage – the landward limit of the model. For the low flow case zero river flow was included in the model.

The post works model results were compared to the baseline case to enable the footprint and magnitude of any changes to the hydrodynamics to be presented.

4.3. Flow modelling results

4.3.1. Solid quay

Figure 4.2 shows the model representation of the solid quay option. The extension of the dredged channel landward at -14.1 mCD is shown as are the dredged approaches to the proposed quay and the deep berth pocket along the length of the quay. The change in bed level associated with the proposed dredging is shown in Figure 4.3. Increases in bed depth of more than 10 m are shown along the proposed quay line.

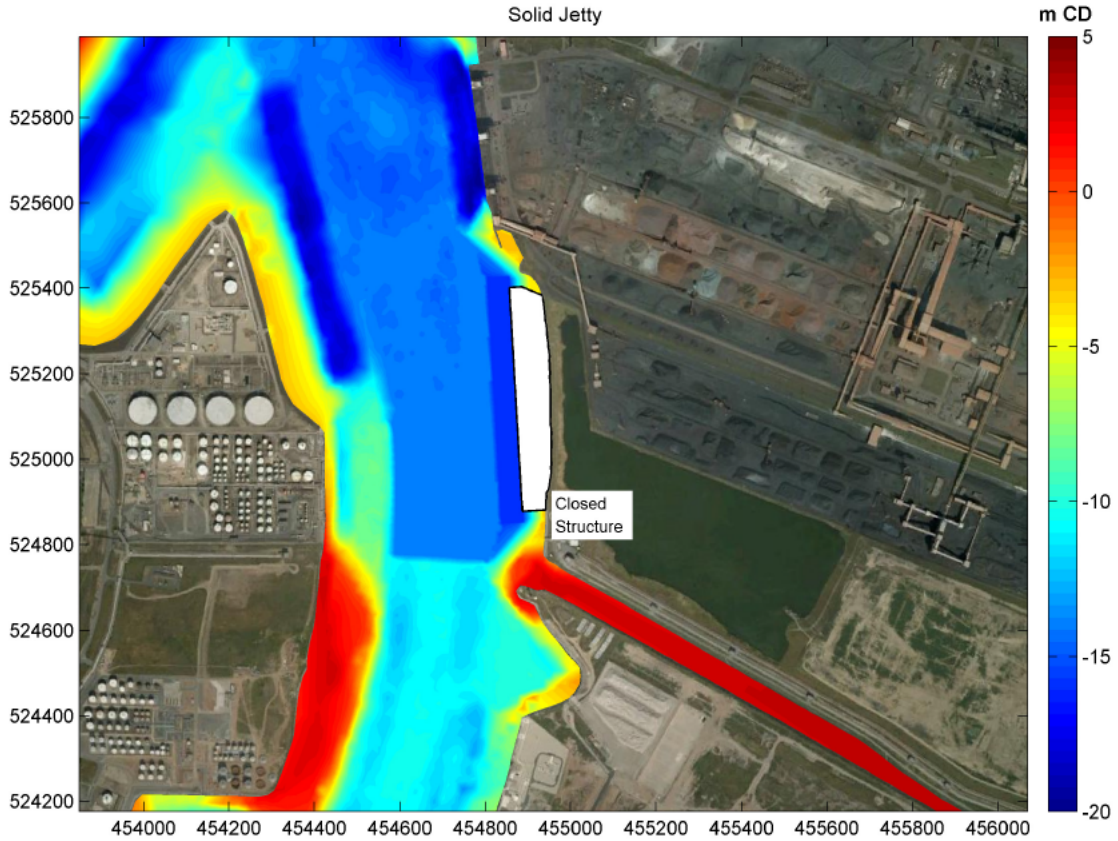

Figure 4.2: Model representation of the solid quay option

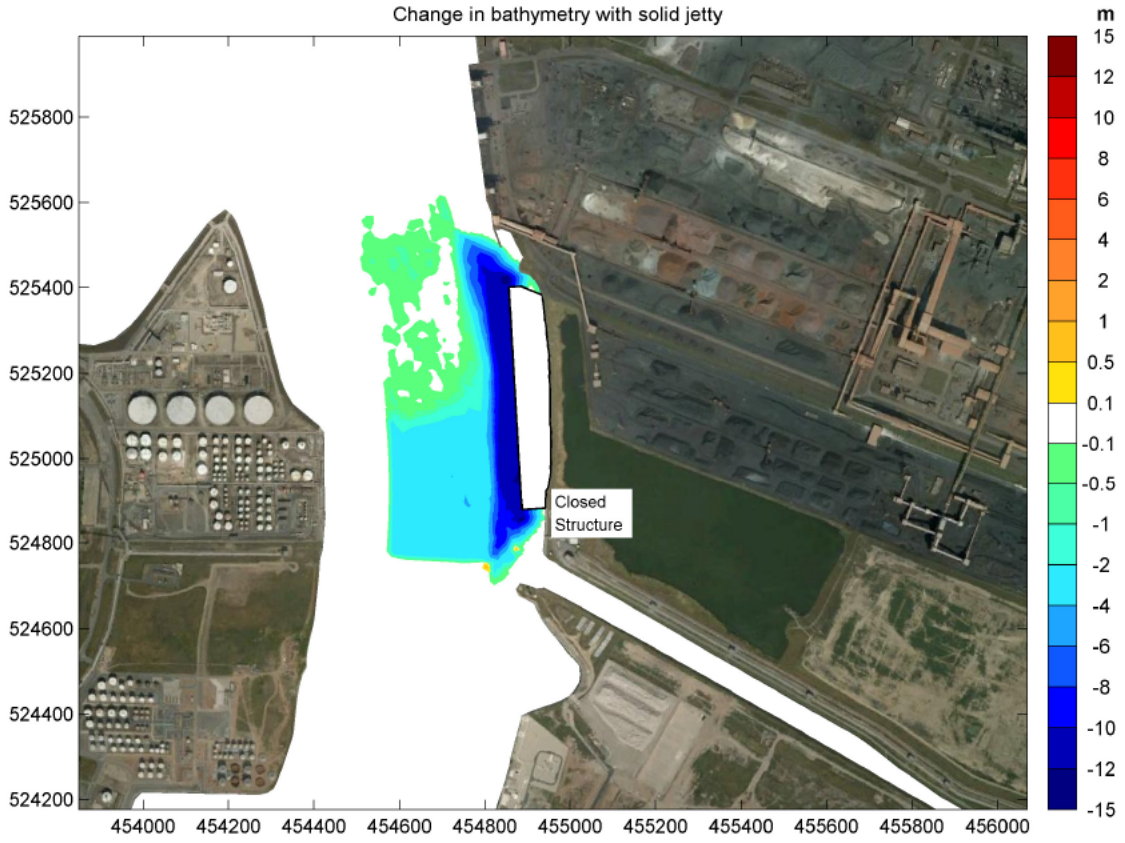

Figure 4.3: Change in bathymetry associated with solid quay option

Figure 4.4 to Figure 4.7 show the effect of the proposed development on tidal currents for low river flow, spring tide conditions at times of peak ebb (Figure 4.4 and Figure 4.5) and flood (Figure 4.6 and Figure 4.7) tides. The left hand frame shows the depth averaged current magnitude overlaid by vectors showing the current direction and the right hand frame shows the difference in current compared to baseline conditions. Increasingly dark blue colours indicate reduced currents and yellow to red colours indicate current increases.

The results show speed decreases in the extended area of -14.1 m CD channel and approaches to the quay. There is some evidence of flow being drawn towards the quay line as speed increases are predicted along the Redcar Bulk Terminal frontage during the ebb tide and adjacent to Dabholm Gut during the flood tide. The predicted changes are generally very small as anticipated considering the low baseline currents in the study area and are therefore unlikely to have consequences for navigation.

The modelling results for the other tide / river flow combinations are provided in Appendix A. These results show a consistent pattern of effects of the solid quay option on tidal currents across the range of tide / river flow cases studied.

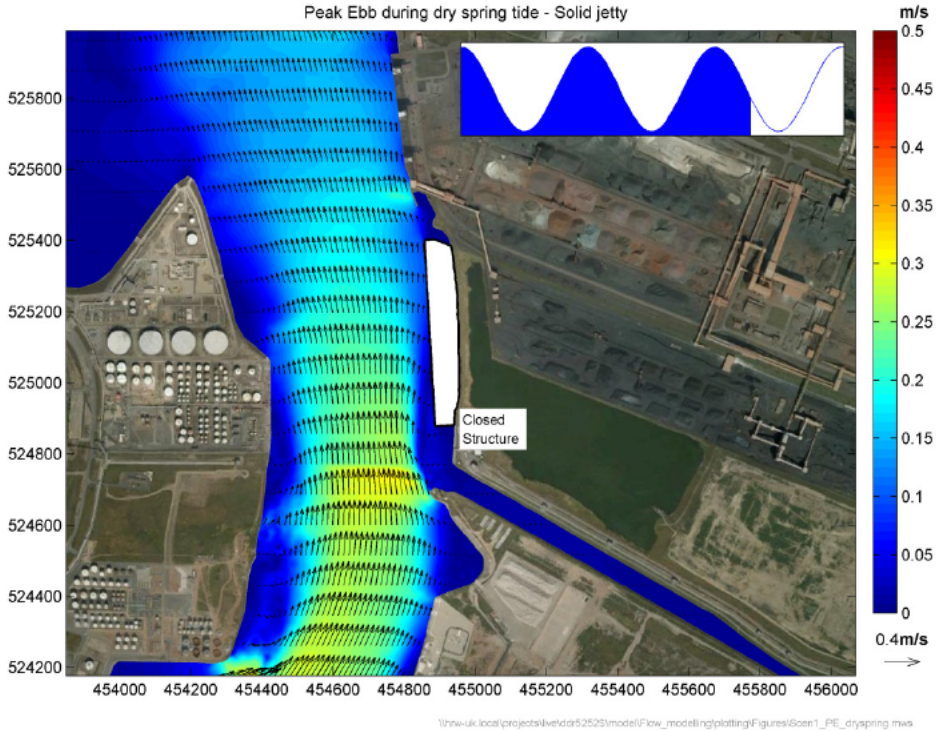

Figure 4.4: Depth average currents at peak ebb tide for solid quay, spring tide low river flow

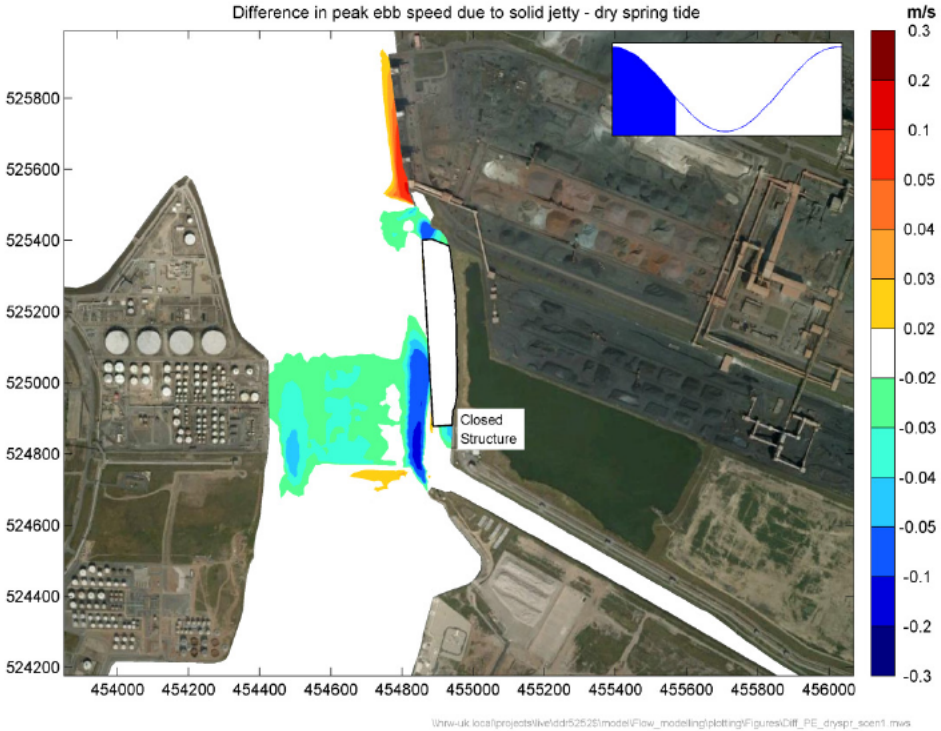

Figure 4.5: Change in depth average currents at peak ebb tide for solid quay, spring tide low river flow

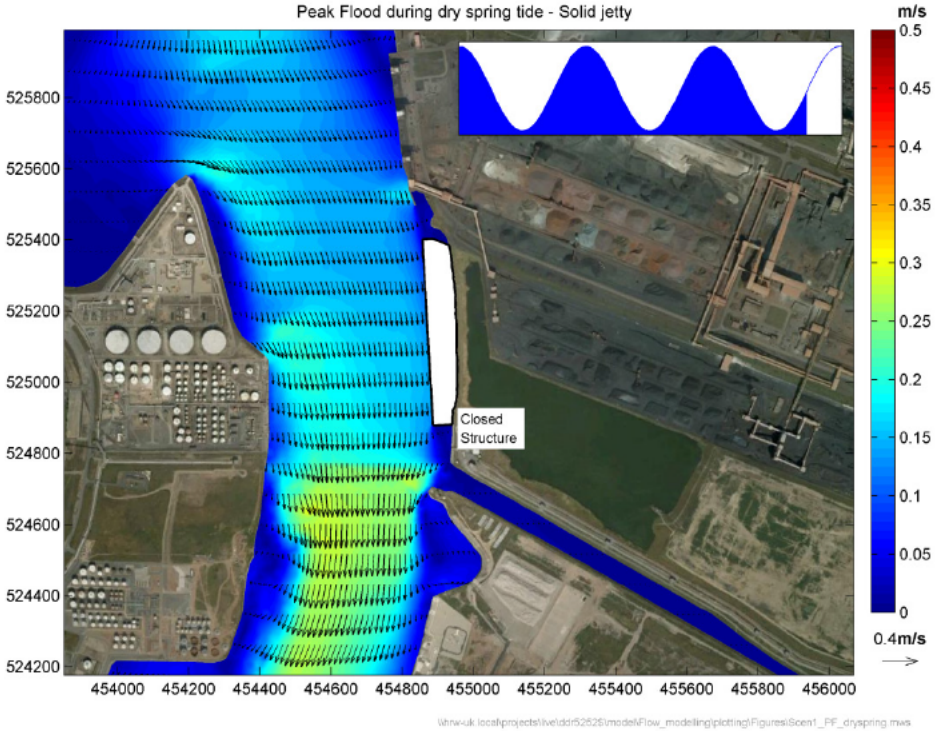

Figure 4.6: Depth average currents at peak flood tide for solid quay, spring tide low river flow

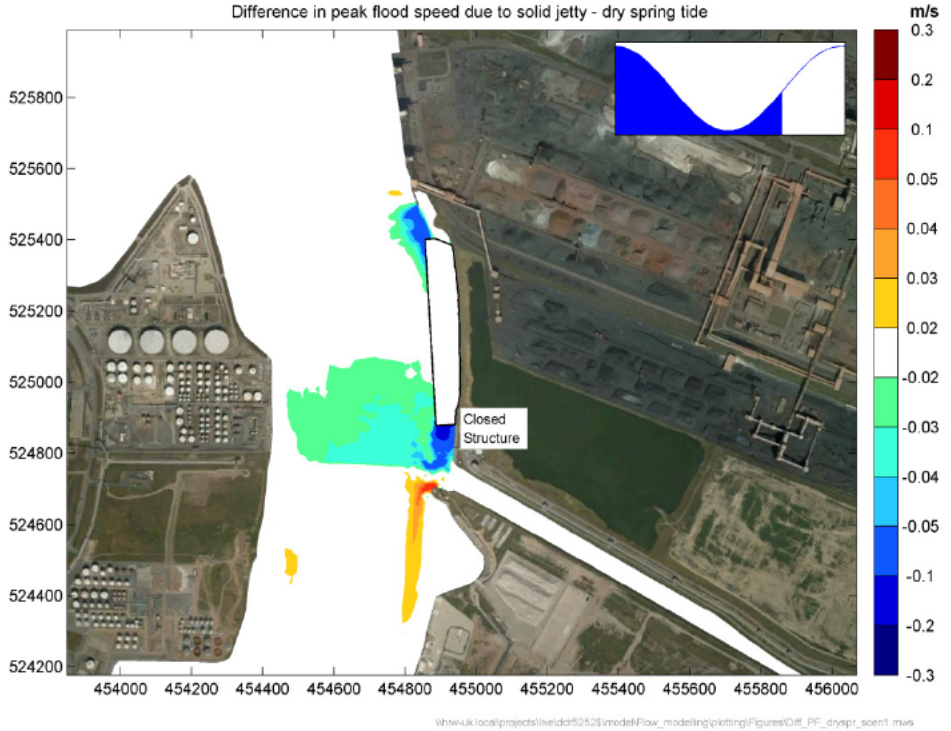

Figure 4.7: Change in depth average currents at peak flood tide for solid quay, spring tide low river flow

4.3.2. Open quay

The models representation of the bathymetry with the open quay in place is shown in Figure 4.8 with the change in bathymetry associated with this development option shown in Figure 4.9. Dredging of the channel, berth approaches and berth pocket are the same as the solid quay case however in this case the area between the dredged berth pocket and the bank is profiled under the quay to increase slope stability. The piles themselves were represented in the model via the inclusion of the drag force of the piles on the passing flow.

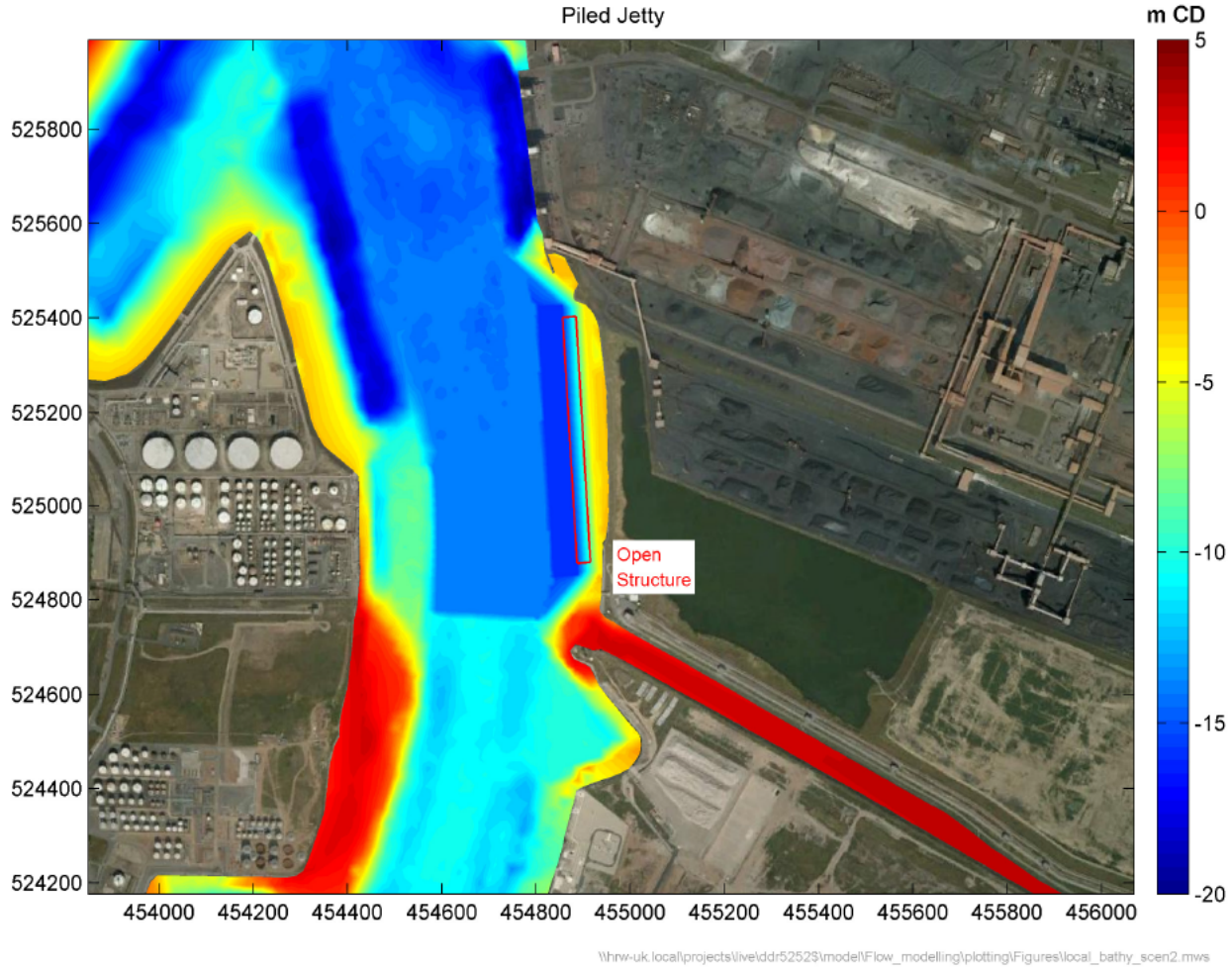

Figure 4.8: Model representation of the open quay option

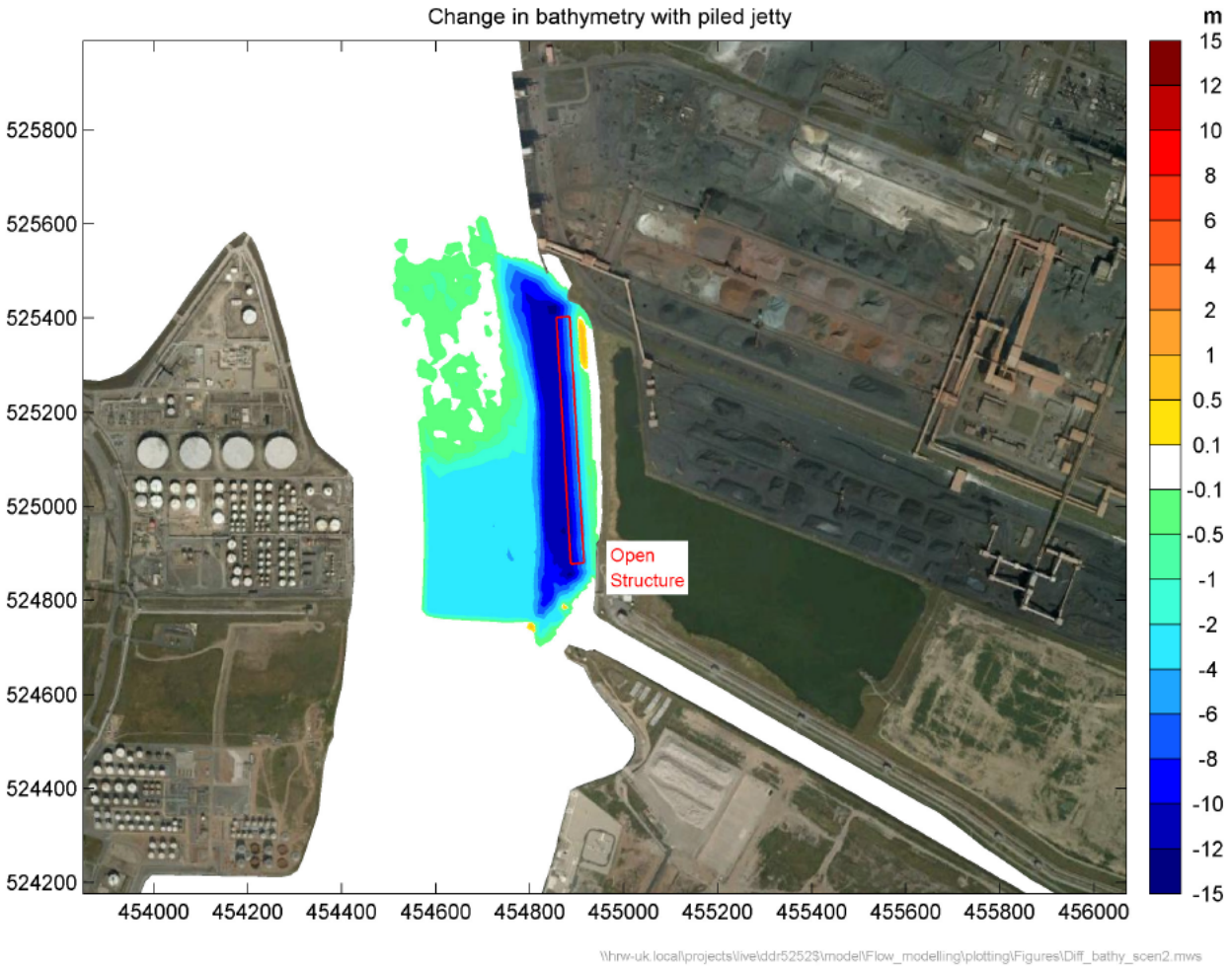

Figure 4.9: Change in bathymetry associated with the open quay option

As for the solid quay option the full set of flow model results is provided in Appendix B. In this case the effect of the works for low river flow, spring tide conditions are shown at times of peak ebb (Figure 4.10 and Figure 4.11) and flood (Figure 4.12 and Figure 4.13) tides. The left hand frame shows the depth averaged current magnitude overlaid by vectors showing the current direction and the right hand frame shows the difference in current compared to baseline conditions. Increasingly dark blue colours indicate reduced currents and yellow to red colours indicate current increases.

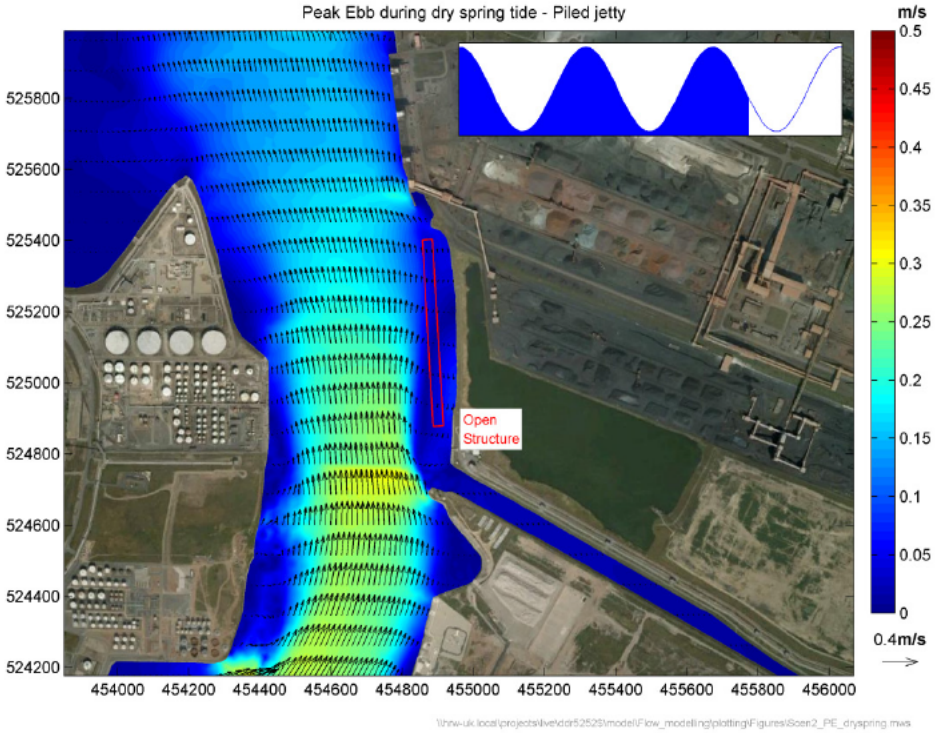

Figure 4.10: Depth average currents at peak ebb tide for open quay, spring tide low river flow

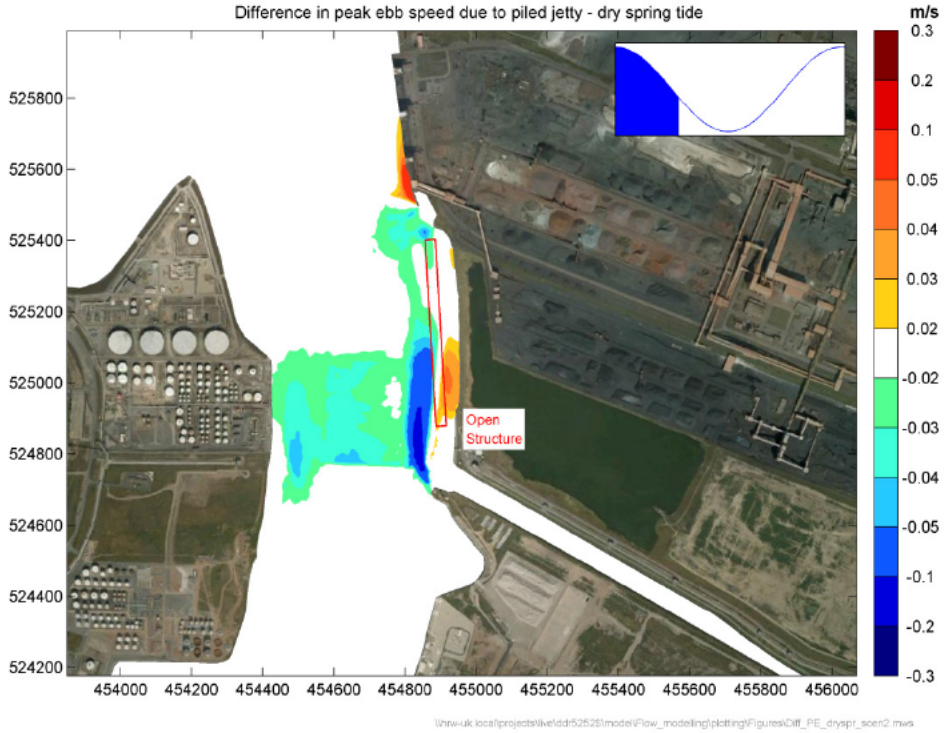

Figure 4.11: Change in depth average currents at peak ebb tide for open quay, spring tide low river flow

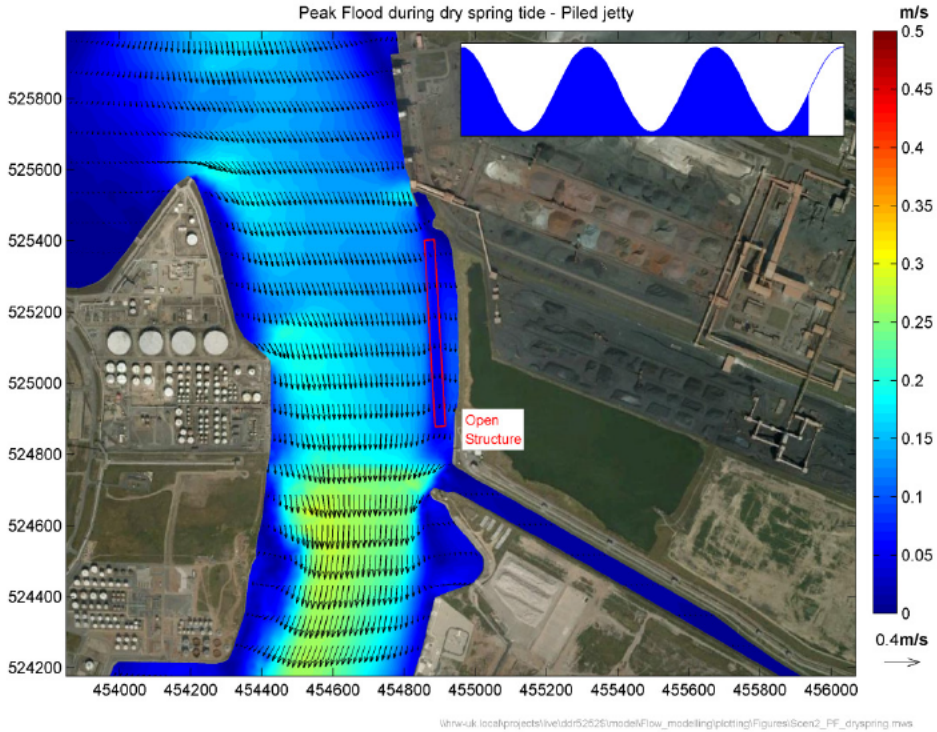

Figure 4.12: Depth average currents at peak flood tide for open quay, spring tide low river flow

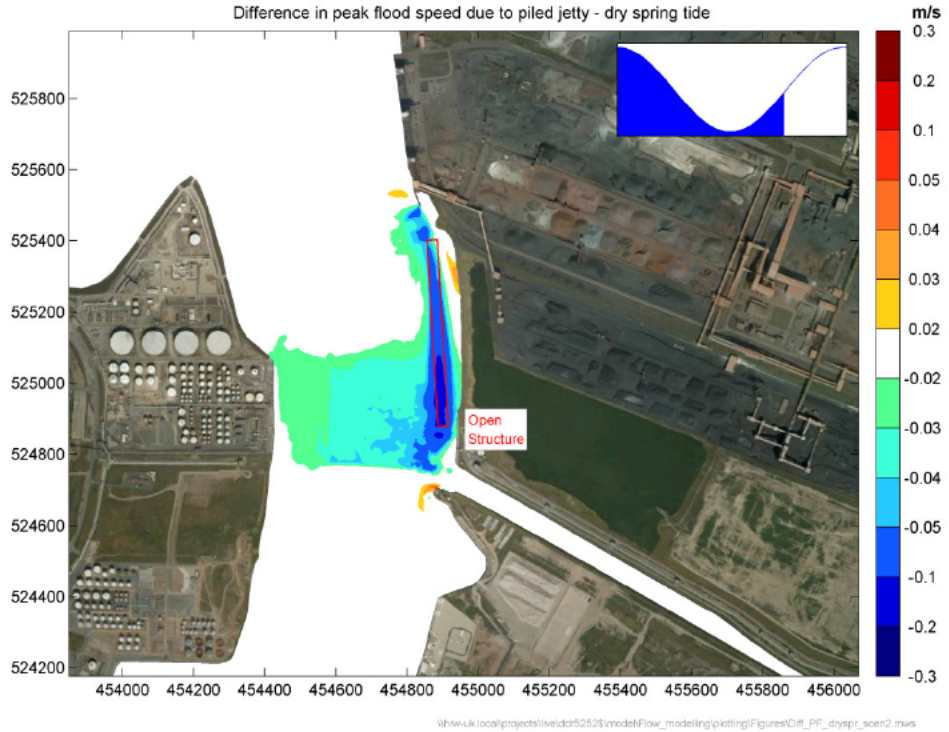

Figure 4.13: Change in depth average currents at peak flood tide for open quay, spring tide low river flow

The results show that the footprint of effect of the open quay option is similar to that for the solid quay. The areas of speed increase shown for the solid quay case (Redcar Bulk Terminal during the ebb tide and Dabholm Gut for the flood tide) are now not seen. This difference is probably due to the drag effect of the piles further slowing the flow along the quay line compared to less frictional effect of the solid quay. At time of peak ebb tide an area of speed increase is shown to the rear of the open quay, associated with changes to the position of the eddy generated at the site of the open quay by the interaction of the ebbing flow exiting Dabholm Gut with that in the main estuary. In this area of speed increase the magnitude of change is less than 0.1 m/s and so erosion of the bed is not likely from this magnitude of change to the tidal hydrodynamics.

4.4. Discussion

The results plotted above show the instantaneous effects of the development on hydrodynamics at the times of largest currents. The largest footprint and magnitude of effect would be expected at these times as the baseline currents, on which the effects of the development will act, are at their largest.

To confirm that the plotted results have captured the largest effect, a series of time series of currents have been extracted at sites throughout the study area. Figure 4.14 shows the locations of the extracted time series. The full set of results for all locations and all tide types are included in this report as Appendix C. Figure 4.15 to Figure 4.18 show the time series results at a representative point near the quay line (Point 3). These four figures show the time series results for each tide / river flow condition and both the solid quay and open quay results are overlaid on the baseline variation in current. The time series results do show some variation in the predicted effects of the works particularly for the high river flow cases when 3D current effects are also included. However, from these figures it is confirmed that the largest effects are shown at times of largest baseline current and, therefore, the results as plotted at these times provide an appropriate view of the greatest effect of the development options on currents in the Tees Estuary.

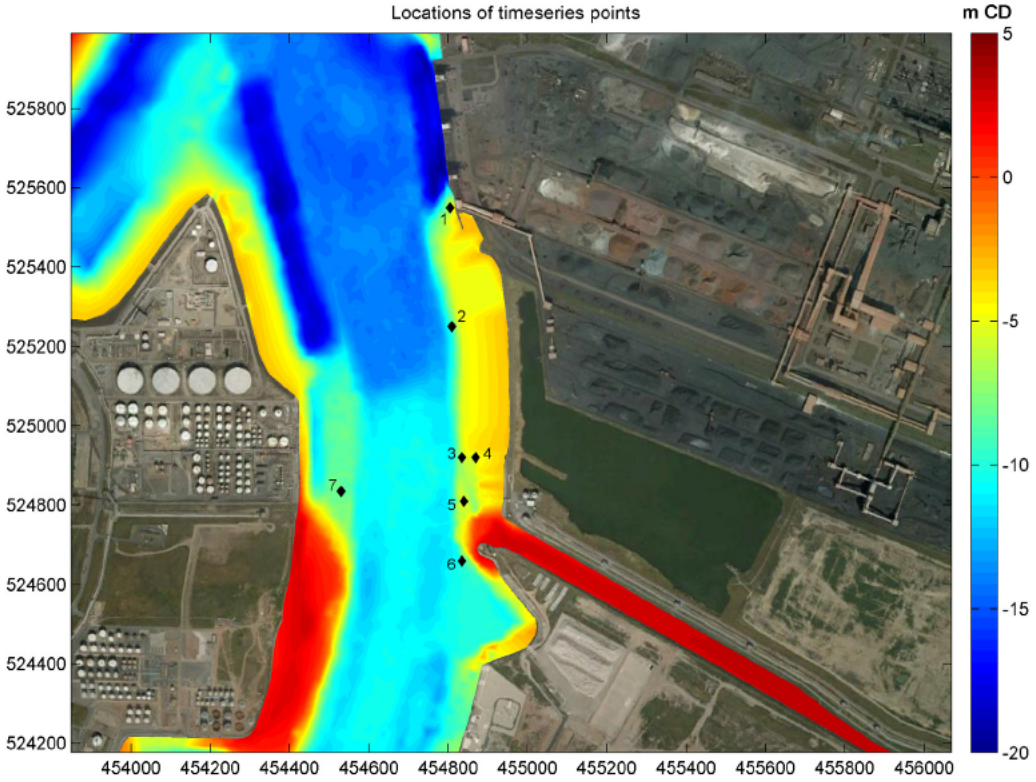

Figure 4.14: Extracted time series locations

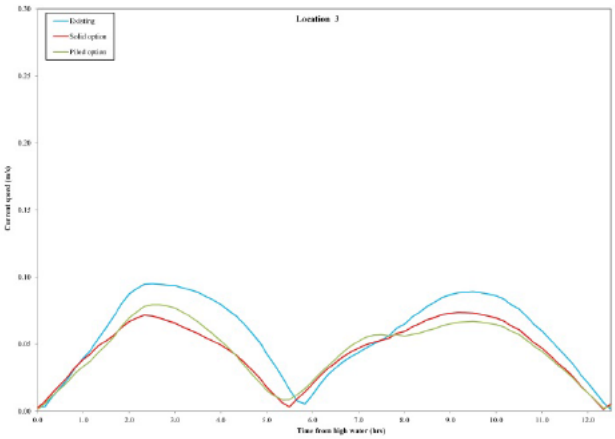

Figure 4.15: Time series of currents at Point 3, neap tide , low river flow

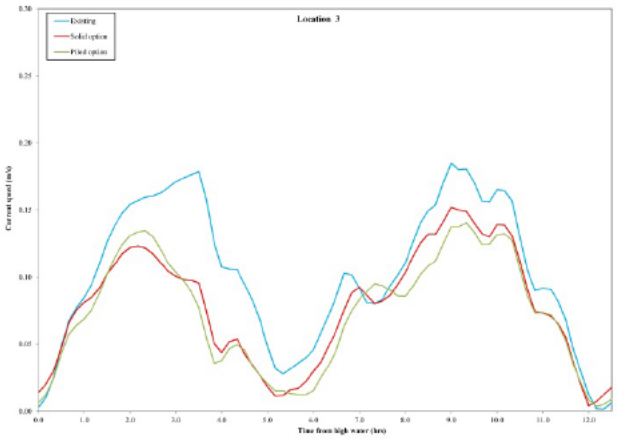

Figure 4.16: Time series of currents at Point 3, spring tide , low river flow

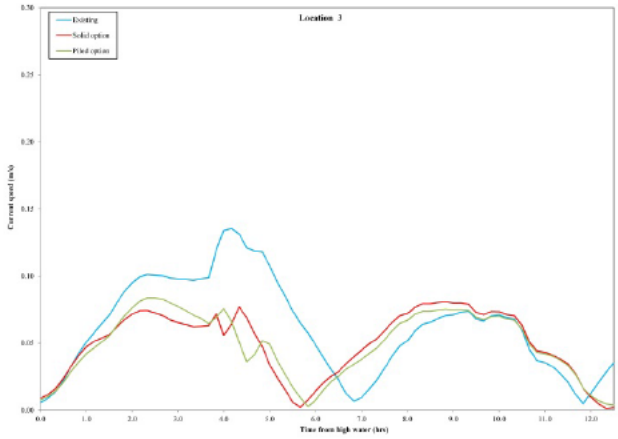

Figure 4.17: Time series of currents at Point 3, neap tide , high river flow

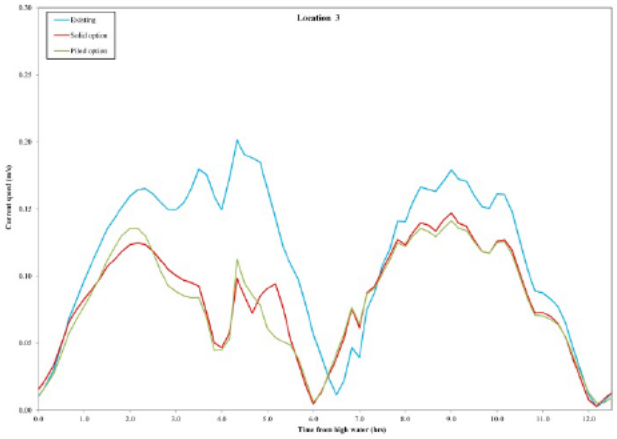

Figure 4.18: Time series of currents at Point 3, spring tide , high river flow

5. Sediment transport modelling of operational impacts

5.1. Background

Mud transport modelling has been undertaken to examine the behaviour of the mud fraction with the potential that the proposed development may alter the fine sediment dynamics of the Tees Estuary. Furthermore, information on the typical concentrations in the area and rates of accretion in the proposed dredged areas were required to understand the potential changes to the maintenance dredging volumes in the area and in the proposed berth itself.

The baseline situation for sediment transport in the Tees is an average total infill rate of approximately 800,000 m^3 per year. This total has been reduced from the historical levels by the impacts of the Tees Barrage. Within the estuary and approaches the areas of maintenance dredging are divided into a series of Chart areas (Shown in Figure 5.1). The proposed scheme is within Chart area 8. This Chart area has had an average annual infill rate of approximately 84,000 m^3 per year since the Tees Barrage was constructed in 1995.

Bed sampling undertaken by Bridgland (shown in Halcrow, (1991)) indicates that in Chart area 8, 83% of the material dredged is in the fine silts and clay fractions. The most significant source of this fine material is marine sources with sediment brought into suspension during storm periods. The density induced, landward, near-bed flow acts to bring the fine suspended sediments into the estuary. Once within the estuary, wave and tidal energies reduce and the material settles. Within the estuary reaches of the Tees (Chart areas 1-9) total fine sediment infill has been in the range 100,000-600,000 m^3 per year with an average of 300,000 m^3 per year.

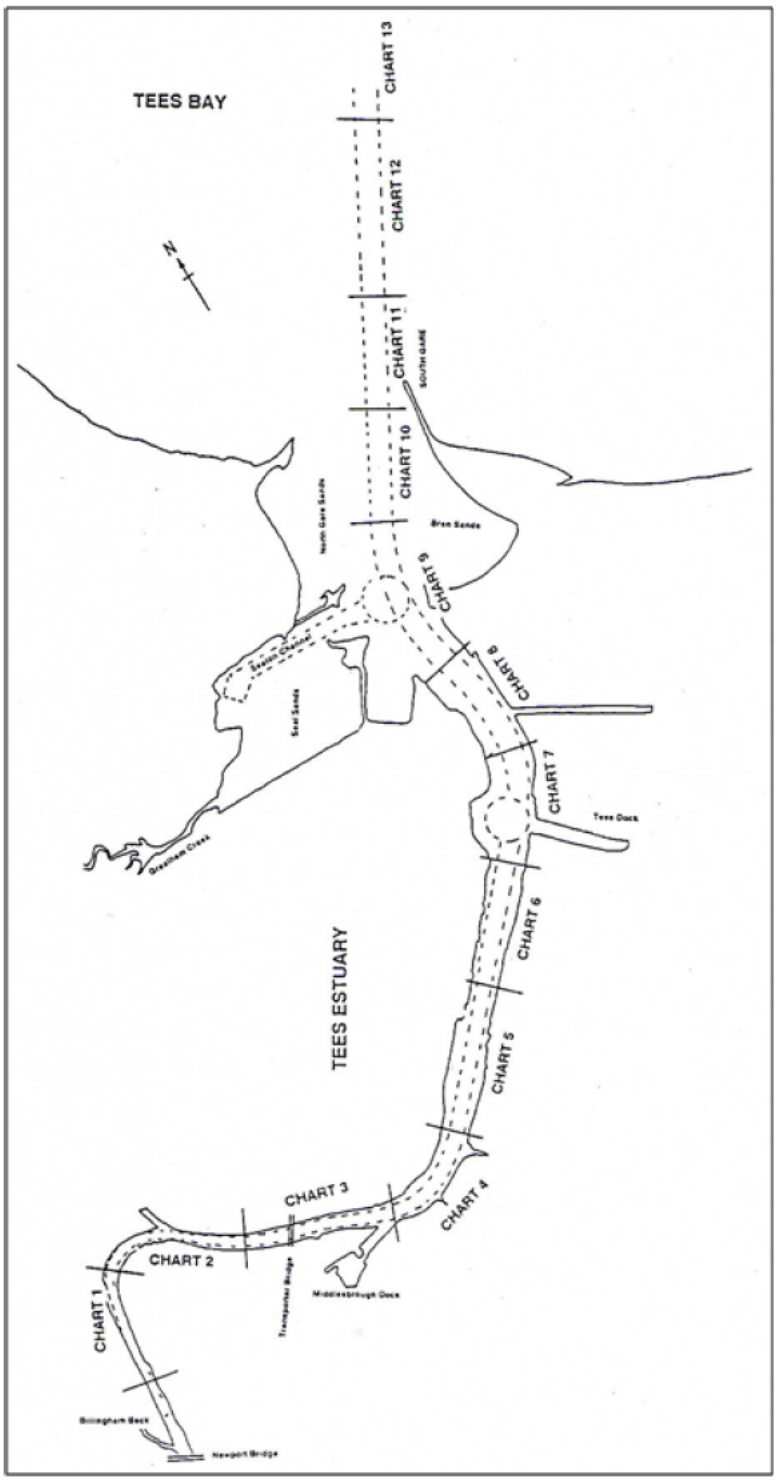

Figure 5.1: Tees Estuary Chart areas

5.2. Sediment modelling method

The chosen model for the study of mud transport was DELWAQ. This model is a generic transport and water quality model originated by Deltares. It has been integrated to the TELEMAC system as part of both systems development paths. DELWAQ is able to read in directly the 3D flow results produced by TELEMAC3D and use them to model the transport of fine sediments, also in 3D.

As for the NGCT studies (HR Wallingford, 2006) four tide/freshwater combinations were run in the hydrodynamics and these were combined in the mud transport model with a range of offshore concentrations to allow simulation of the variability of likely suspended sediment concentrations in the estuary. The offshore boundary is considered to be the main source of sediment in the Tees as material is resuspended in Tees Bay by wave action before being taken in suspension into the estuary. To include the effect of wave activity a generic distribution of wave height was extracted from the wave modelling studies undertaken for the present study which was the multiplied appropriately to correspond with the larger offshore concentrations. Figure 5.2 and Figure 5.3 show the distribution of wave height used for the simulations. From these figures it can be seen that wave energies reduce markedly in the approaches to the proposed development site. There are some small differences in wave height in the vicinity of the development site due to the additional wave reflection from the solid quay.

The exchange of mud to and from the bed was parameterised in the model with the commonly used formulae of Krone and Parthenaides. Above a critical bed shear stress of 0.12 N/m^2, erosion of the bed was initiated. The rate of erosion was parameterised with a Parthenaides constant of $4x10^{-5}$ $kg/m^2/s$. Deposition to the bed was assumed to occur continuously in the model. The settling velocity of the suspended mud was represented using a constant value of 0.5 mm/s which was reduced in the model if the concentration exceeded 2,000 mg/l when it was assumed hindering of the settling due to particle interactions was initiated.

As was done for the NGCT studies, the offshore boundary was the only source of sediment in the area. No initial concentration or deposition patterns were imposed. The simulations were undertaken for a set of repeating tidal cycles, until the simulated suspended sediment concentration was sufficiently repeating.

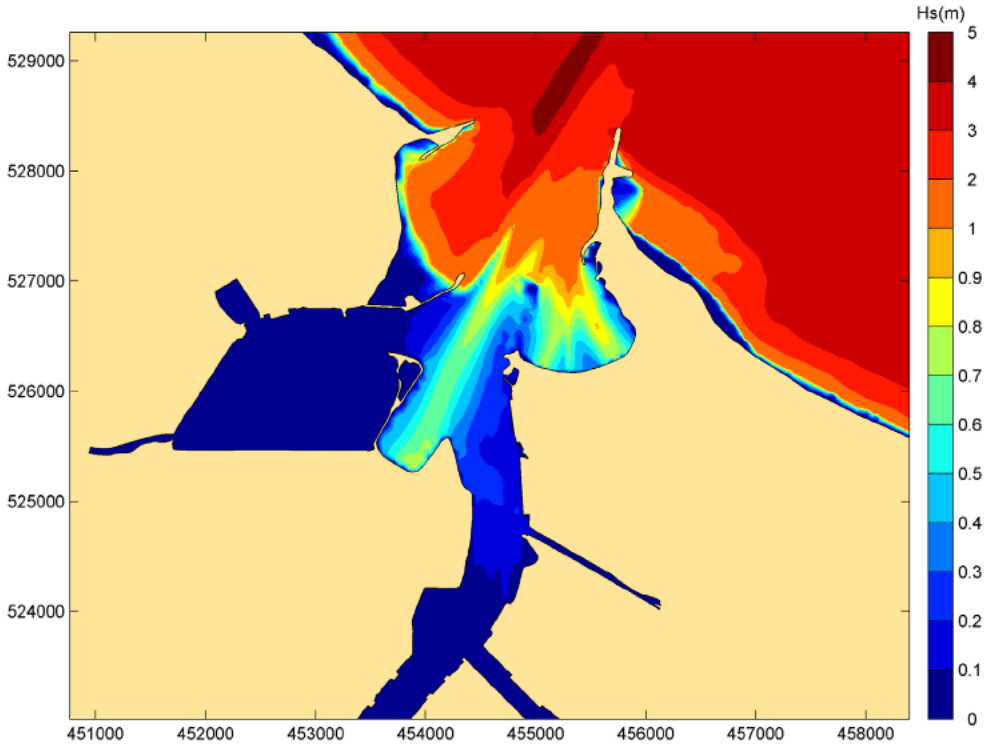

Figure 5.2: Input wave energy distribution for solid quay case

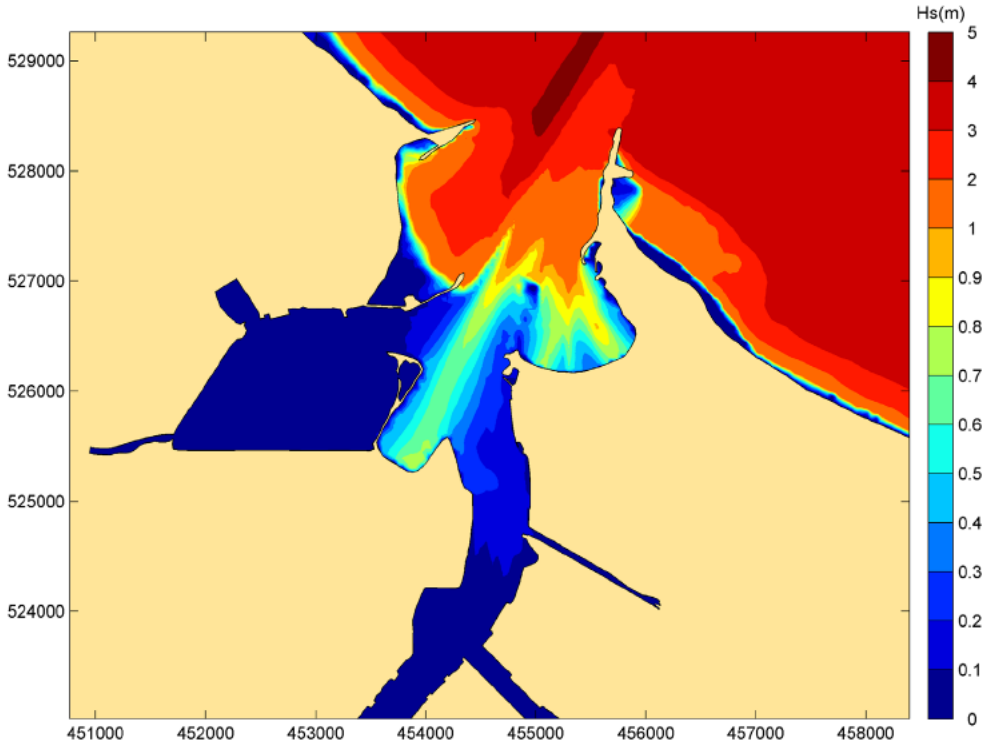

Figure 5.3: Input wave energy distribution for open quay case

5.3. Sediment modelling results

The model simulated an overall import of fine sediment of 430,000 m^3 into Chart areas 1–9 which is within the range observed since the Tees Barrage was constructed. In Chart area 8 the model predicted 88,000 m^3 per year fine sediment infill which is very close to the observed annual average value. All infill predictions were made assuming a representative density of 500 kg/m^3 for deposited sediment.

The results for the post development cases show a negligible effect on the overall import of fine sediment into the estuary – less than 0.5 %. This is to be expected because the width and depth of the channel at the entrance to the estuary unchanged by the proposed works so the potential for changes to the amount of sediment imported though this route is also unchanged. The predicted very small change in overall fine sediment regime in the Tees will not alter the present maintenance dredging frequency or methodology.

At the study site in Chart area 8, the predicted infill rate is reduced by 2-3% for the two development options compared to baseline conditions. This effect is associated with a small increase in fine sediment infill in Chart area 9 - about 1%. However, it should be noted that these changes are extremely small and are well within any natural variability in infill associated with, for example, variation in duration of storm wave conditions during any given year.

In the berth pocket and approaches for the proposed facility the medium term average infill rates are predicted to be 5,100 m^3 per year for the reclaimed quay case and 5,900 m^3 per year for the open quay case. This calculation included the foreshore surrounding the facility as these areas may also act as sediment supply into the berth pocket; therefore it is not surprising that the reclaimed case (which removes some foreshore) has less infill predicted than the open quay case.

The footprints of predicted changes to infill rate are shown in Figure 5.4 and Figure 5.5. In these plots the orange colours indicate an increase in annual infill and the blue colours show a predicted decrease in infill. The solid quay case (Figure 5.4) shows some areas of distribution in infill although of relatively small magnitude, less than 0.2 m per year. The small changes plotted are consistent with the small changes in the total infill calculated. No changes in infill pattern are shown in Seal Sands or the other intertidal areas around Teesmouth.

The open quay case (Figure 5.5) shows an even smaller effect with no predicted changes to annual accretion greater than 0.05 m per year. The open quay case does not show the redistribution of infill around the Redcar Bulk Terminal as was shown by the solid quay, which is probably linked to the smaller area of footprint in predicted change to the hydrodynamics.

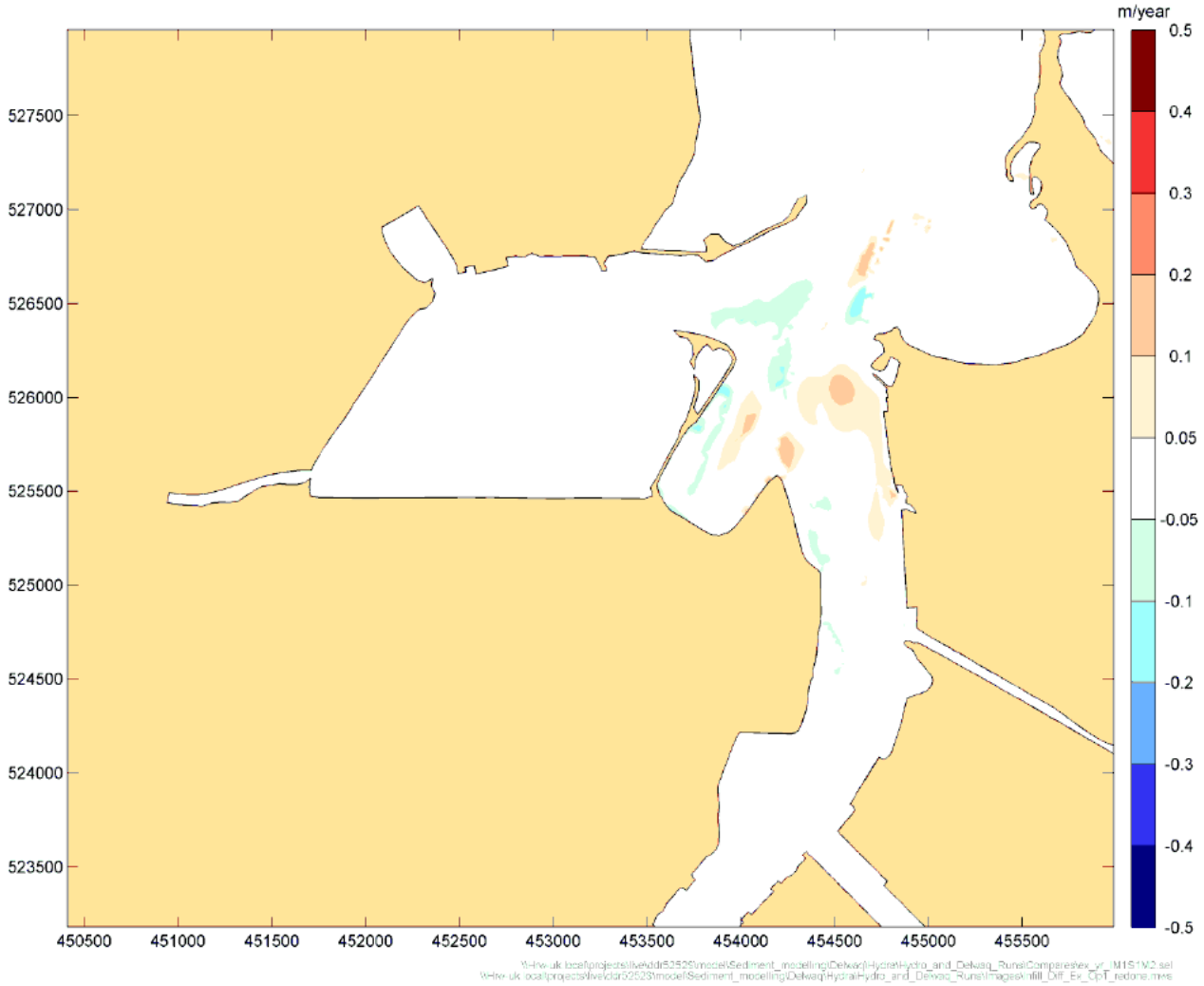

Figure 5.4: Predicted change in annual accretion rate, solid quay case

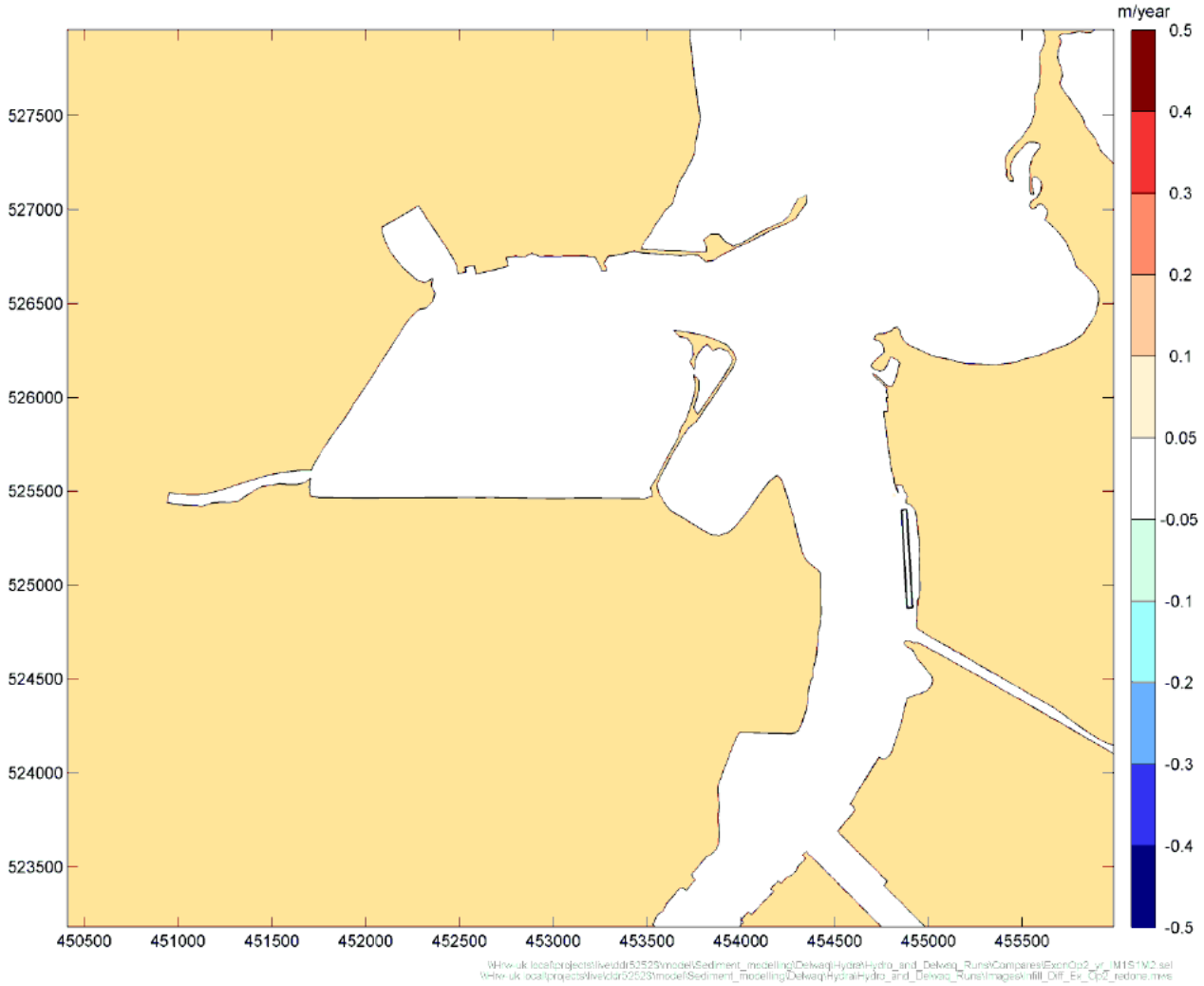

Figure 5.5: Predicted change in annual accretion rate, open quay case

6. Conclusions

A set of established modelling tools have been used to predict the effects of the construction and operation of two options of the York Potash facility on flows, waves and sediment transport.

During the construction phase

The plume dispersion simulations show the following key features:

- The effects of backhoe dredging are relatively small compared to those of CSD and barge or TSHD.
- The CSD and barge overflowing produce considerable deposition of fine sediment locally on the bed while the TSHD dredging results in the release of more sediment into the water column.
- The CSD footprint of effect is smaller than that of TSHD dredging.

- On average predicted mean concentration increases outside of the dredging area are a few tens of mg/l at most. Peak predicted concentration increases are larger possibly rising to 100 or 200 mg/l outside of the dredging area for short periods.
- The footprint of effects of dredging for high river flow, neap tide conditions is considerably smaller than that for low river flow, spring tide conditions which extends past South Gare and Tees Dock.
- The predicted deposition is typically of the order of a few millimetres, except in the vicinity of the dredging itself where much higher rates of deposition are predicted. In practice the sediment depositing in the vicinity of the dredging will be re-dredged. During the period of the dredging operation a one off increase of up to 10% to the annual maintenance requirement in the Tees is predicted.

During the operational phase

Wave conditions are increased by the reflection effects of the solid quay. For representative waves (0.1 year return period) wave height increase by up to 0.1 m in the vicinity of the quay. For larger waves with a 5 year return the predicted increases in wave height are in the range 0.1 – 0.15 m in the vicinity of the quay and some changes in the range 0.03 – 0.05 m can occur at the opposite coastline. For the open quay case no effect in changing the distribution of wave energy is predicted.

Currents are predicted to decrease in the dredged areas for both facility options. The solid quay is shown to have a larger footprint of effect with some speed increase predicted at the Redcar Bulk Terminal during the ebb tide and at the mouth of Dabholm Gut during the flood tide. Neither development option results in widespread changes in hydrodynamics.

Both development options show a negligible effect on the overall import of fine sediment into the estuary – less than 0.5 %. The predicted very small change in overall fine sediment regime in the Tees will not alter the present maintenance dredging frequency or methodology.

At the study site in Chart area 8, the predicted infill rate is reduced by 2-3% for the two development options compared to baseline conditions. In the berth pocket and approaches for the proposed facility the medium term average infill rates are predicted to be 5,100 m^3 per year for the reclaimed quay case and 5,900 m^3 per year for the open quay case.

7. References

Allsop N.W.H., 1990. Reflection Performance of Rock Armoured Slopes in Random Waves, Proc. Int. Conf. Coastal Engineering, Delft.

Halcrow, 1991. Tees Estuary Dredging Review. Report for Tees and Hartlepool Port Authority.

HR Wallingford, 2006. Northern Gateway Container Terminal. Hydrodynamic and sedimentation studies; Report EX 5250 May 2006.

Royal HaskoningDHV, 2014. York Potash Marine Export Facility. Preliminary Concept Development Report. Report PB1586/R002/MDG/Newc.

Appendices

A. Solid quay flow modelling results

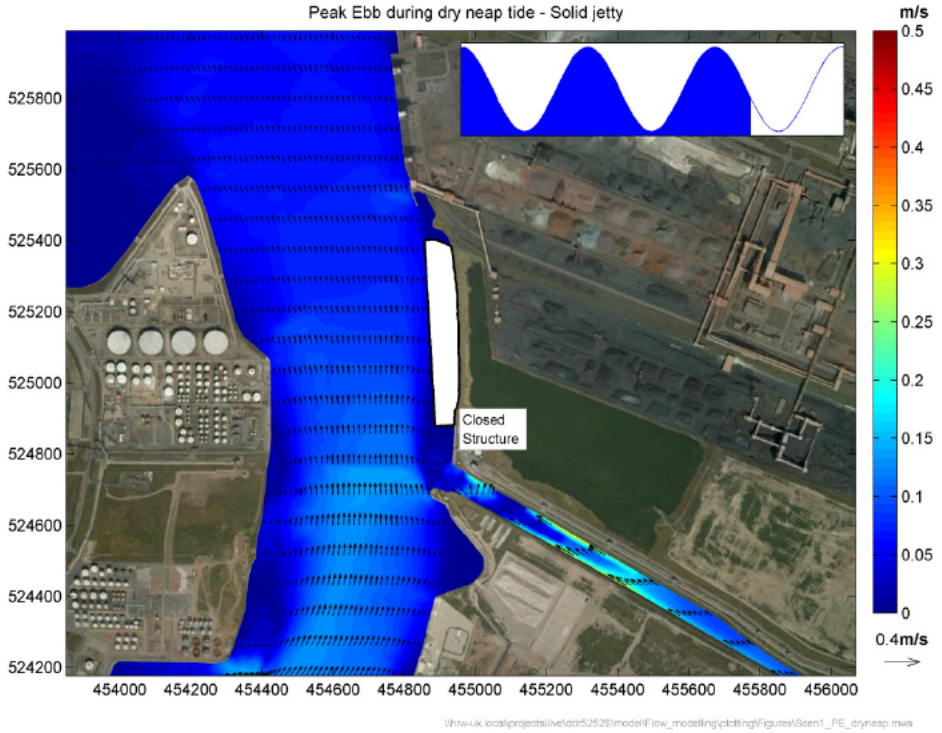

Figure A.1: Depth average currents at peak ebb tide for solid quay, neap tide low river flow

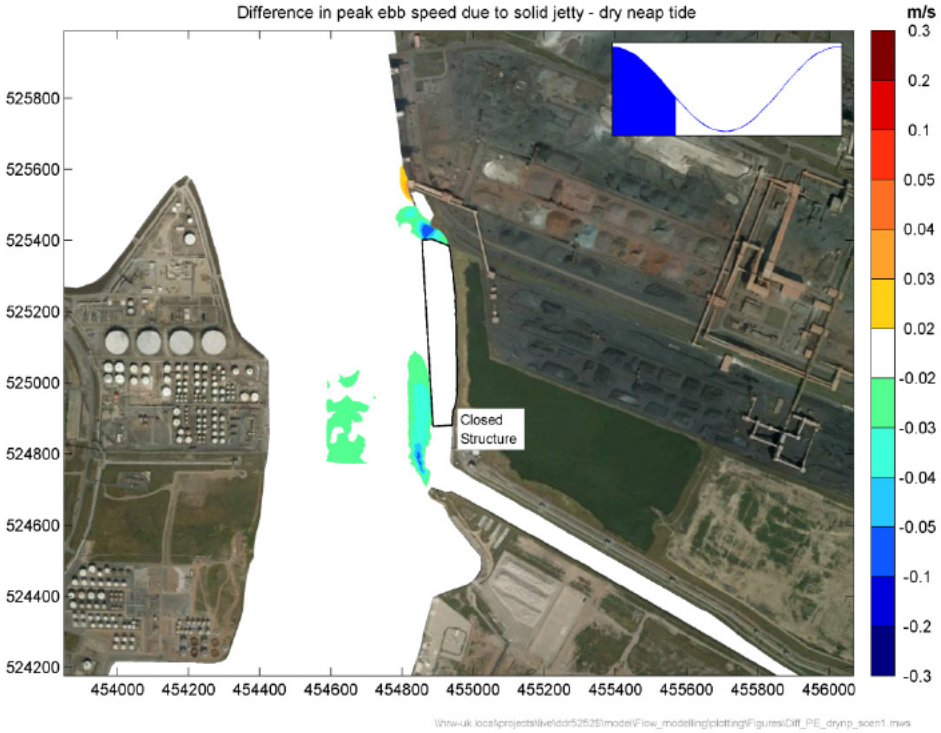

Figure A.2: Change in depth average currents at peak ebb tide for solid quay, neap tide low river flow

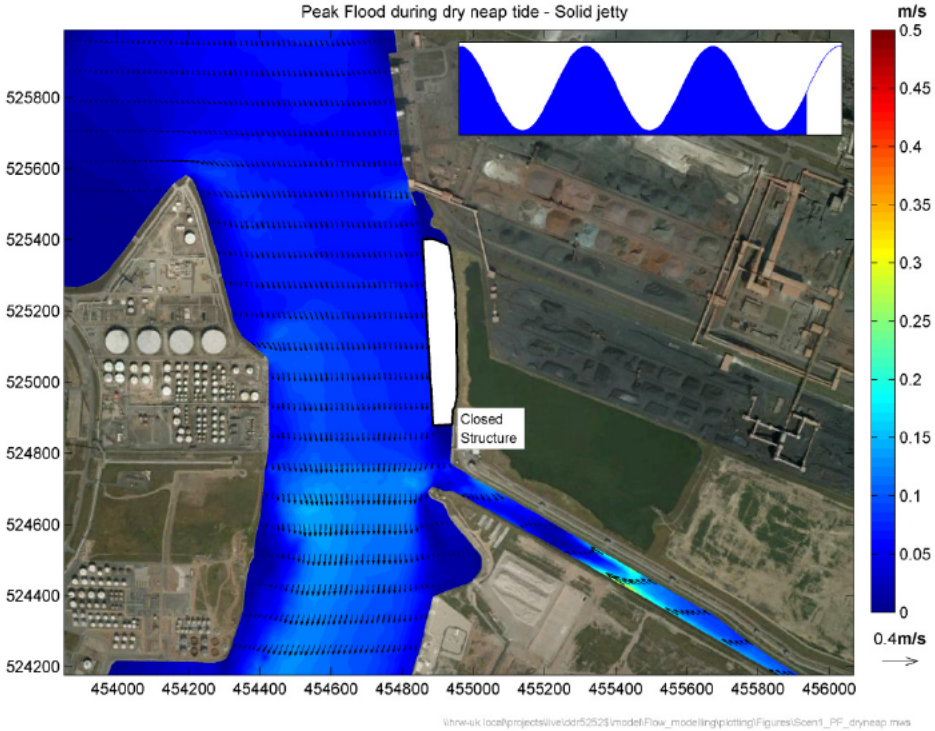

Figure A.3: Depth average currents at peak flood tide for solid quay, neap tide low river flow

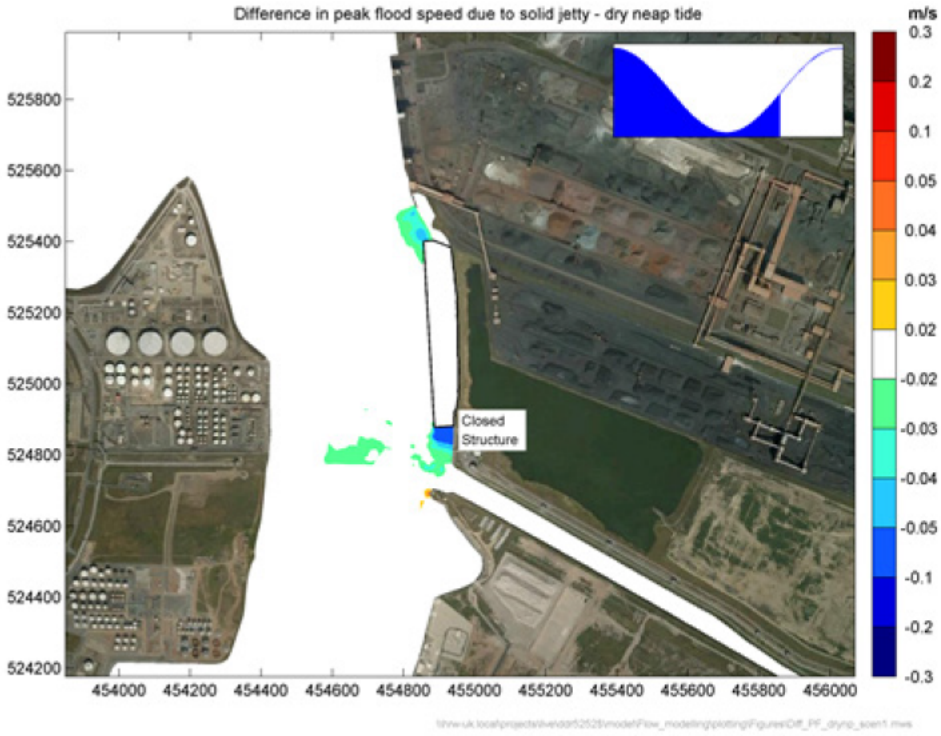

Figure A.4: Change in depth average currents at peak flood tide for solid quay, neap tide low river flow

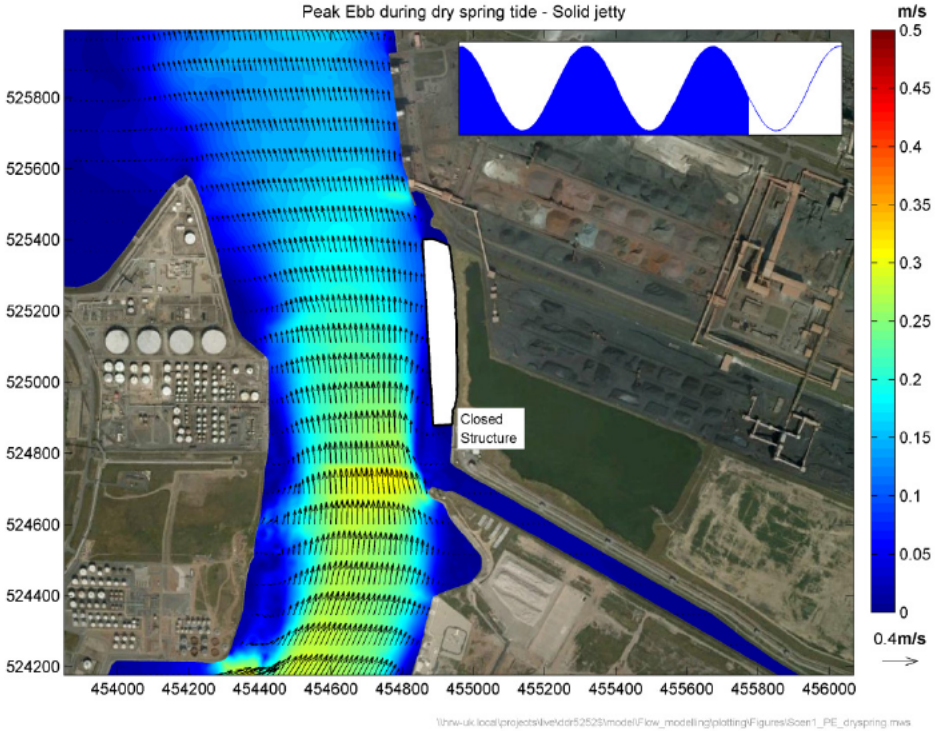

Figure A.5: Depth average currents at peak ebb tide for solid quay, spring tide low river flow

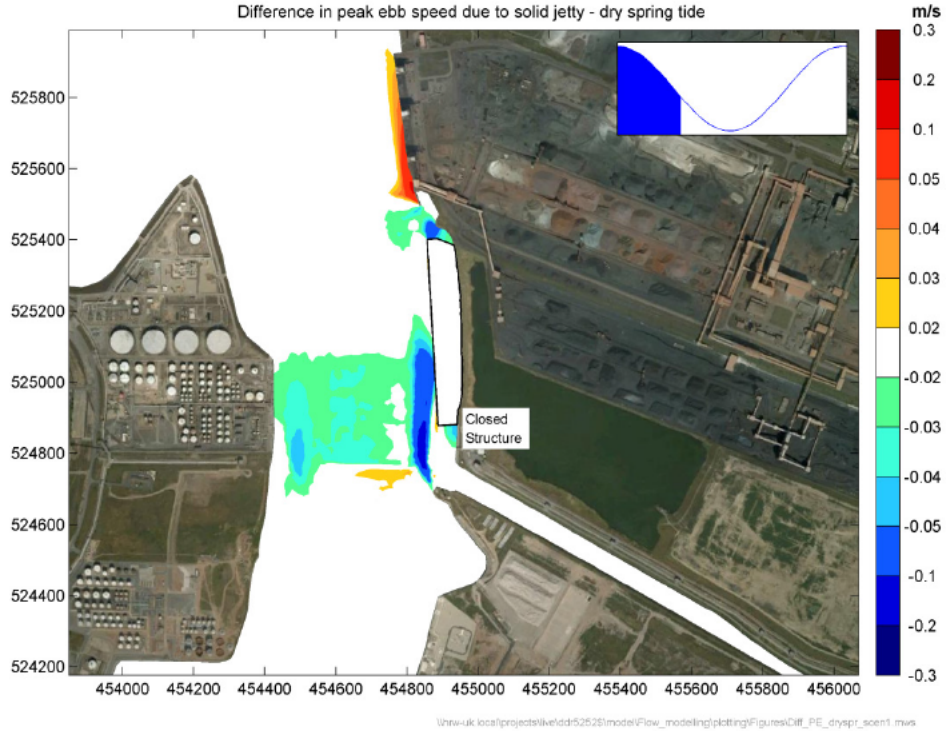

Figure A.6: Change in depth average currents at peak ebb tide for solid quay, spring tide low river flow

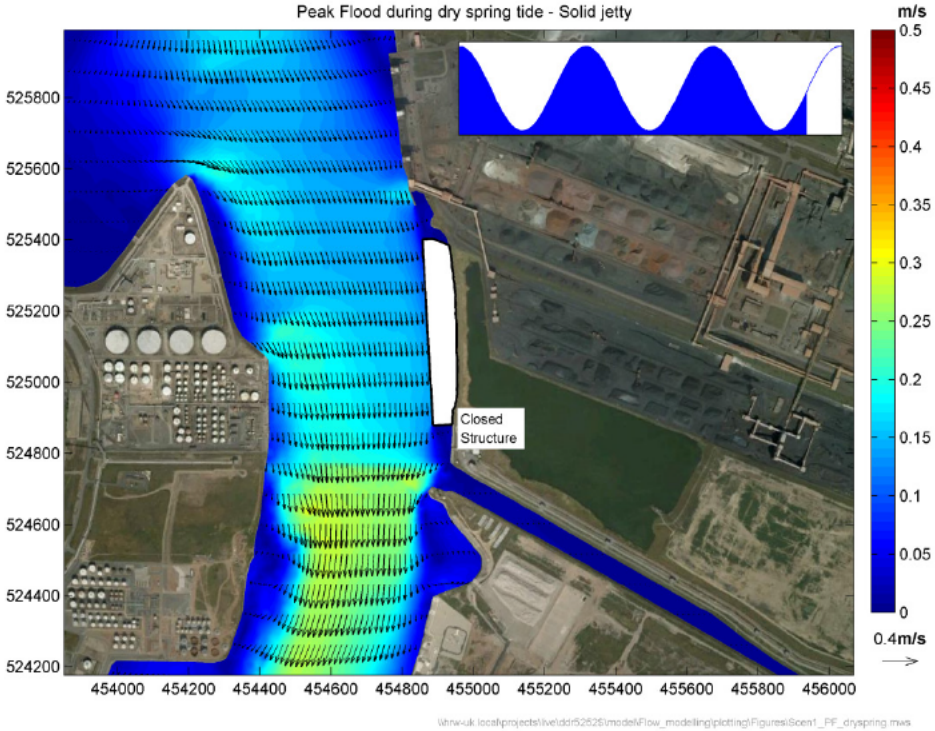

Figure A.7: Depth average currents at peak flood tide for solid quay, spring tide low river flow

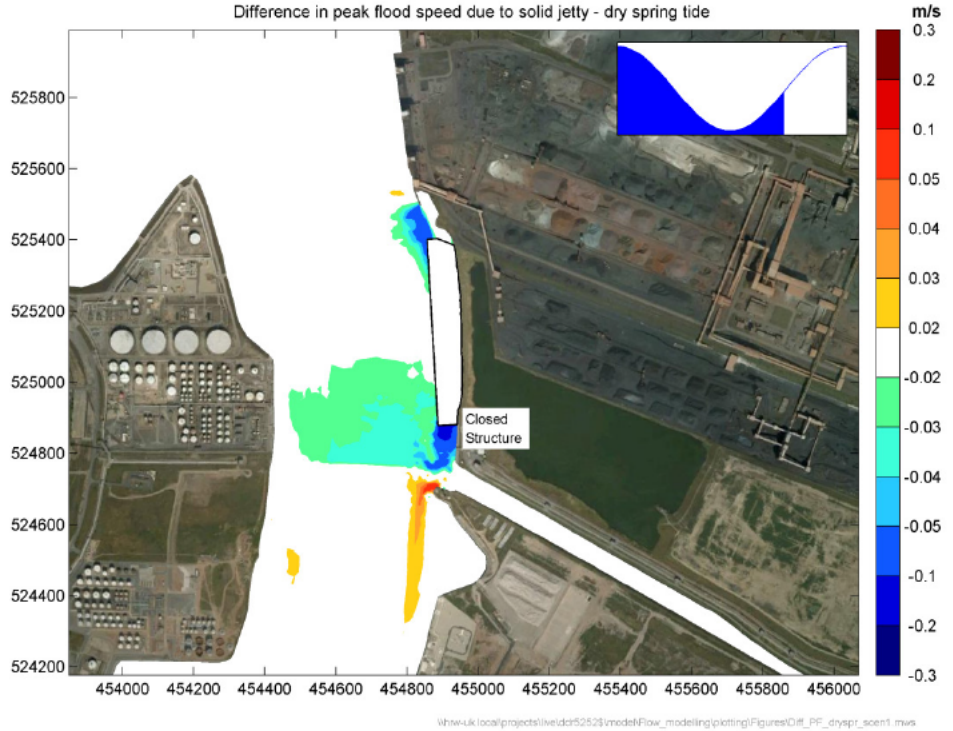

Figure A.8: Change in depth average currents at peak flood tide for solid quay, spring tide low river flow

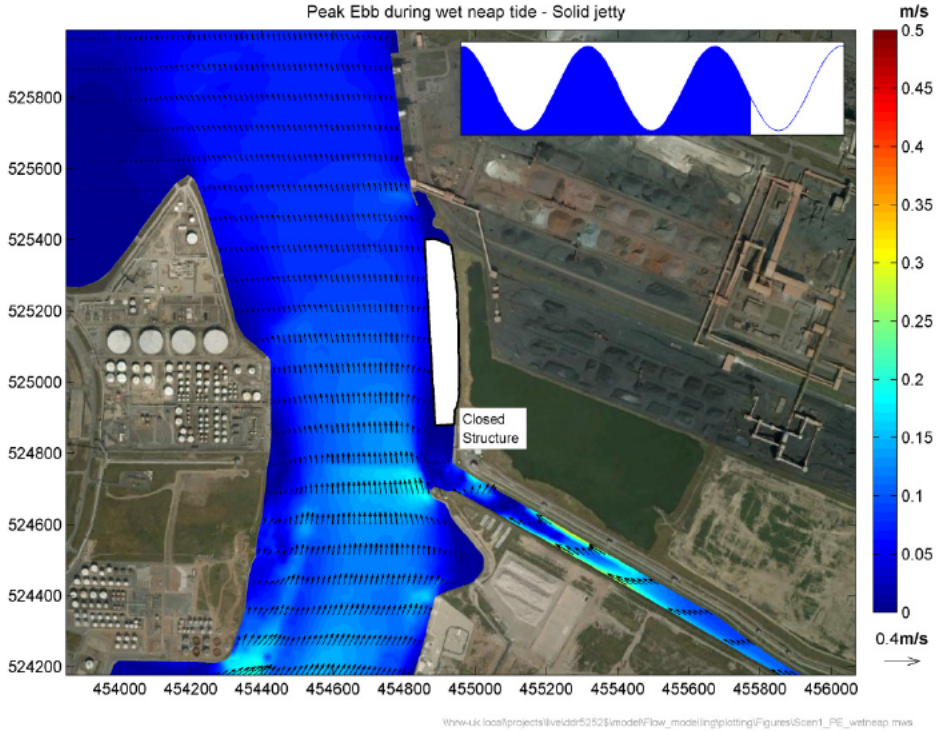

Figure A.9: Depth average currents at peak ebb tide for solid quay, neap tide high river flow

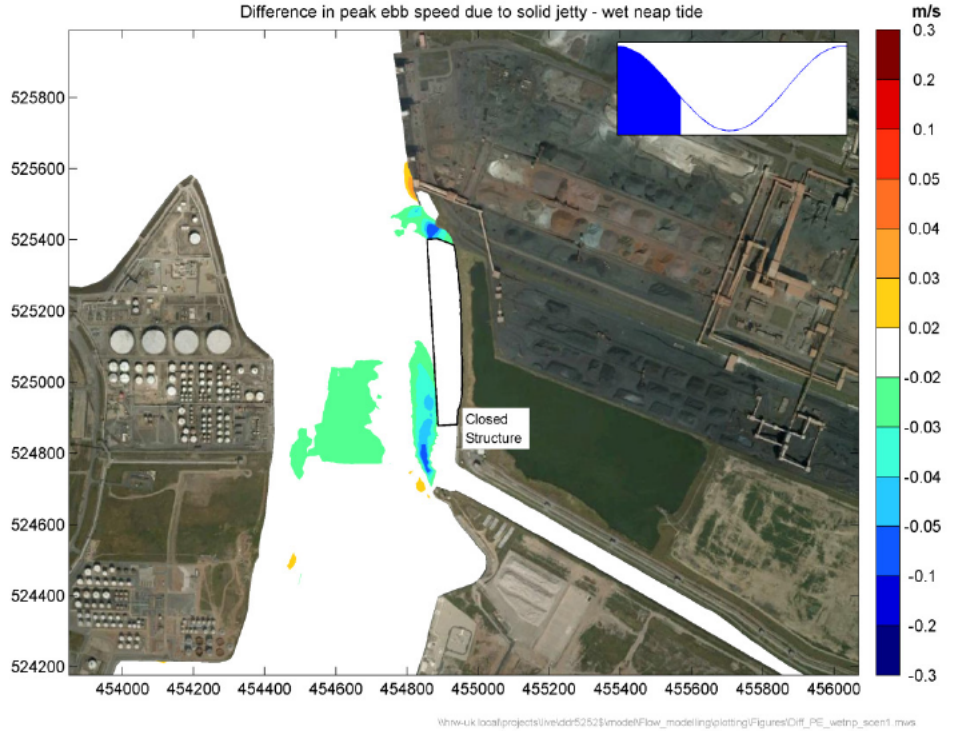

Figure A.10: Change in depth average currents at peak ebb tide for solid quay, neap tide high river flow

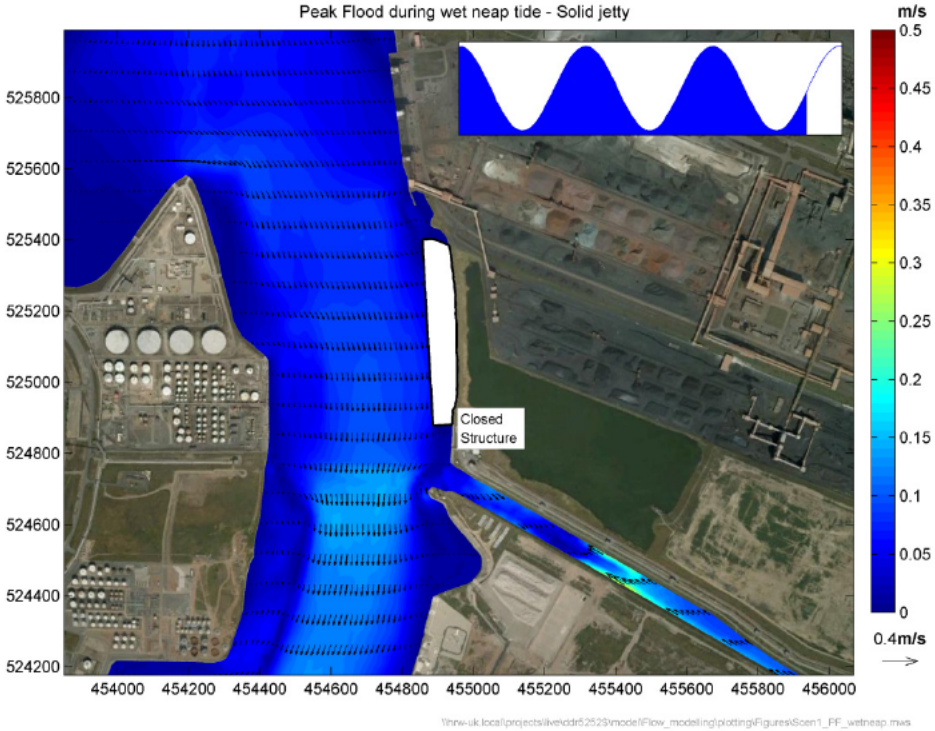

Figure A.11: Depth average currents at peak flood tide for solid quay, neap tide high river flow

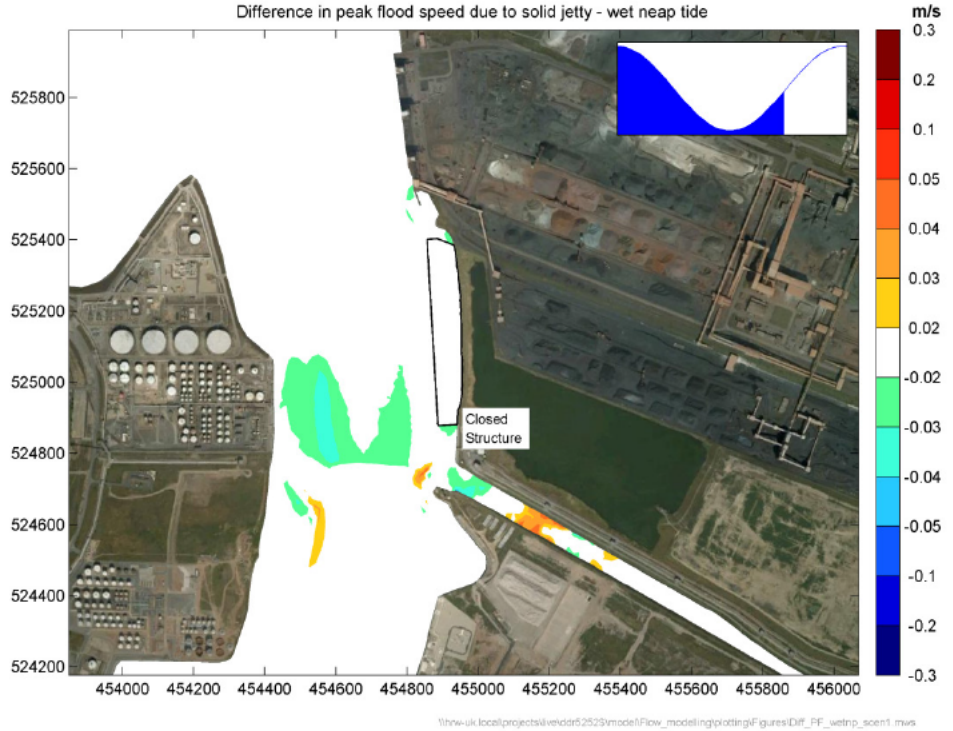

Figure A.12: Change in depth average currents at peak flood tide for solid quay, neap tide high river flow

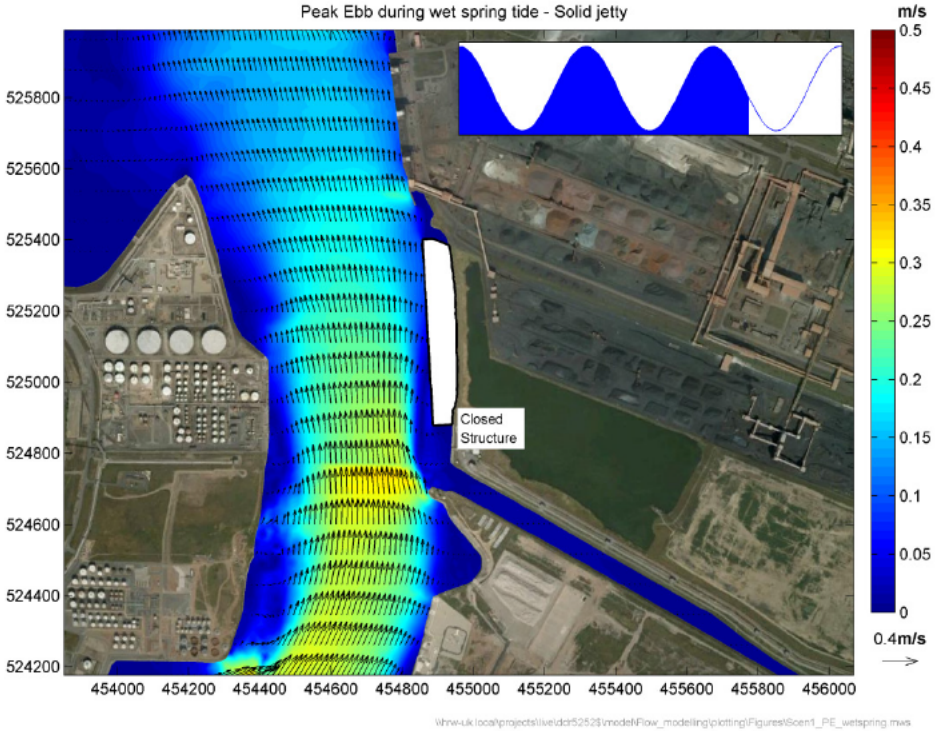

Figure A.13: Depth average currents at peak ebb tide for solid quay, spring tide high river flow

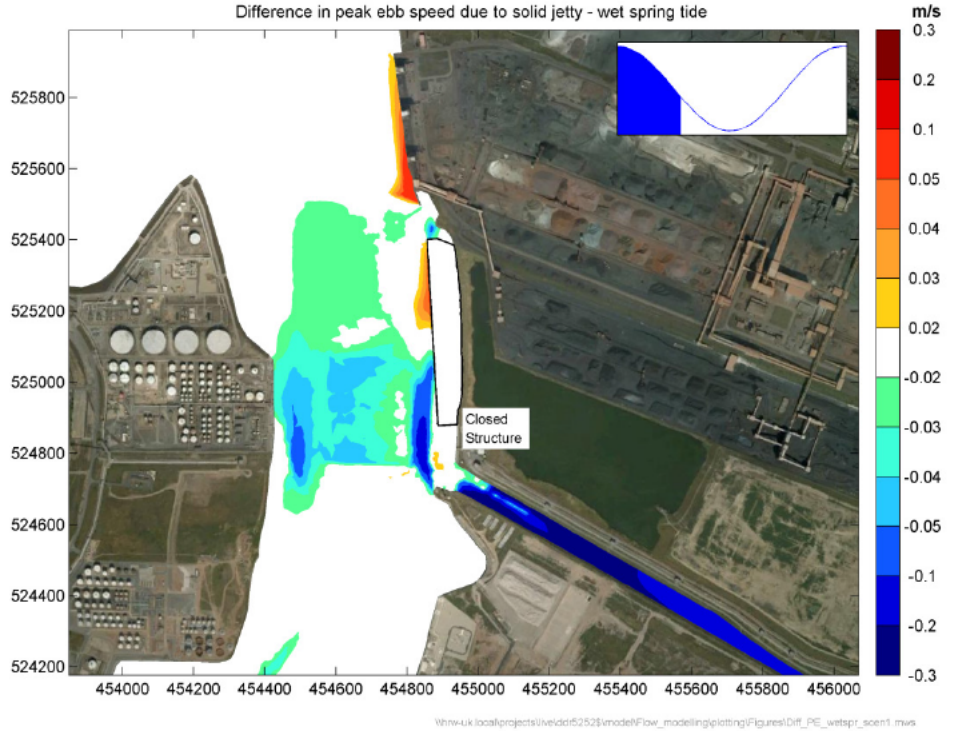

Figure A.14: Change in depth average currents at peak ebb tide for solid quay, spring tide high river flow

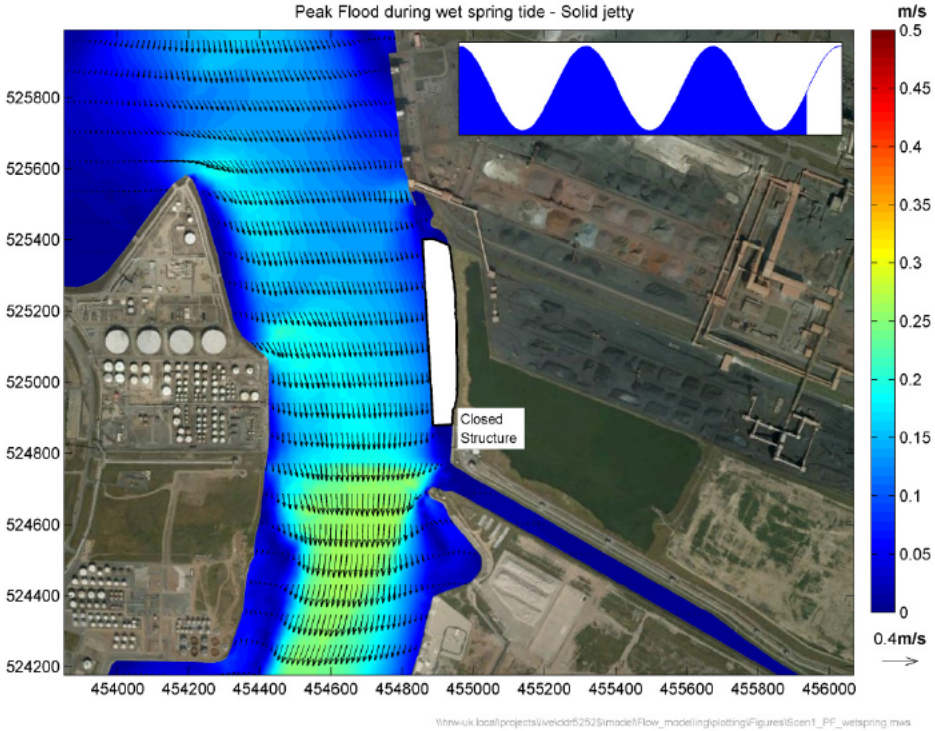

Figure A.15: Depth average currents at peak flood tide for solid quay, spring tide high river flow

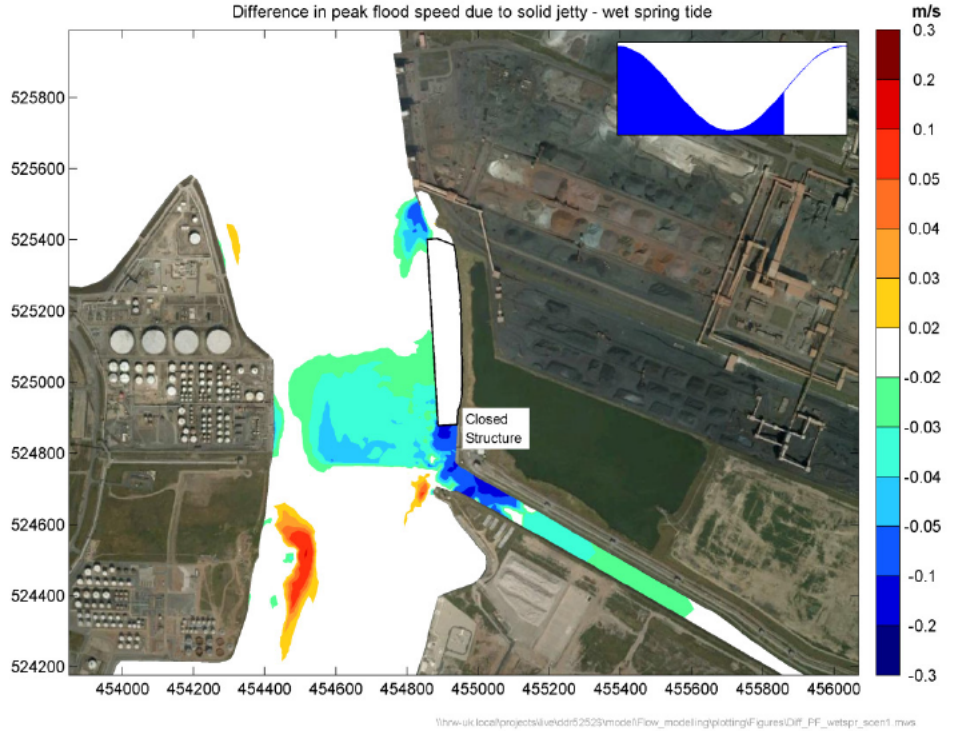

Figure A.16: Change in depth average currents at peak flood tide for solid quay, spring tide high river flow

B. Open quay flow modelling results

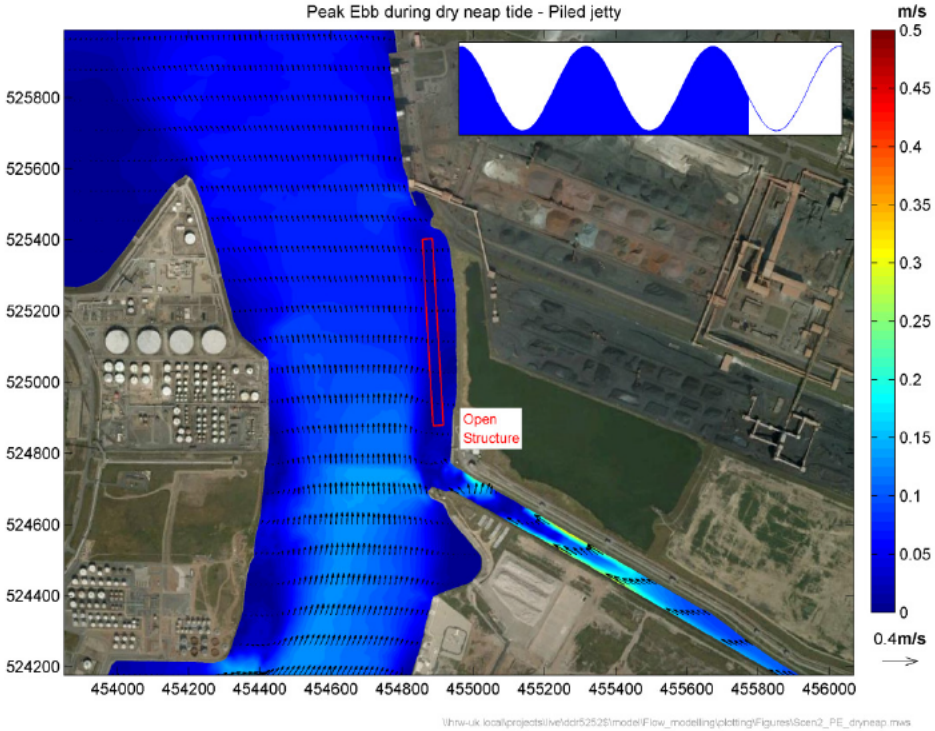

Figure B.1: Depth average currents at peak ebb tide for open quay, neap tide low river flow

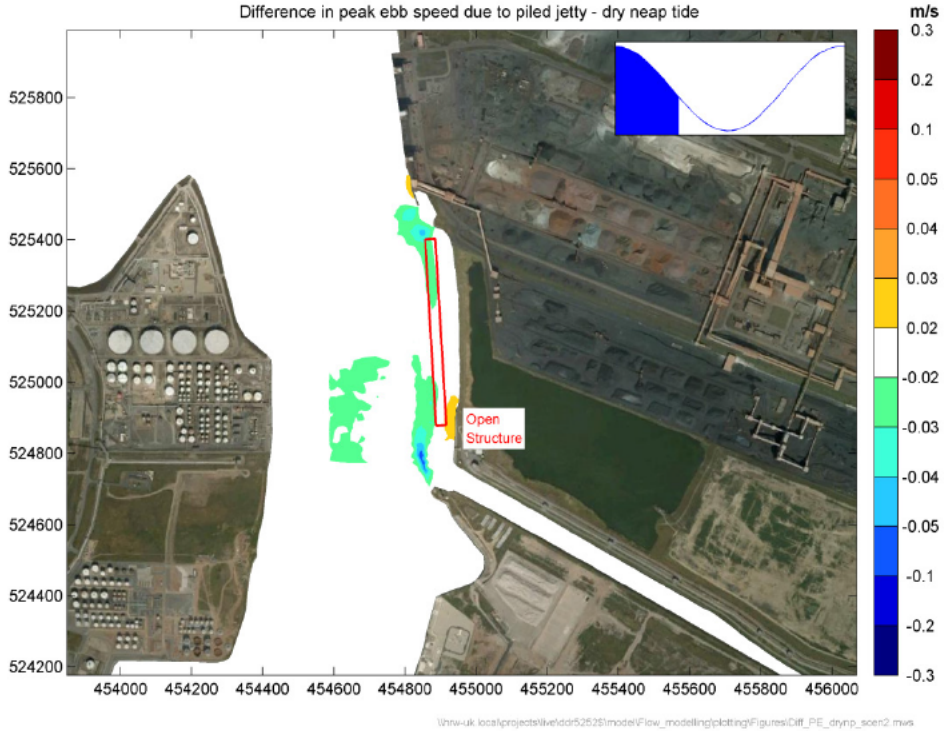

Figure B.2: Change in depth average currents at peak ebb tide for open quay, neap tide low river flow

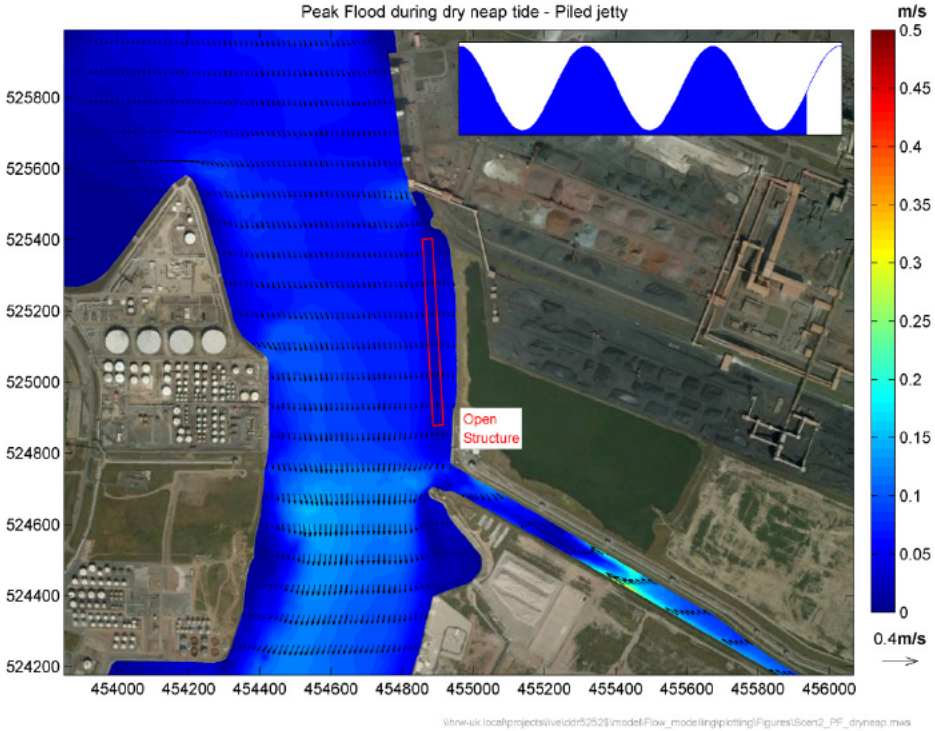

Figure B.3: Depth average currents at peak flood tide for open quay, neap tide low river flow

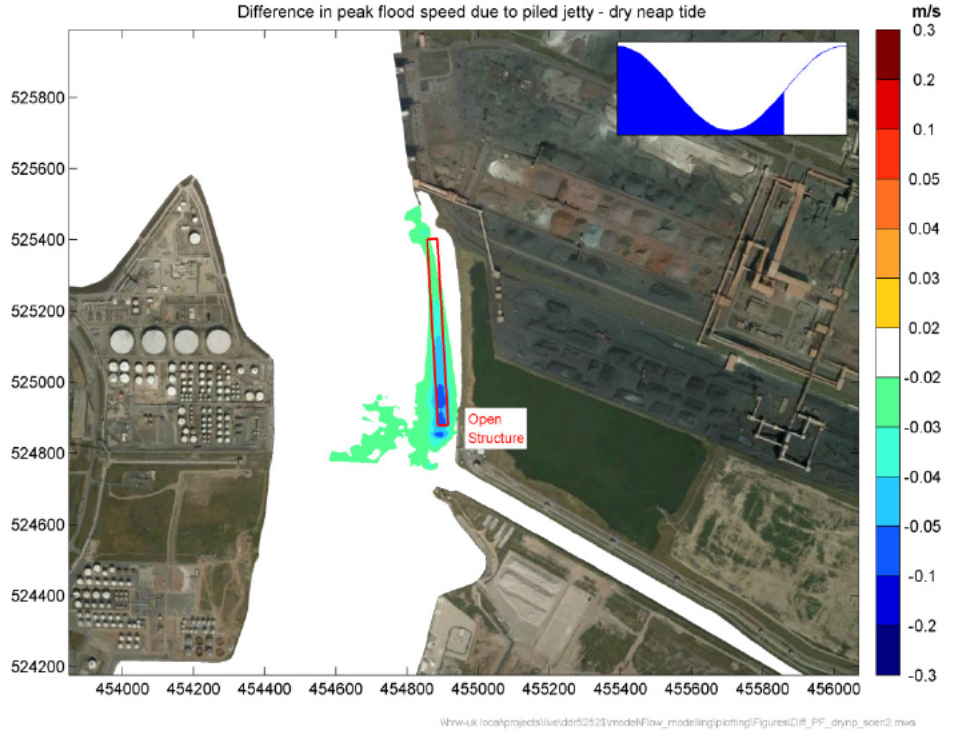

Figure B.4: Change in depth average currents at peak flood tide for open quay, neap tide low river flow

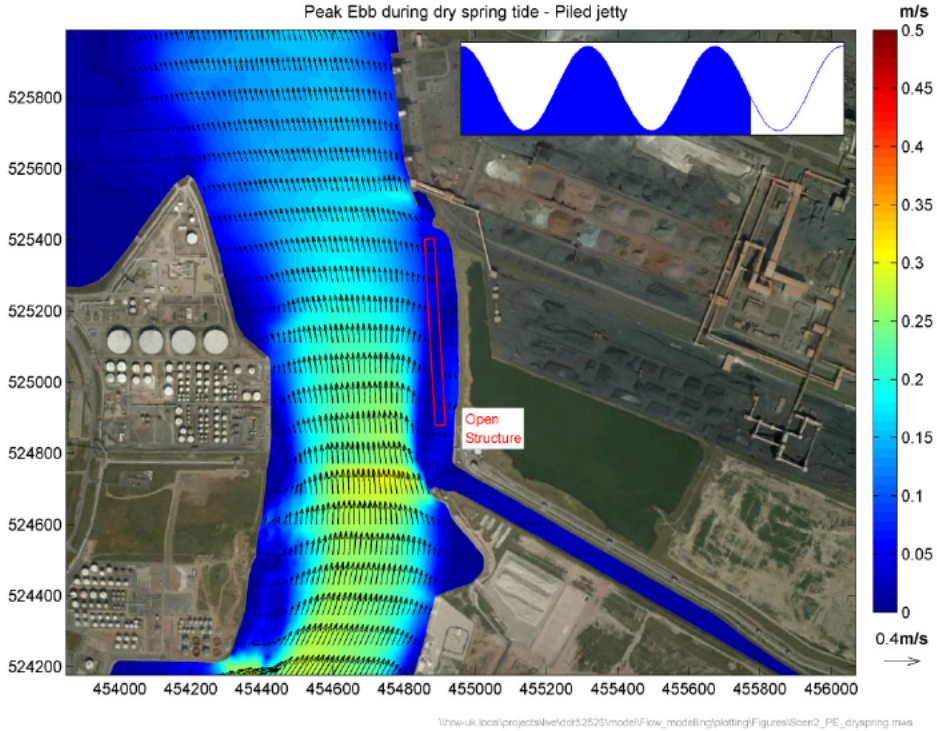

Figure B.5: Depth average currents at peak ebb tide for open quay, spring tide low river flow

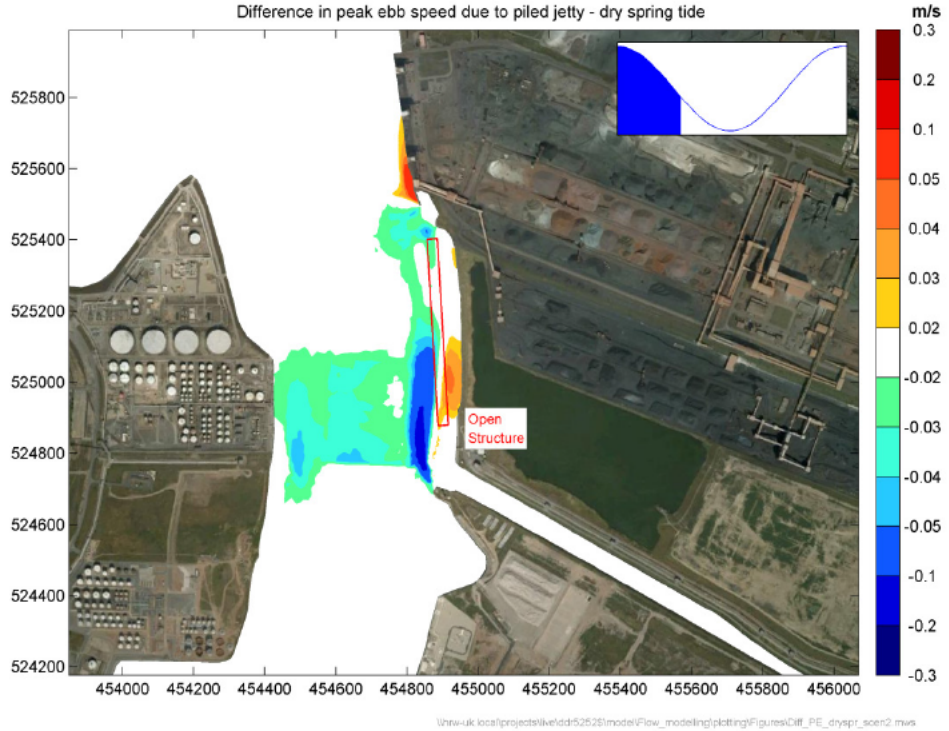

Figure B.6: Change in depth average currents at peak ebb tide for open quay, spring tide low river flow

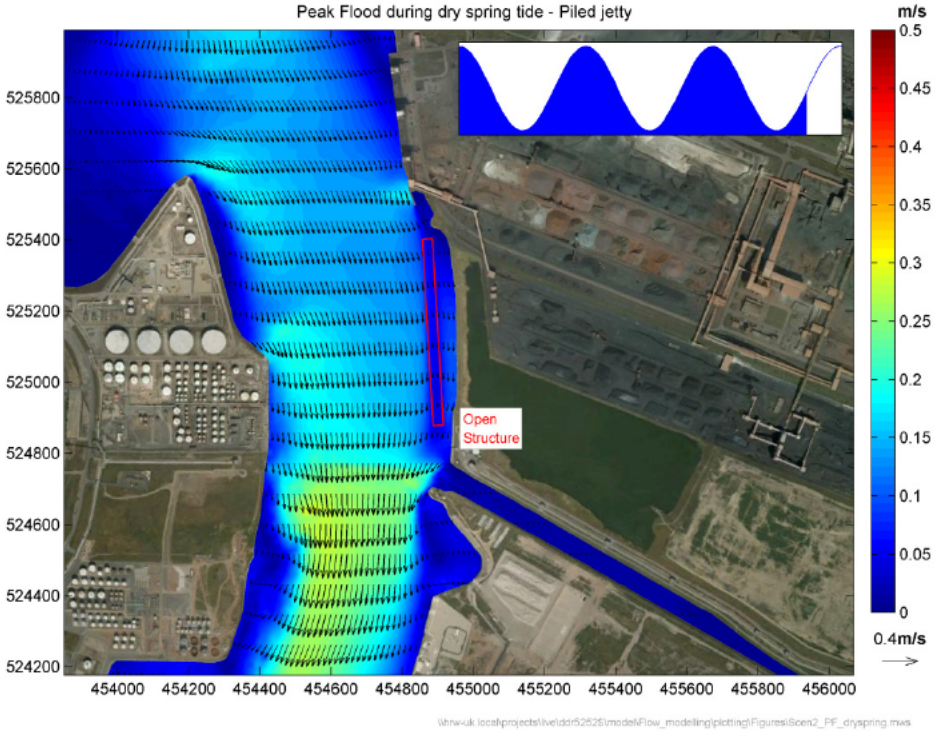

Figure B.7: Depth average currents at peak flood tide for open quay, spring tide low river flow

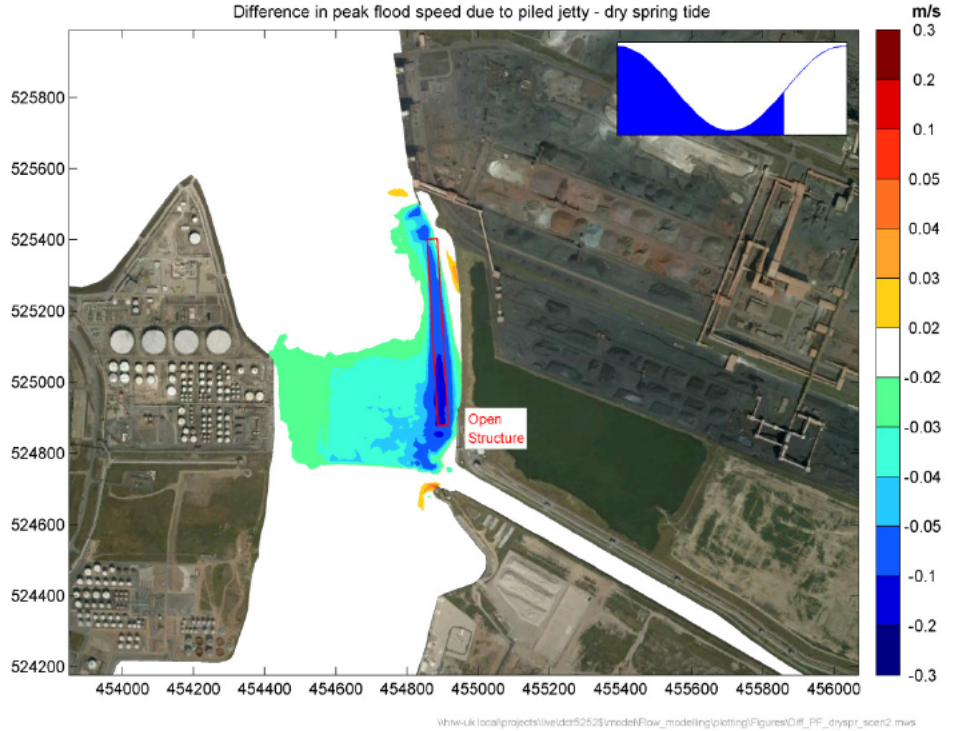

Figure B.8: Change in depth average currents at peak flood tide for open quay, spring tide low river flow

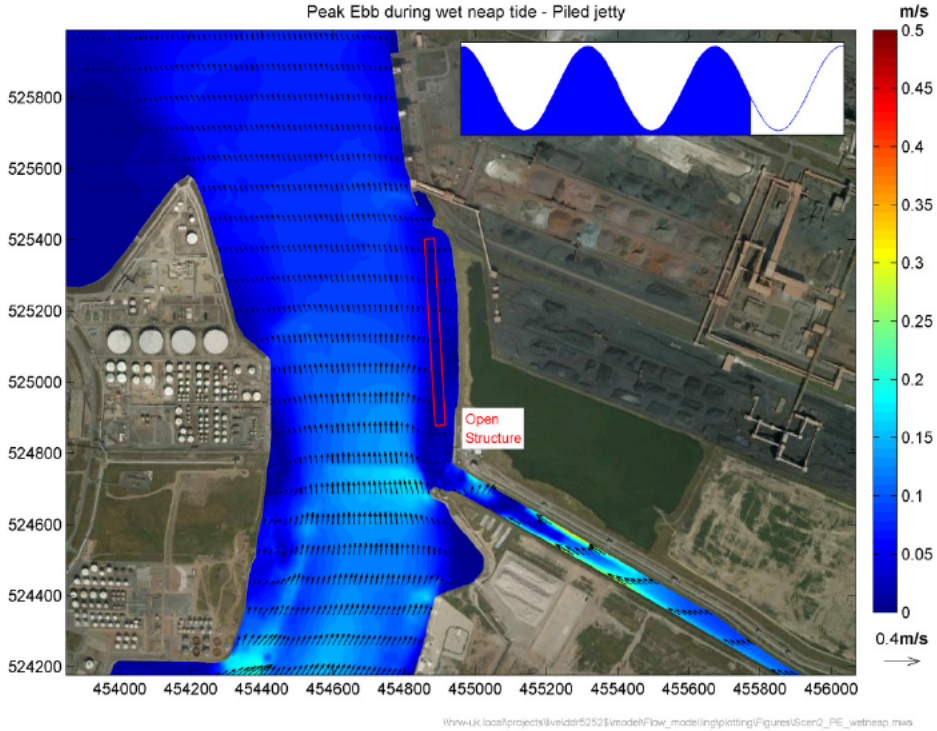

Figure B.9: Depth average currents at peak ebb tide for open quay, neap tide high river flow

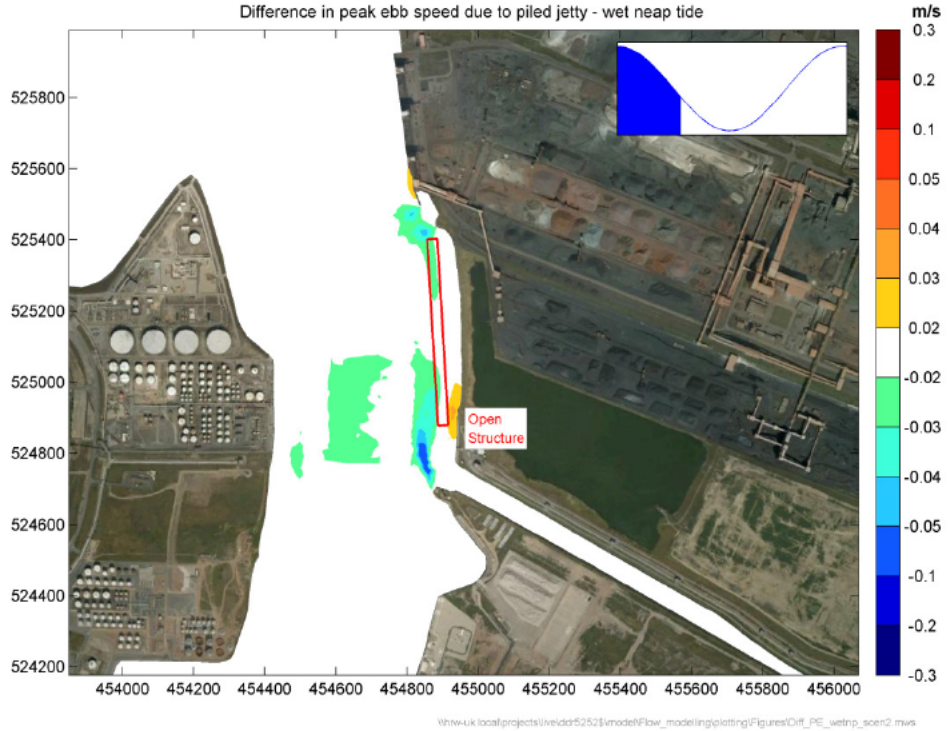

Figure B.10: Change in depth average currents at peak ebb tide for open quay, neap tide high river flow

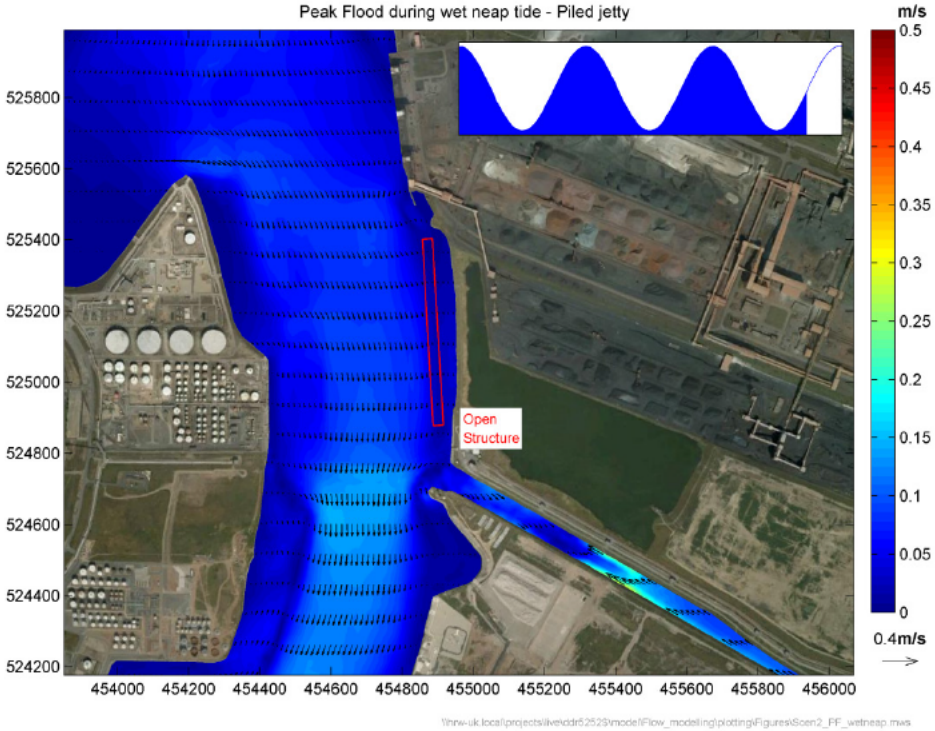

Figure B.11: Depth average currents at peak flood tide for open quay, neap tide high river flow

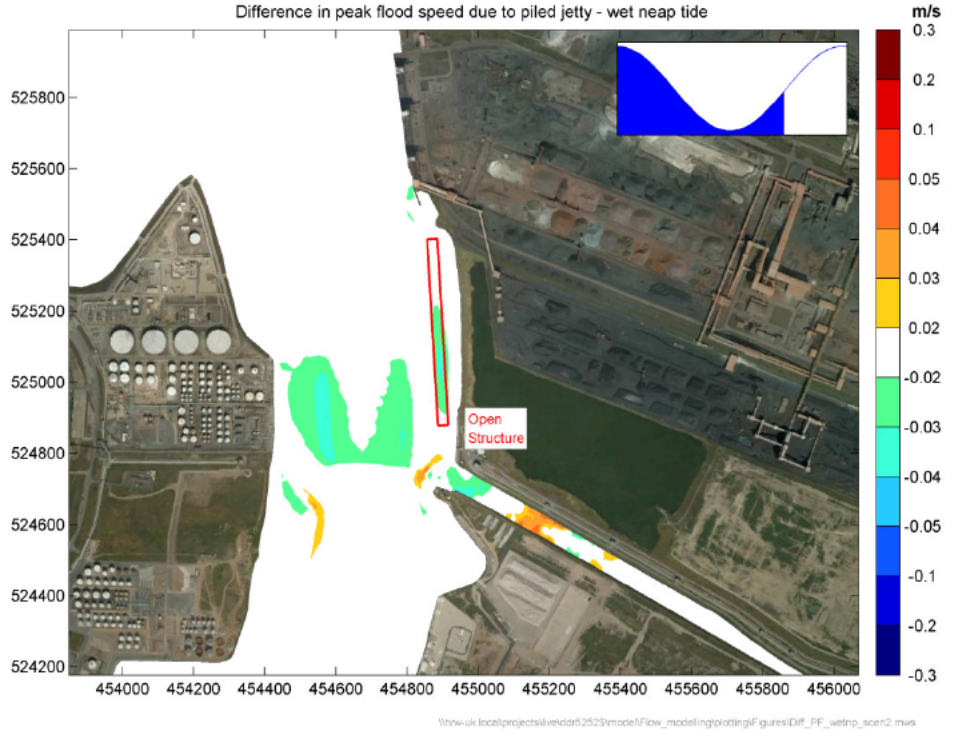

Figure B.12: Change in depth average currents at peak flood tide for open quay, neap tide high river flow

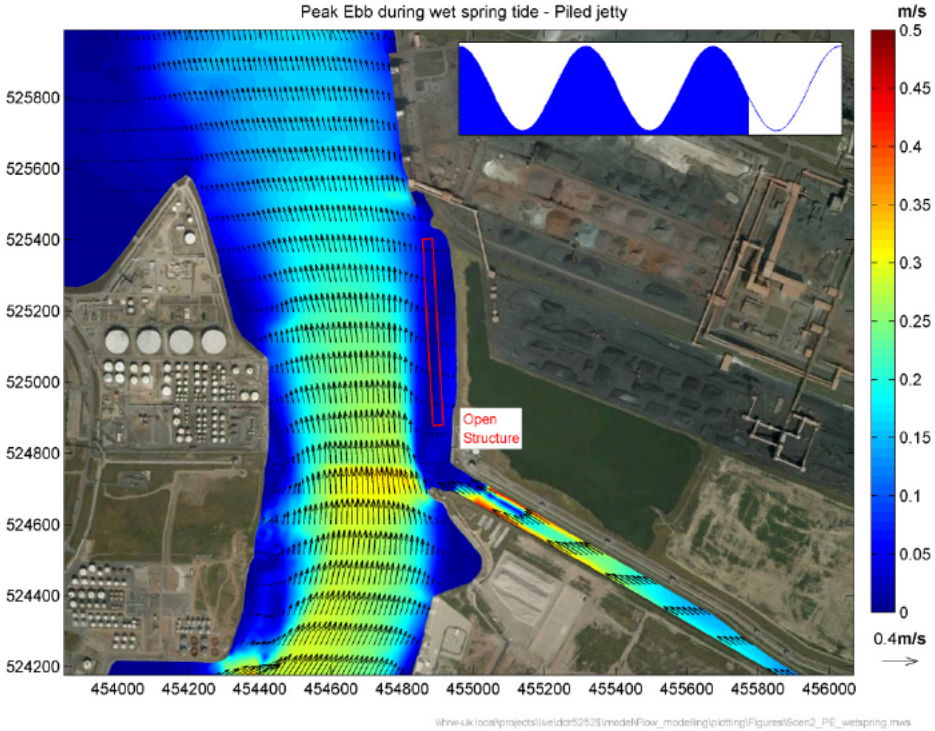

Figure B.13: Depth average currents at peak ebb tide for open quay, spring tide high river flow

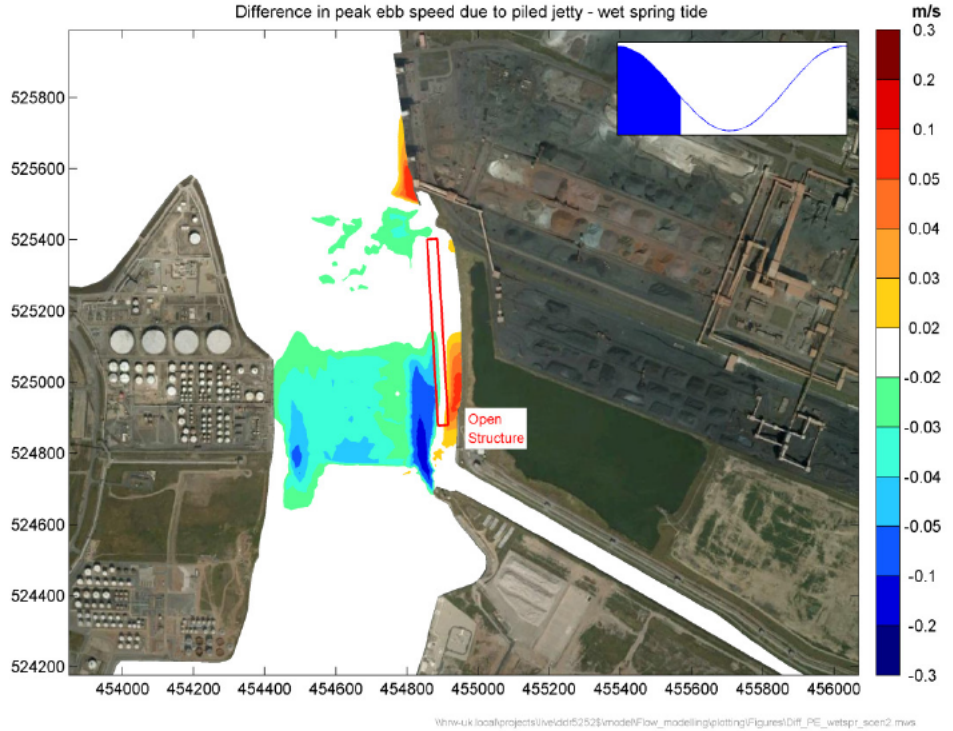

Figure B.14: Change in depth average currents at peak ebb tide for open quay, spring tide high river flow

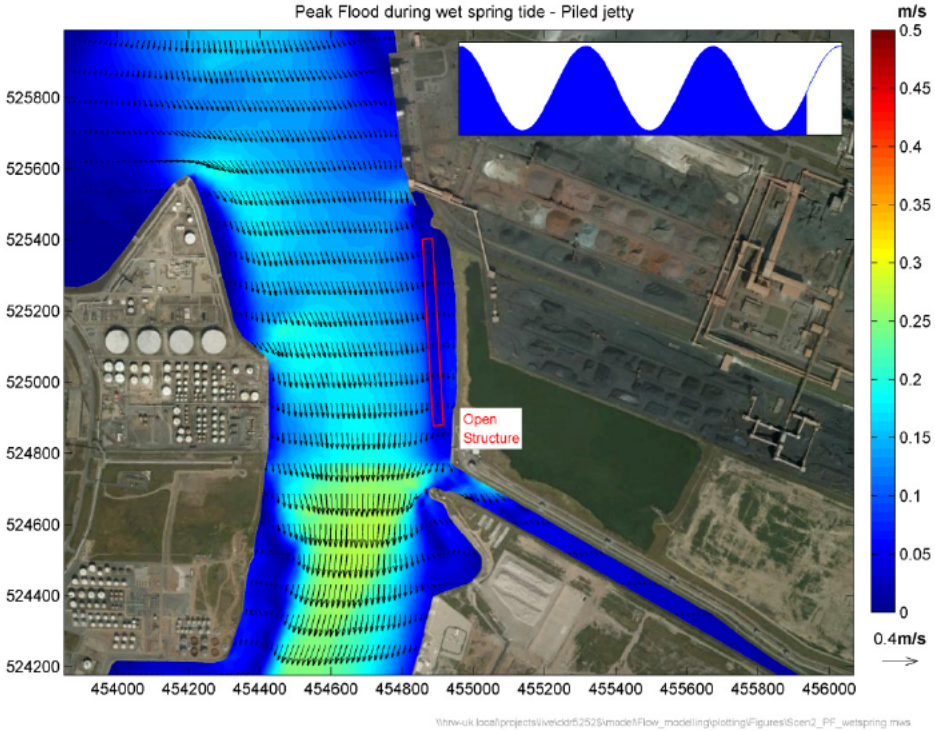

Figure B.15: Depth average currents at peak flood tide for open quay, spring tide high river flow

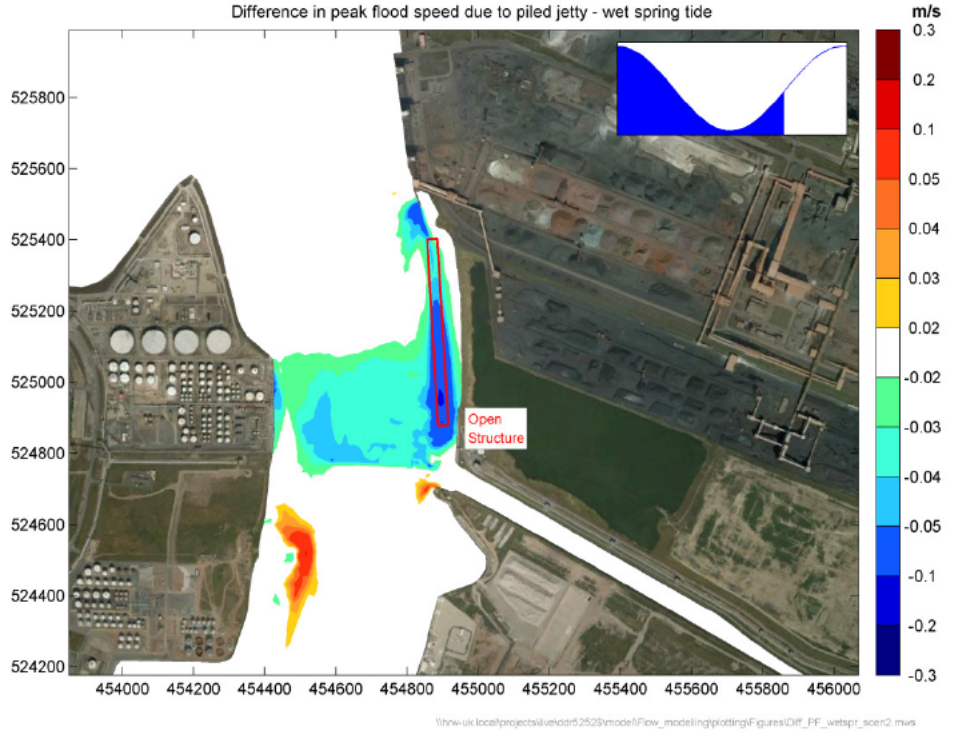

Figure B.16: Change in depth average currents at peak flood tide for open quay, spring tide high river flow

C. Time series results from flow modelling

Neap tide, low river flow

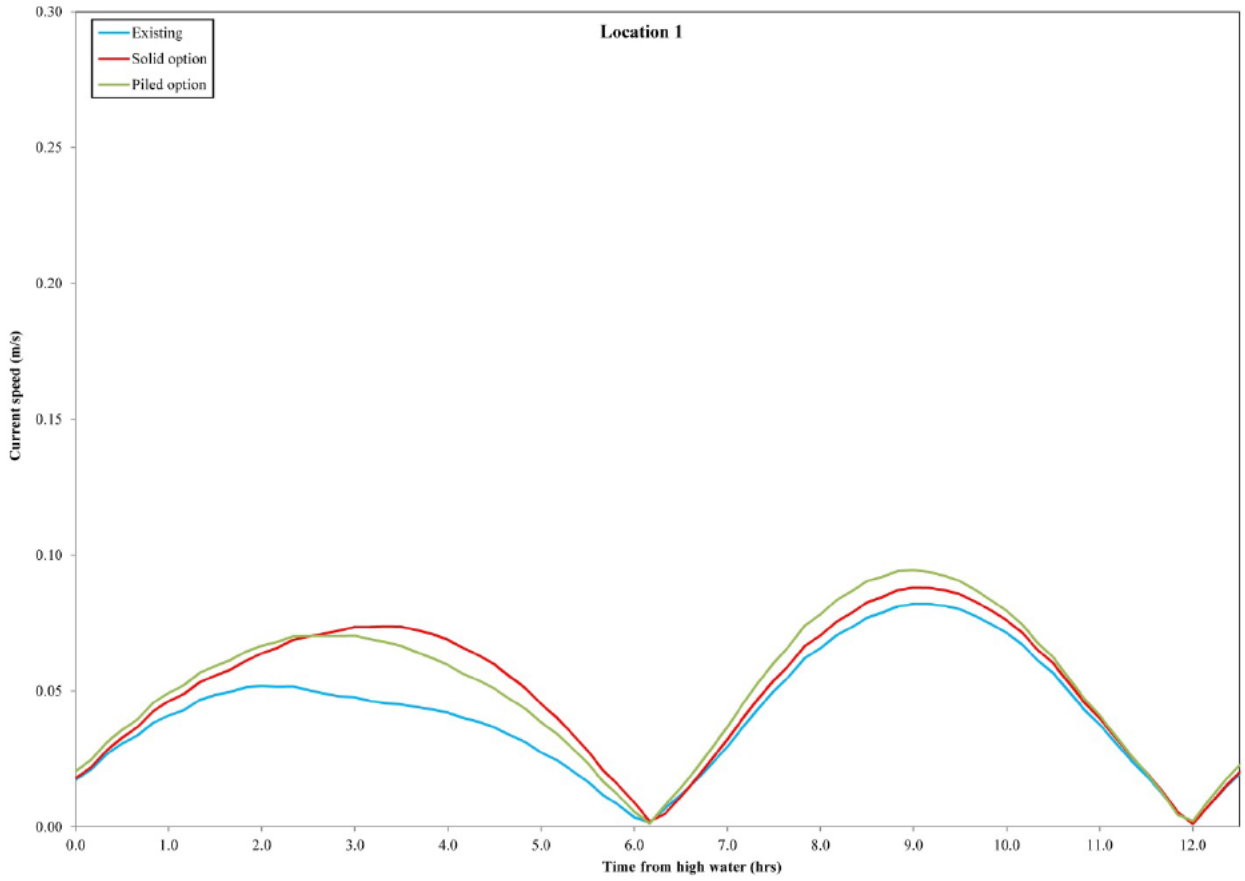

Figure C.1: Time series results at Point 1, neap tide, low river flow

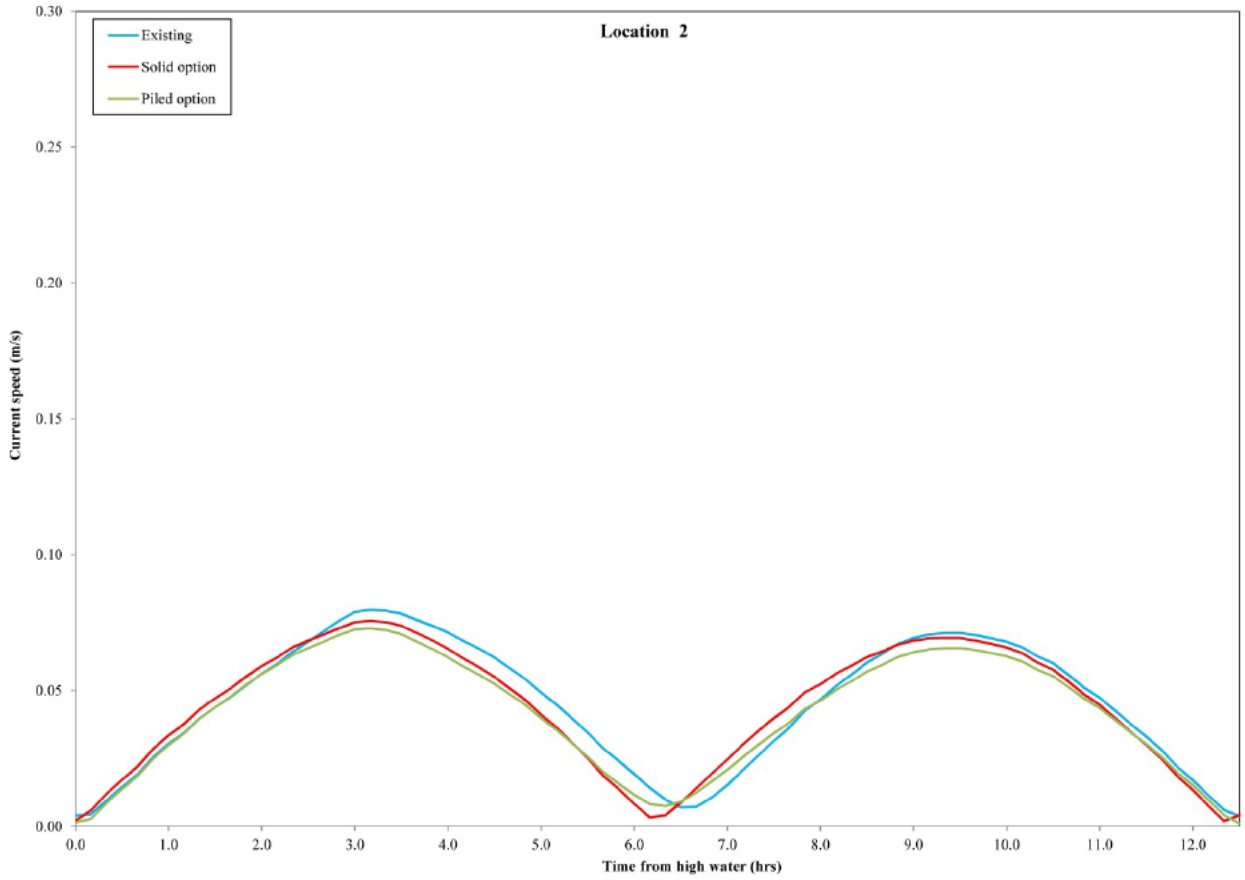

Figure C.2: Time series results at Point 2, neap tide, low river flow

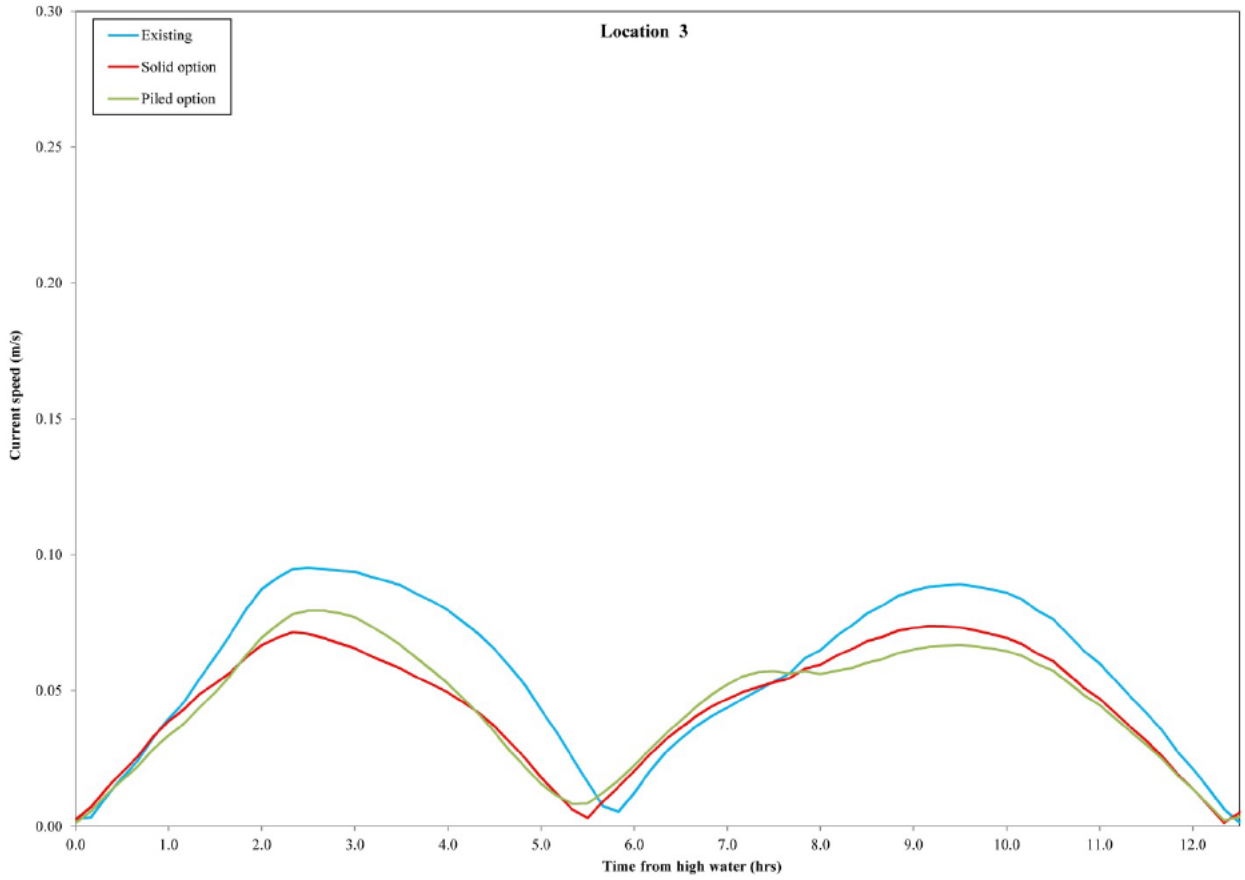

Figure C.3: Time series results at Point 3, neap tide, low river flow

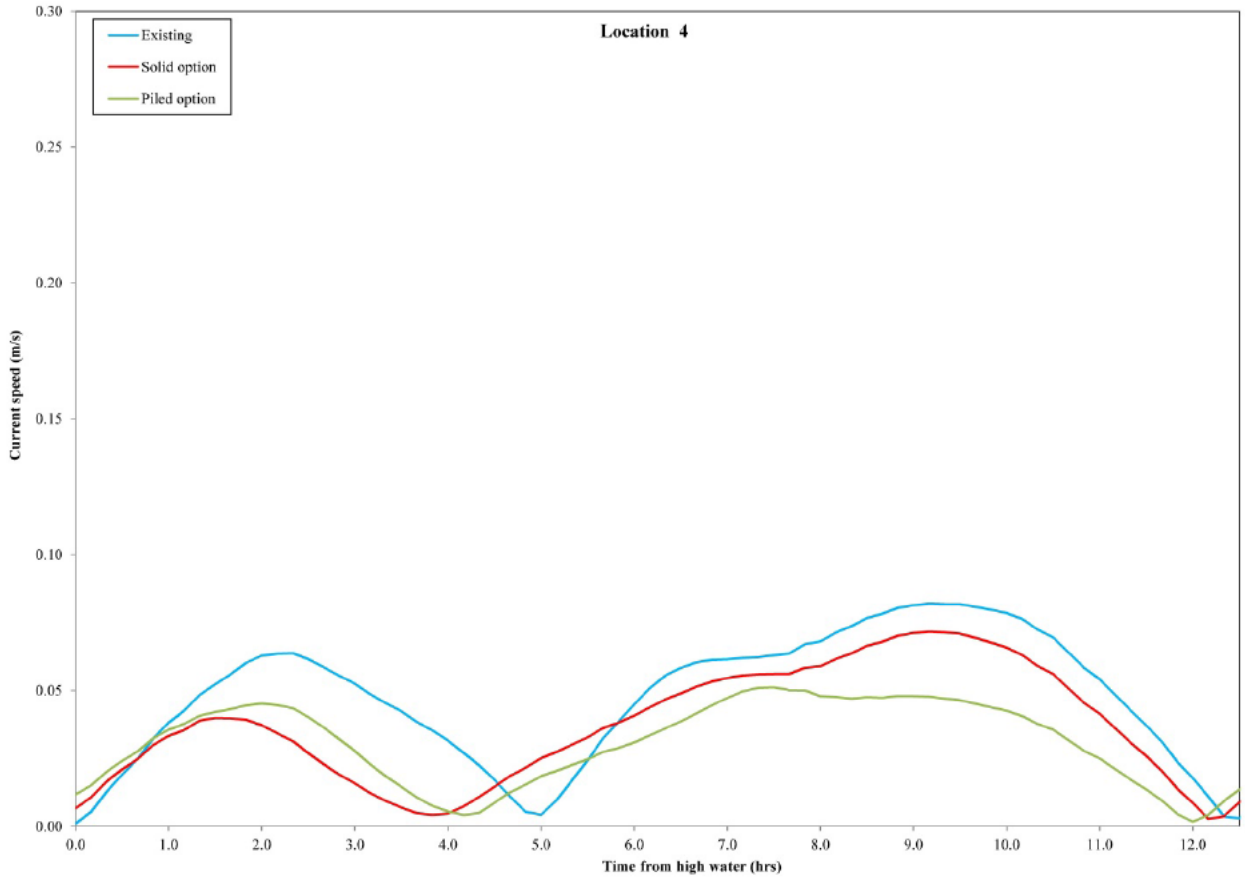

Figure C.4: Time series results at Point 4, neap tide, low river flow

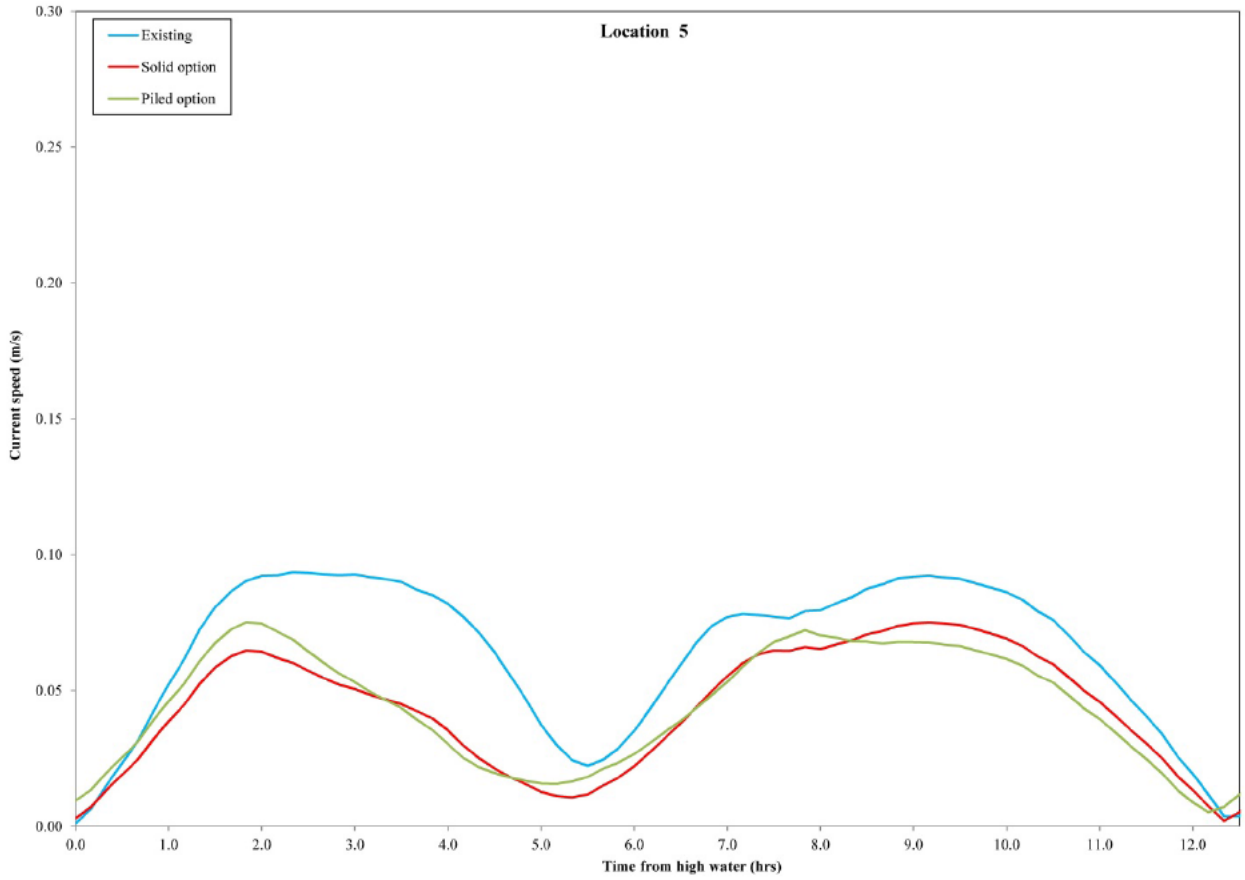

Figure C.5: Time series results at Point 5, neap tide, low river flow

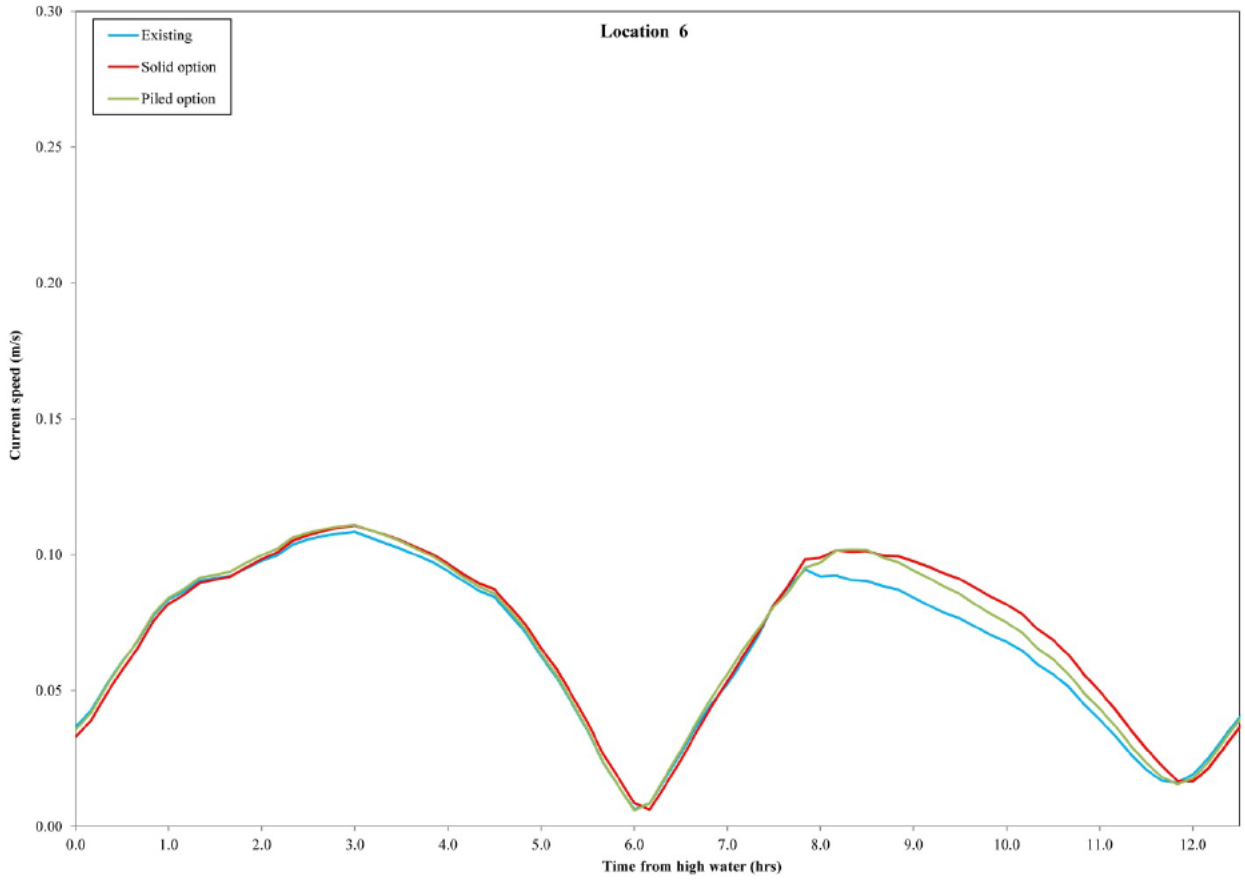

Figure C.6: Time series results at Point 6, neap tide, low river flow

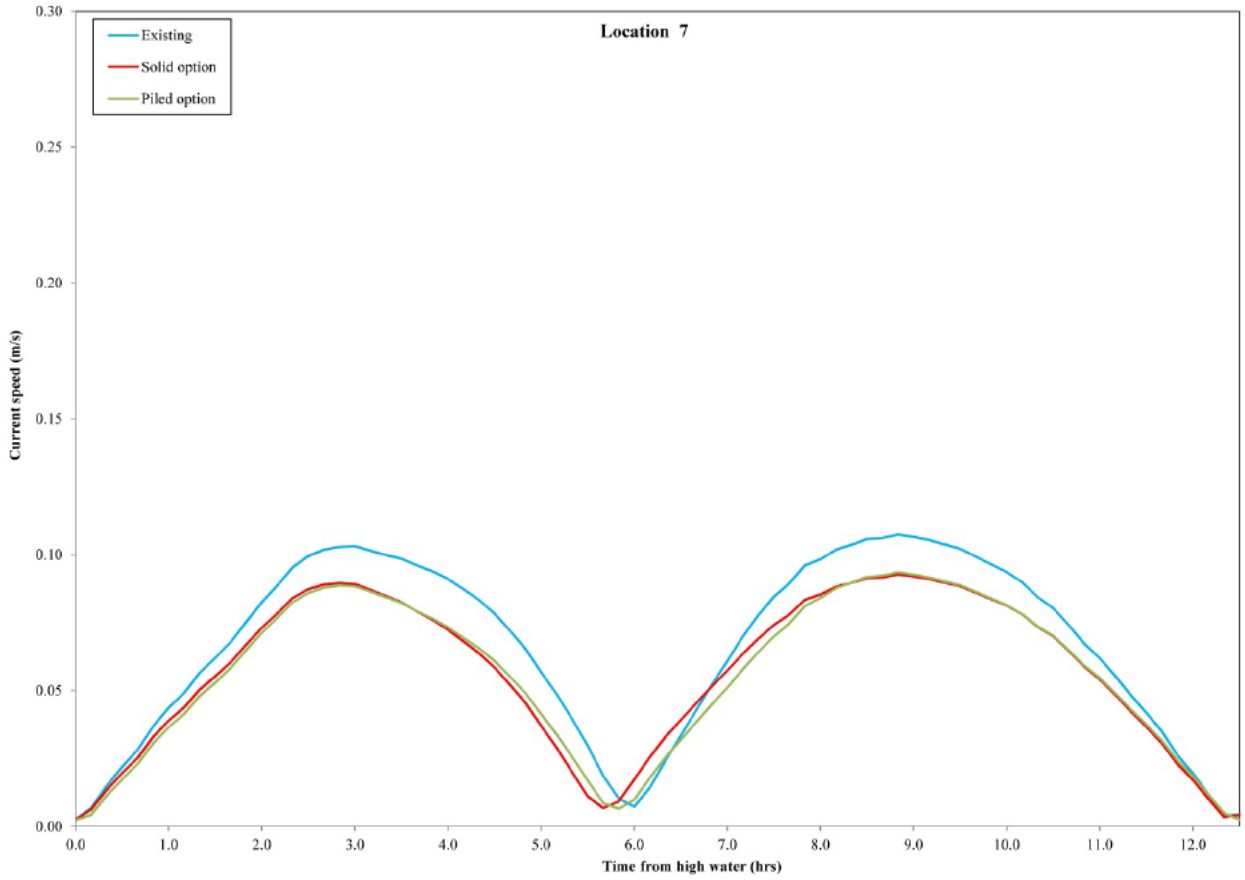

Figure C.7: Time series results at Point 7, neap tide, low river flow

Spring tide, low river flow

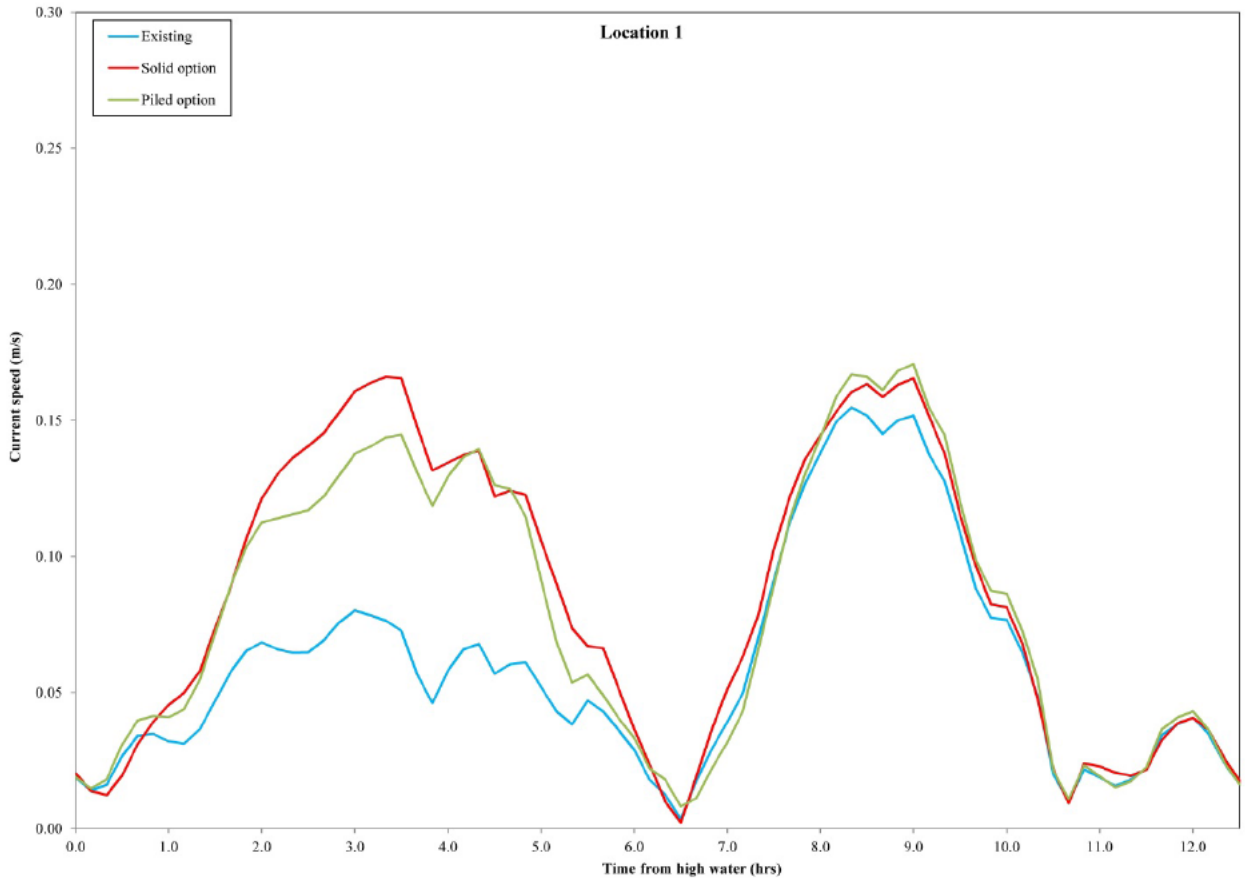

Figure C.8: Time series results at Point 1, spring tide, low river flow

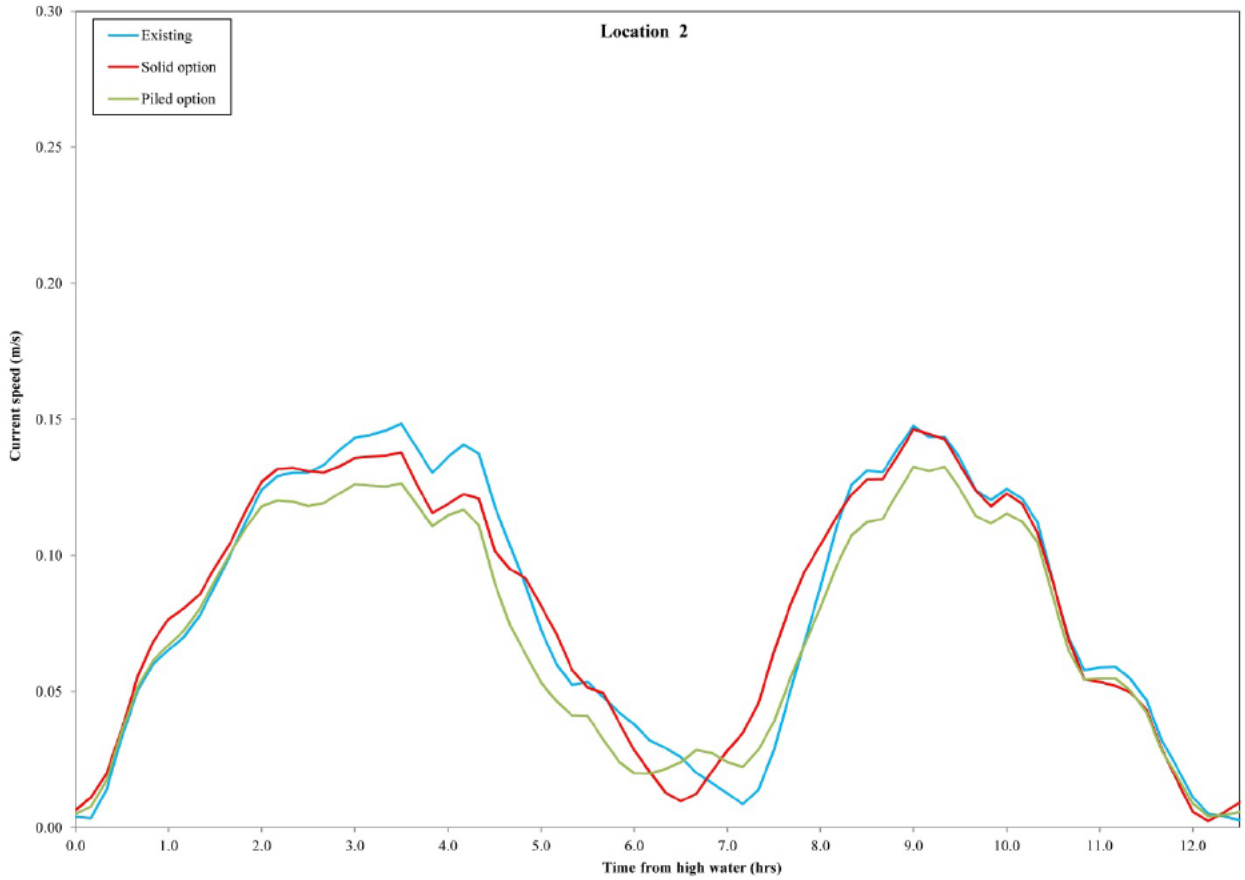

Figure C.9: Time series results at Point 2, spring tide, low river flow

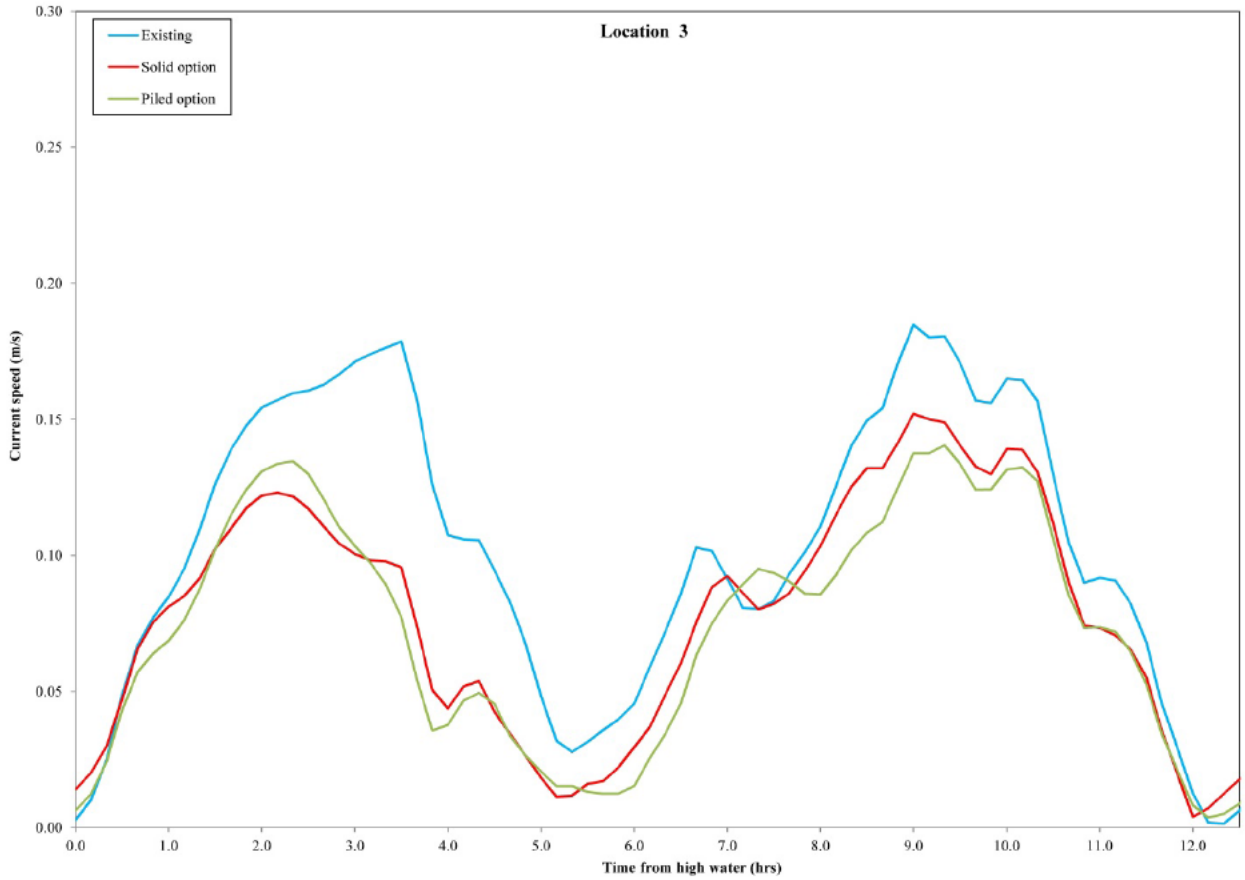

Figure C.10: Time series results at Point 3, spring tide, low river flow

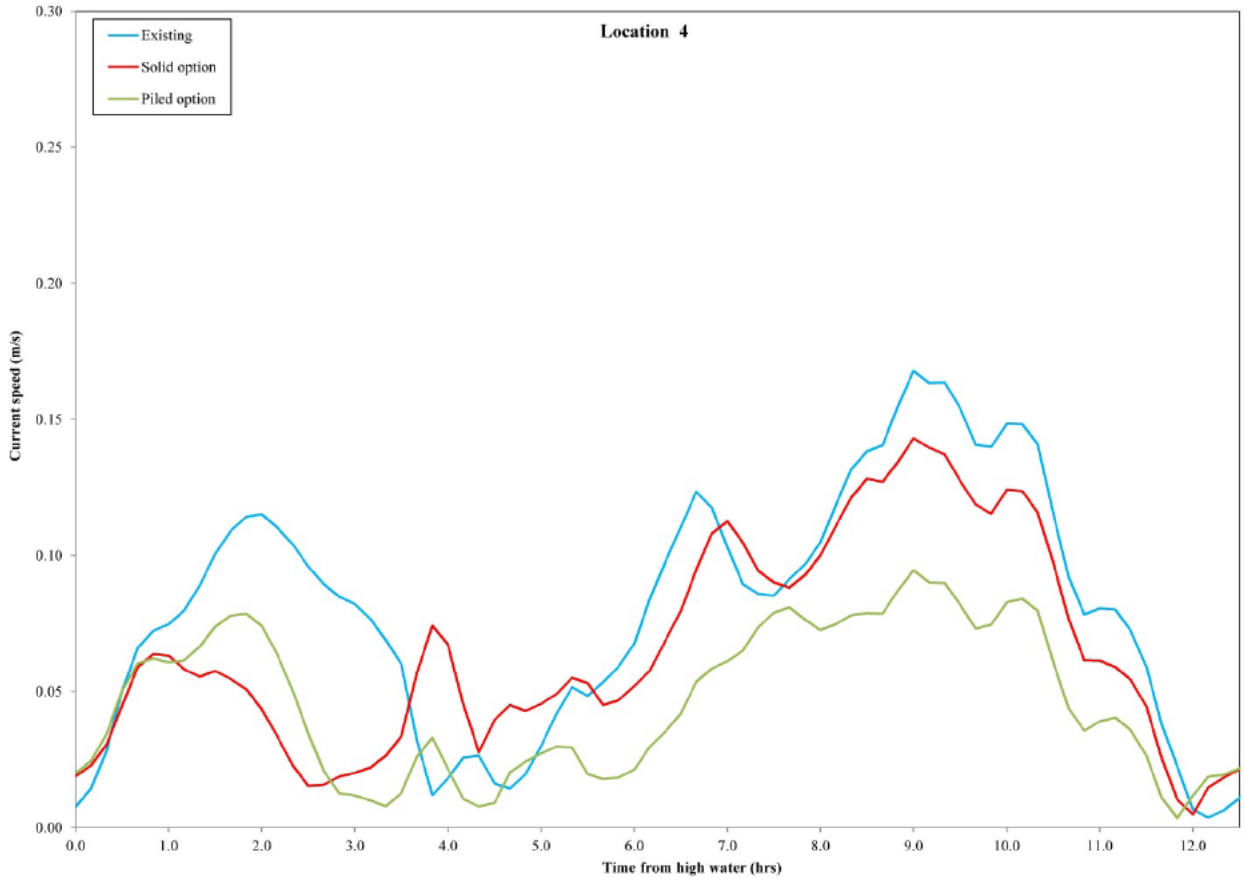

Figure C.11: Time series results at Point 4, spring tide, low river flow

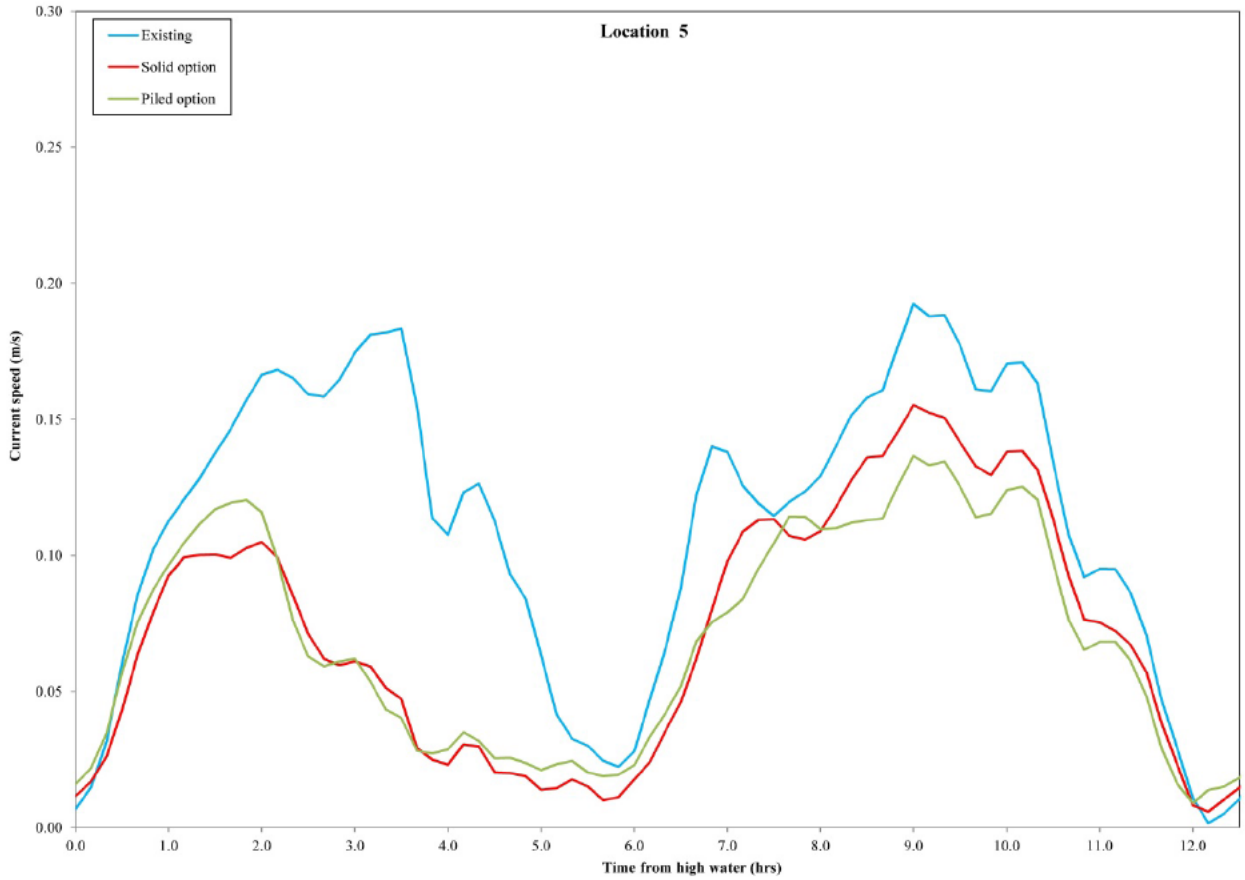

Figure C.12: Time series results at Point 5, spring tide, low river flow

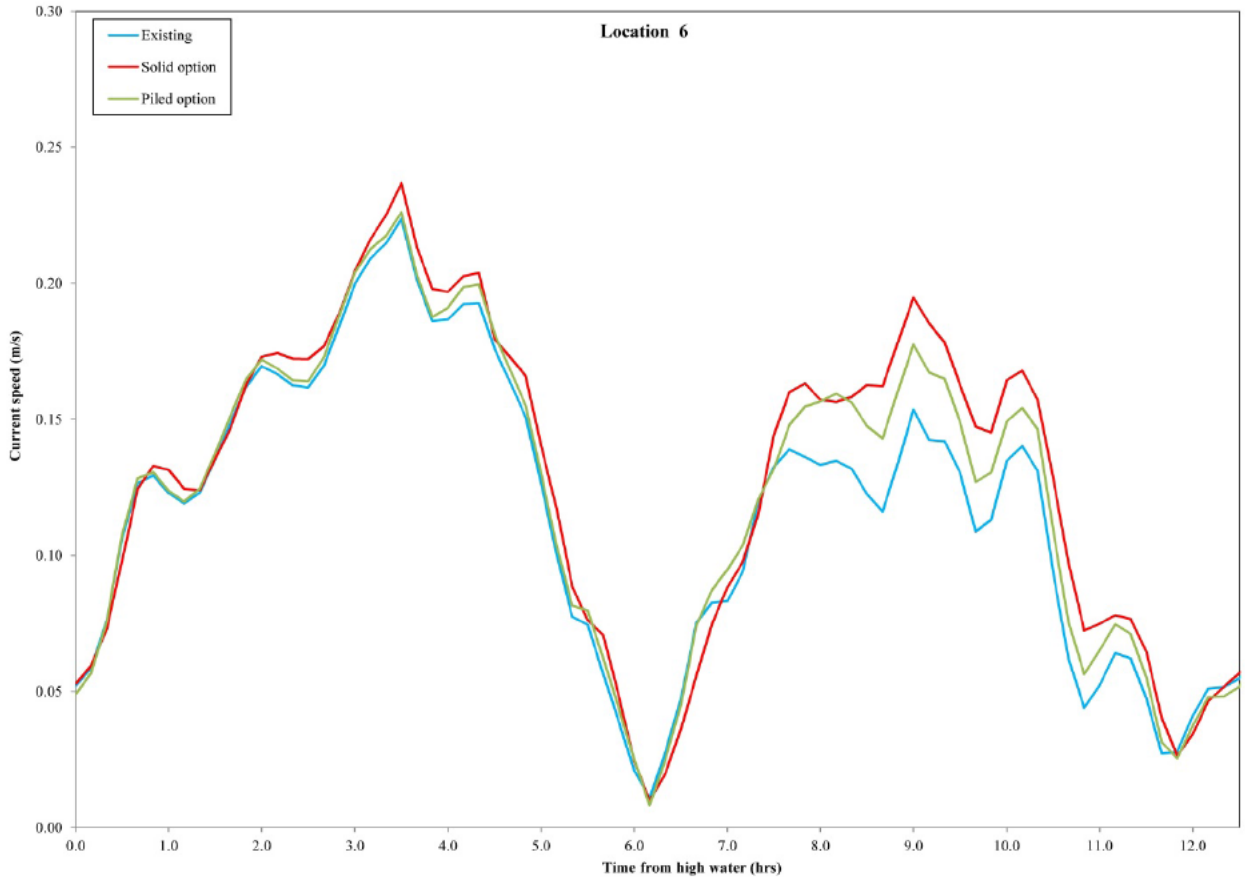

Figure C.13: Time series results at Point 6, spring tide, low river flow

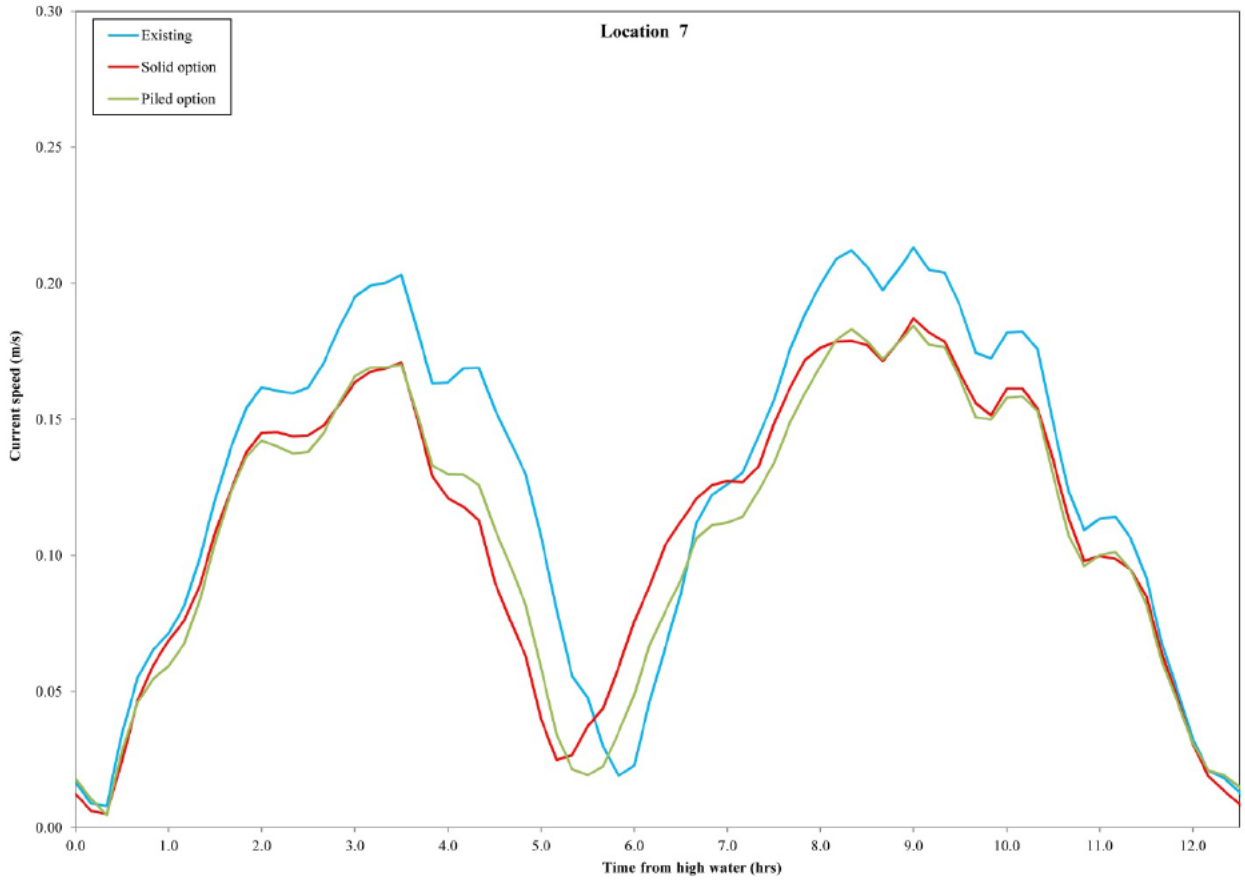

Figure C.14: Time series results at Point 7, spring tide, low river flow

Neap tide, high river flow

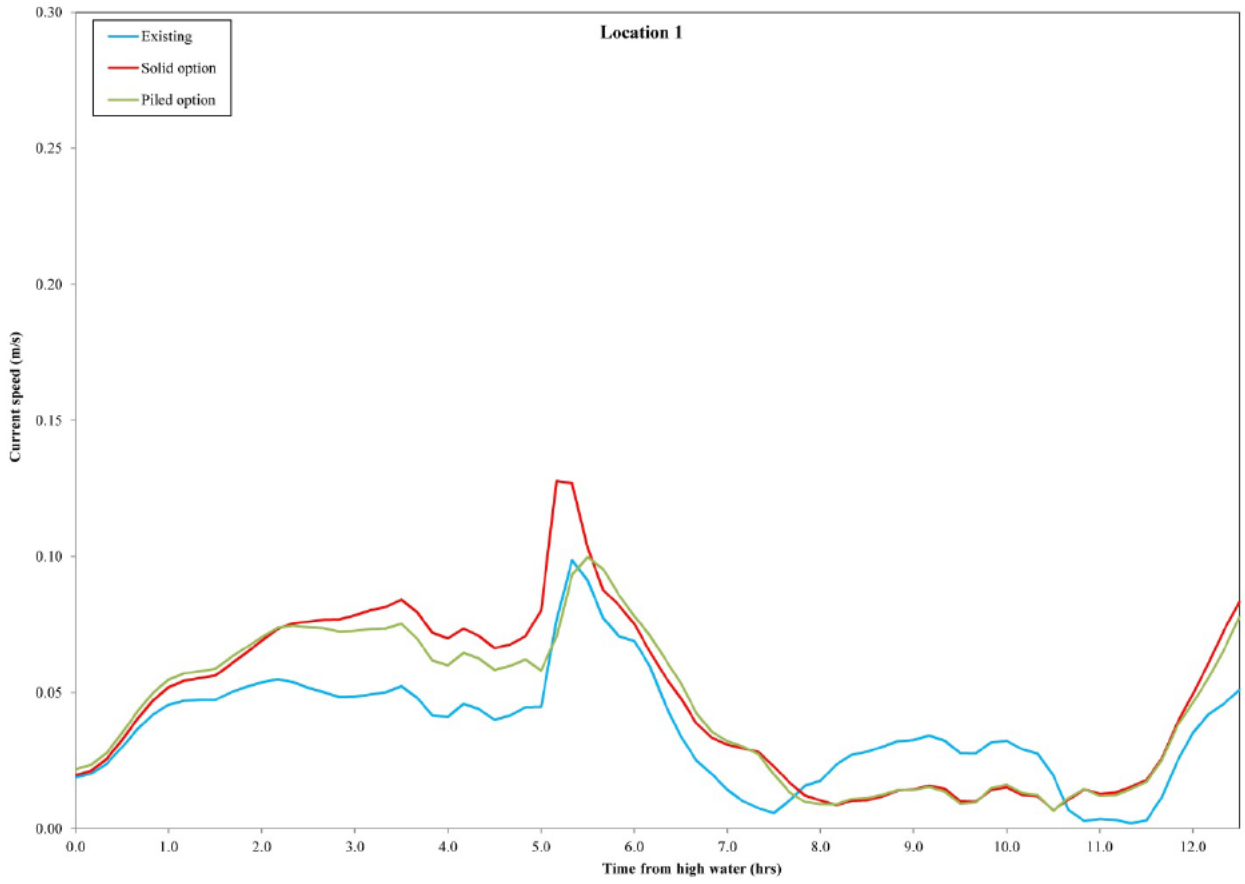

Figure C.15: Time series results at Point 1, neap tide, high river flow

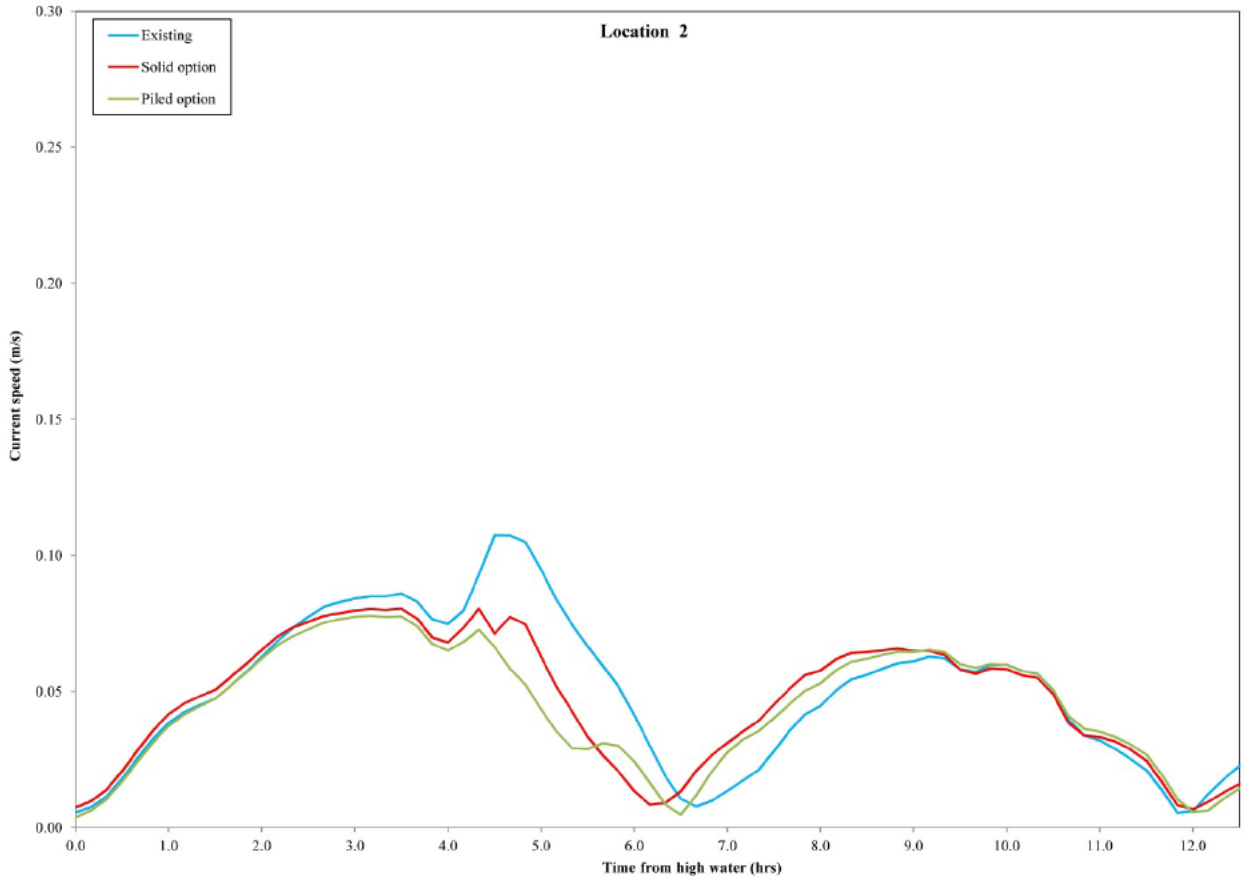

Figure C.16: Time series results at Point 2, neap tide, low river flow

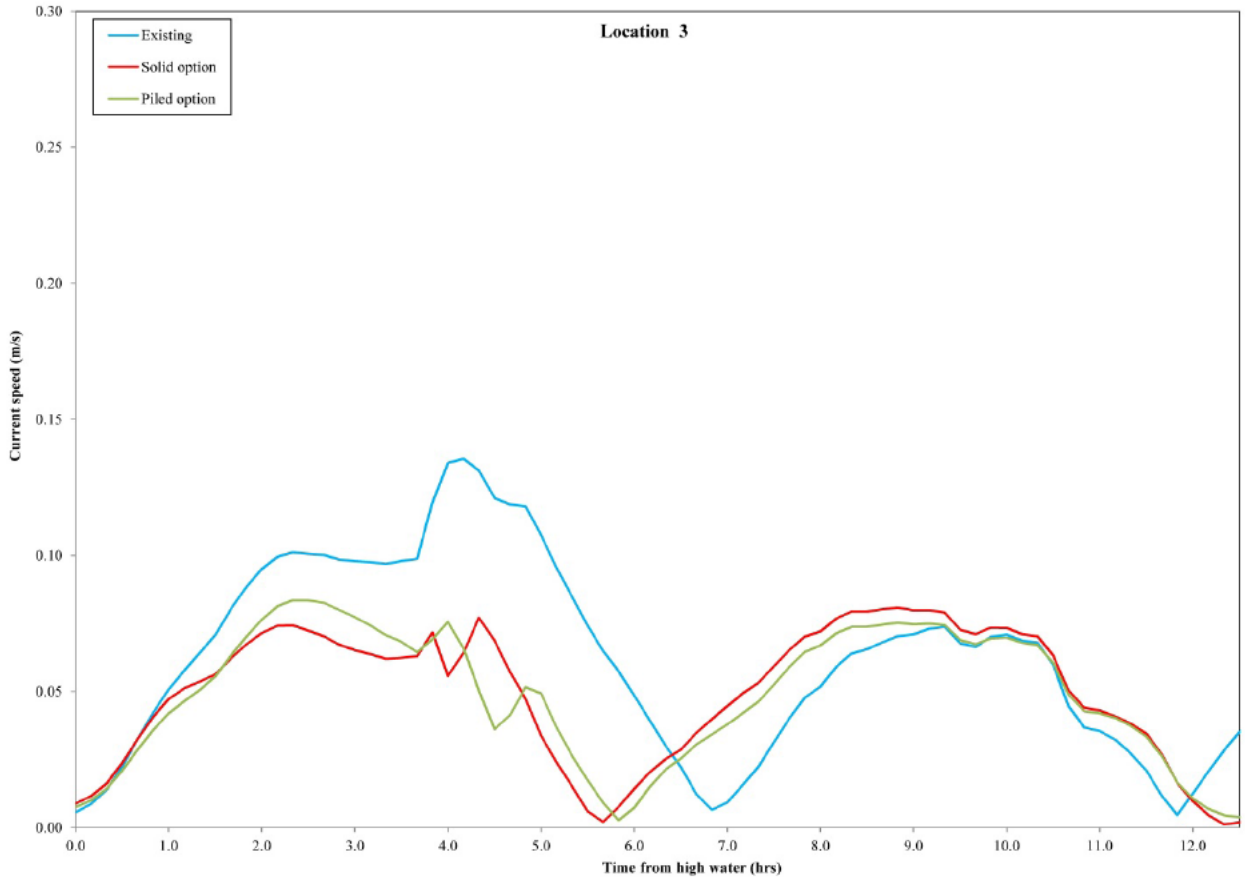

Figure C.17: Time series results at Point 3, neap tide, high river flow

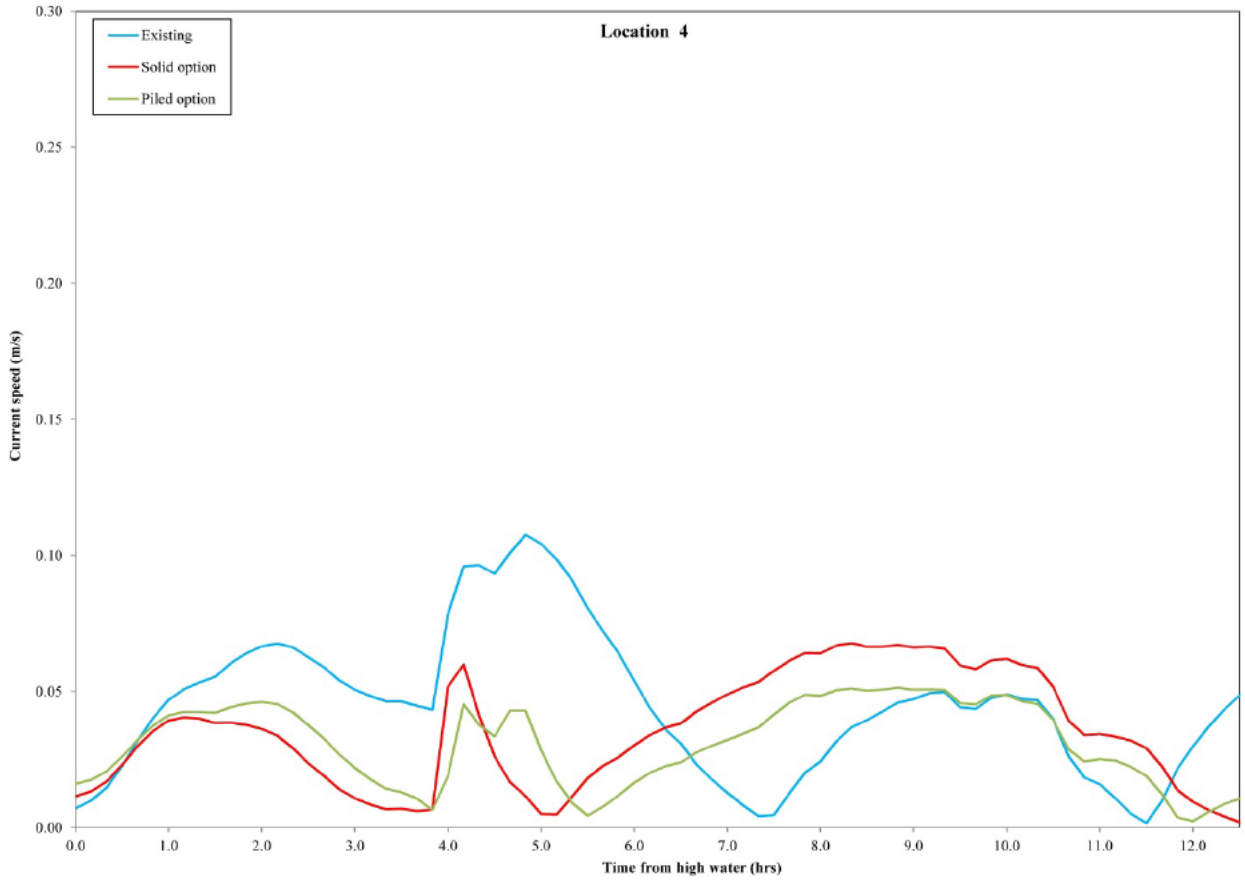

Figure C.18: Time series results at Point 4, neap tide, high river flow

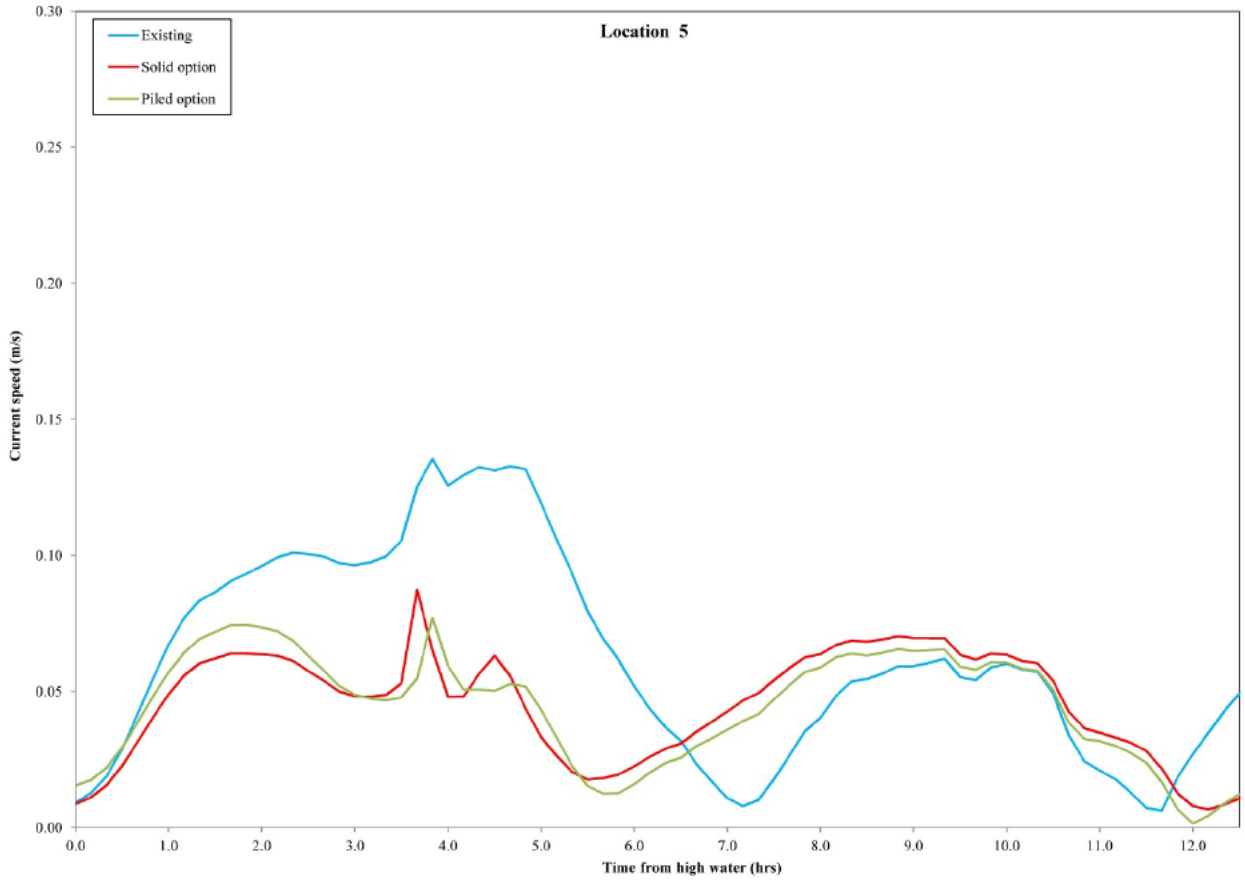

Figure C.19: Time series results at Point 5, neap tide, high river flow

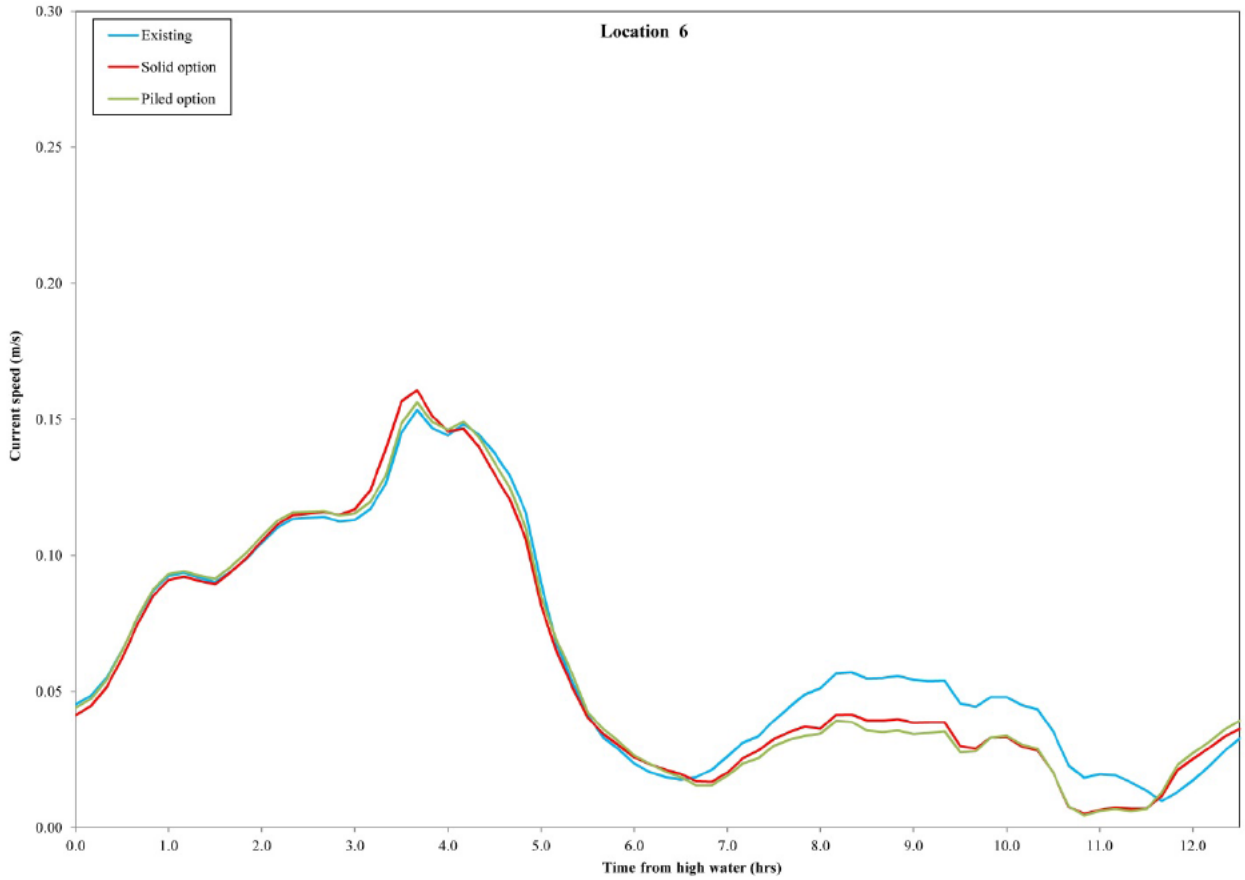

Figure C.20: Time series results at Point 6, neap tide, high river flow

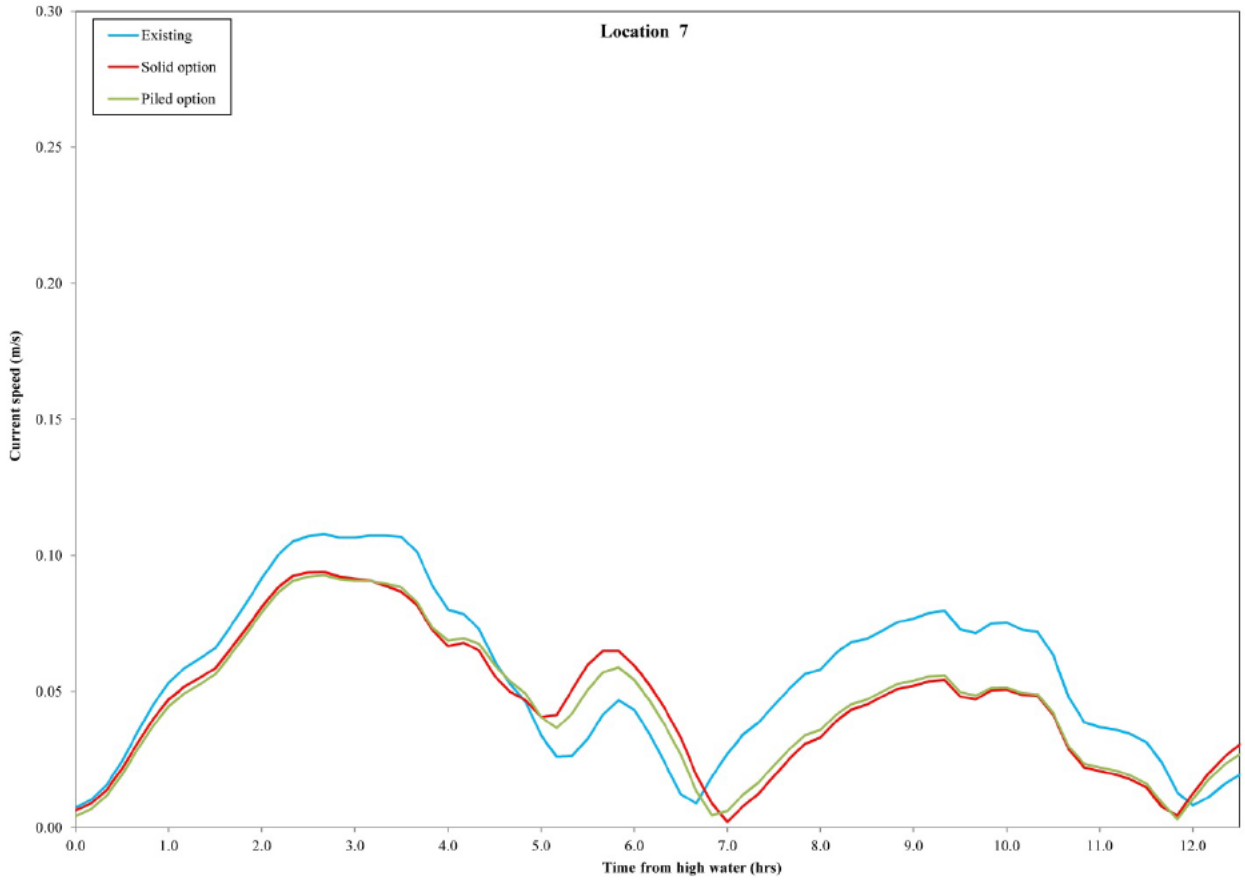

Figure C.21: Time series results at Point 7, neap tide, high river flow

Spring tide, high river flow

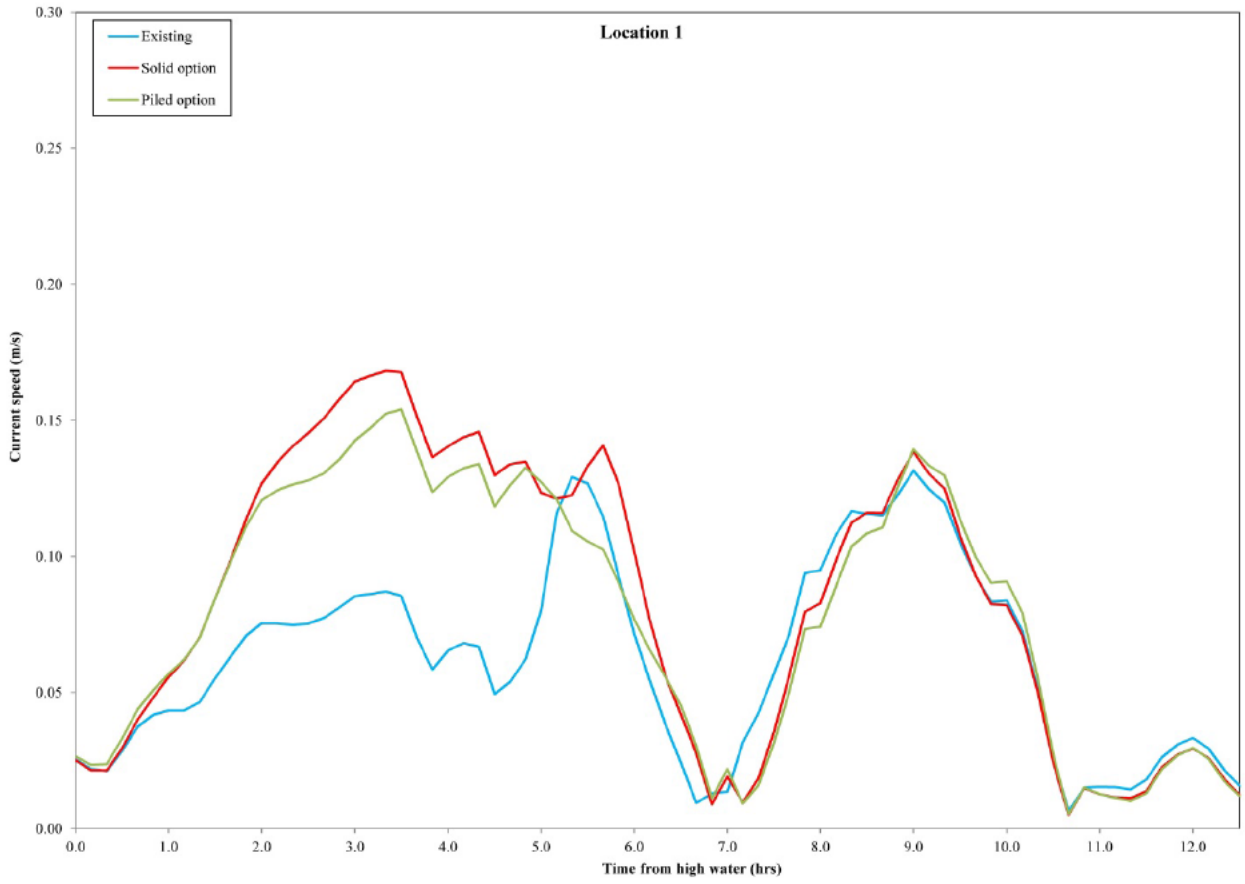

Figure C.22: Time series results at Point 1, spring tide, high river flow

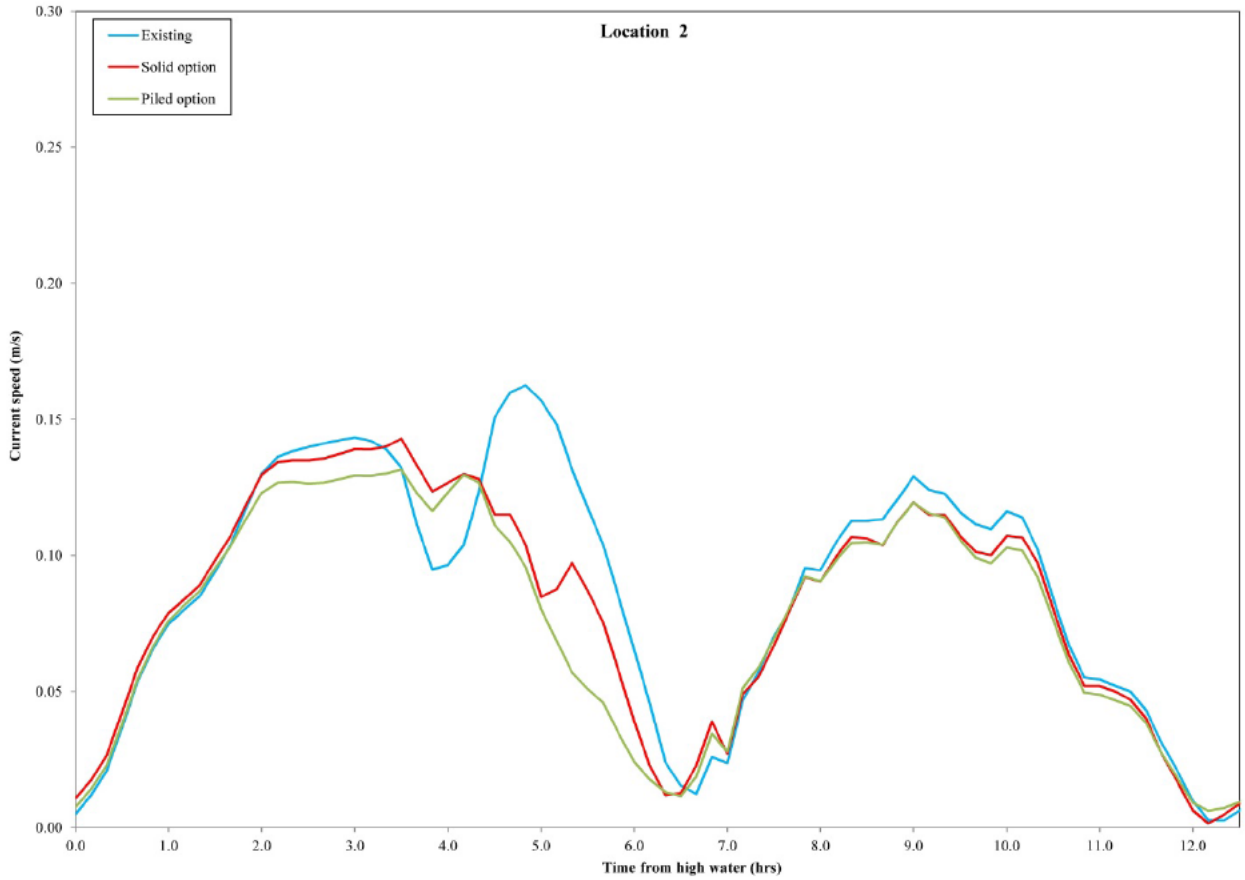

Figure C.23: Time series results at Point 2, spring tide, high river flow

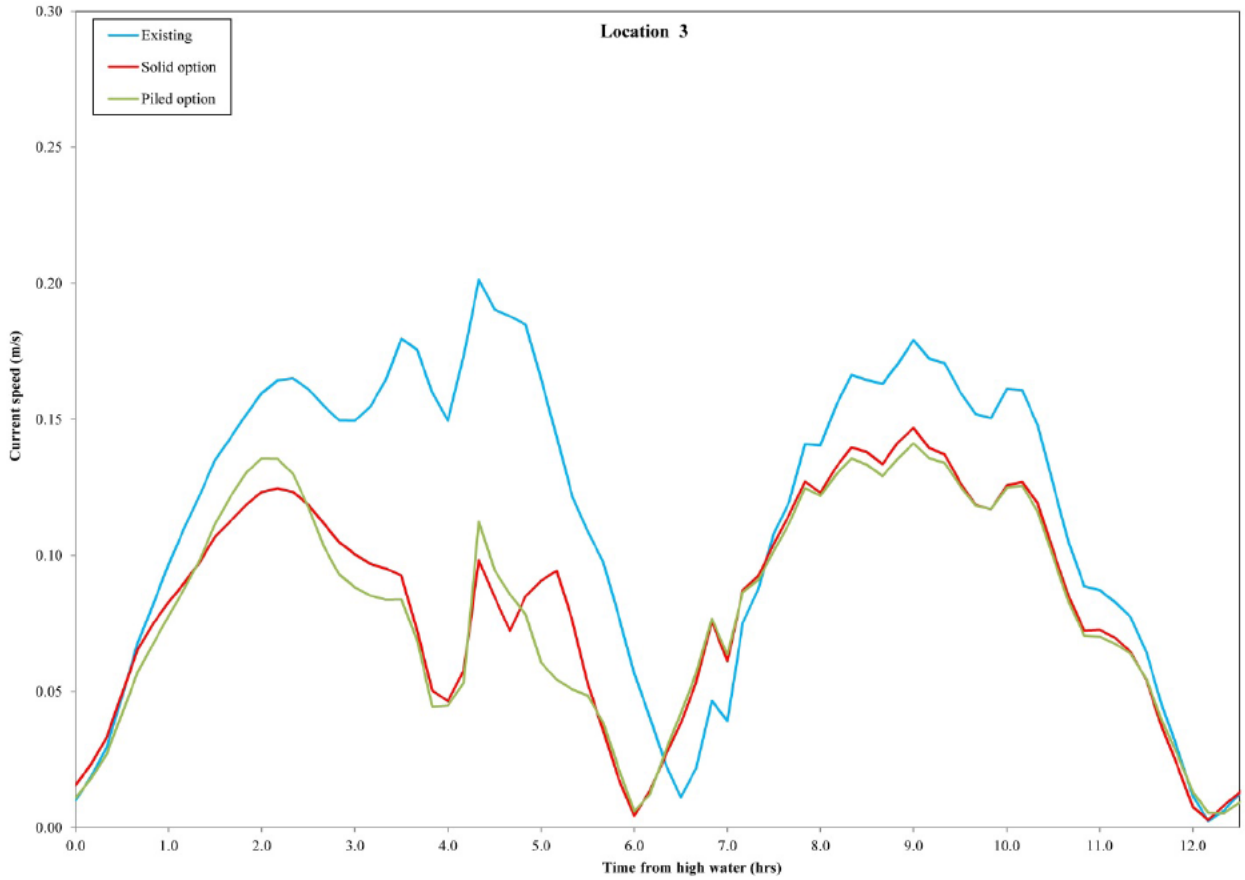

Figure C.24: Time series results at Point 3, spring tide, high river flow

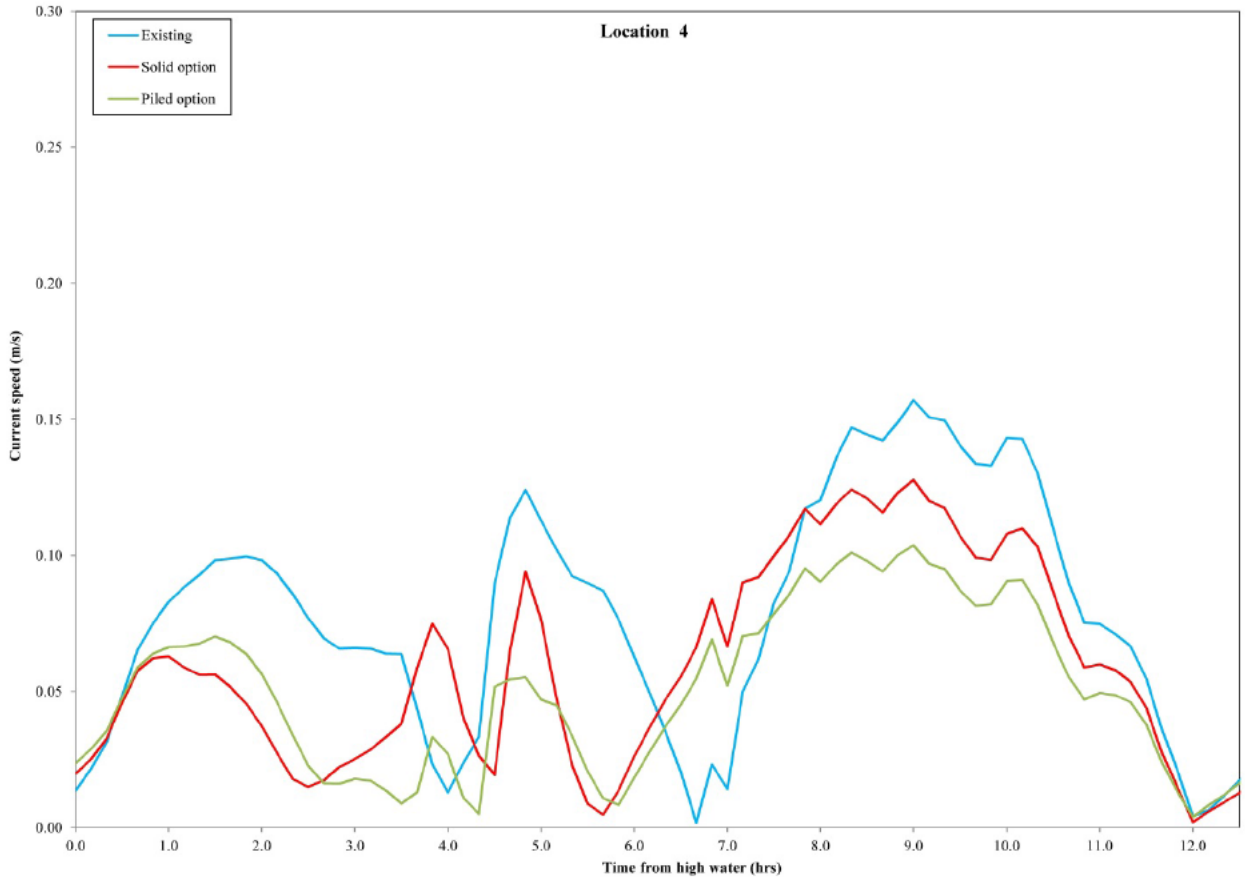

Figure C.25: Time series results at Point 4, spring tide, high river flow

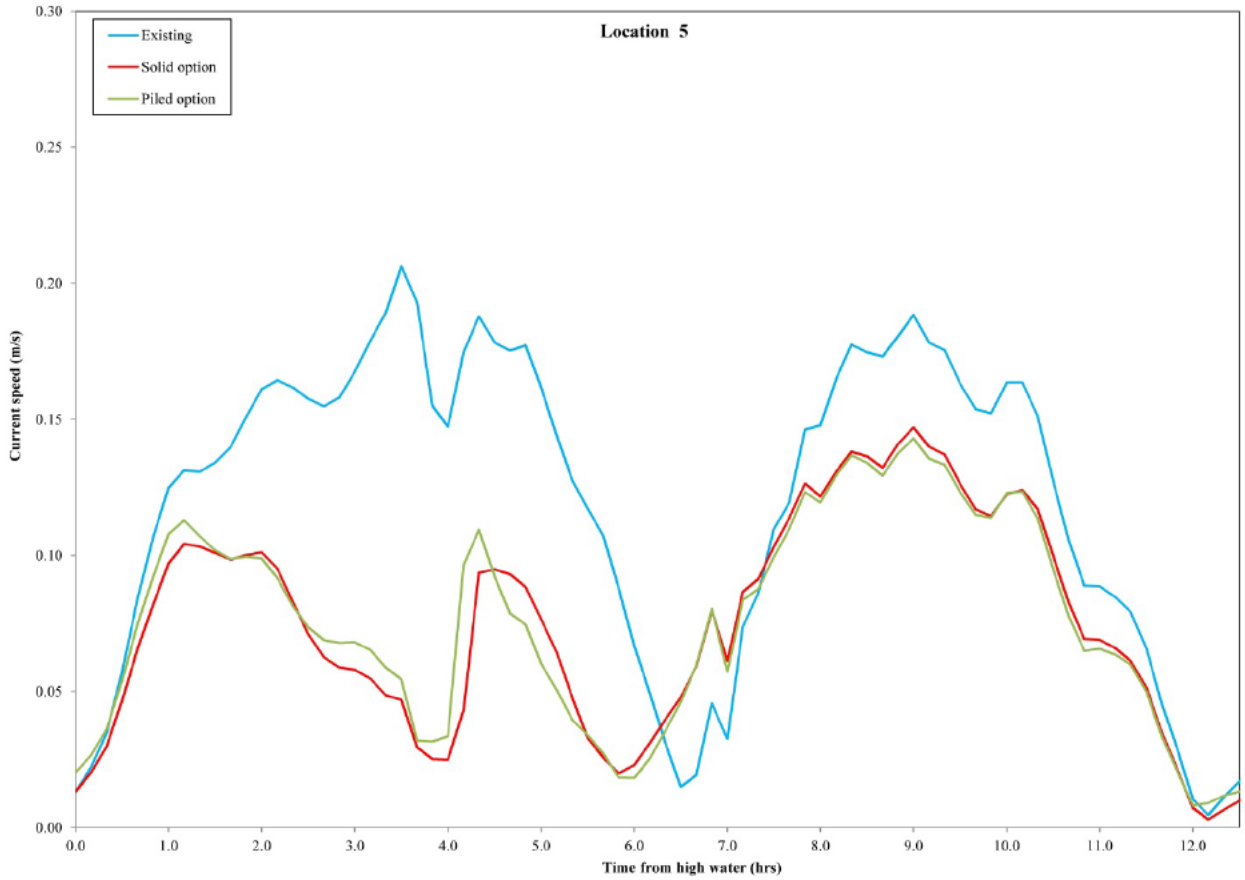

Figure C.26: Time series results at Point 5, spring tide, high river flow

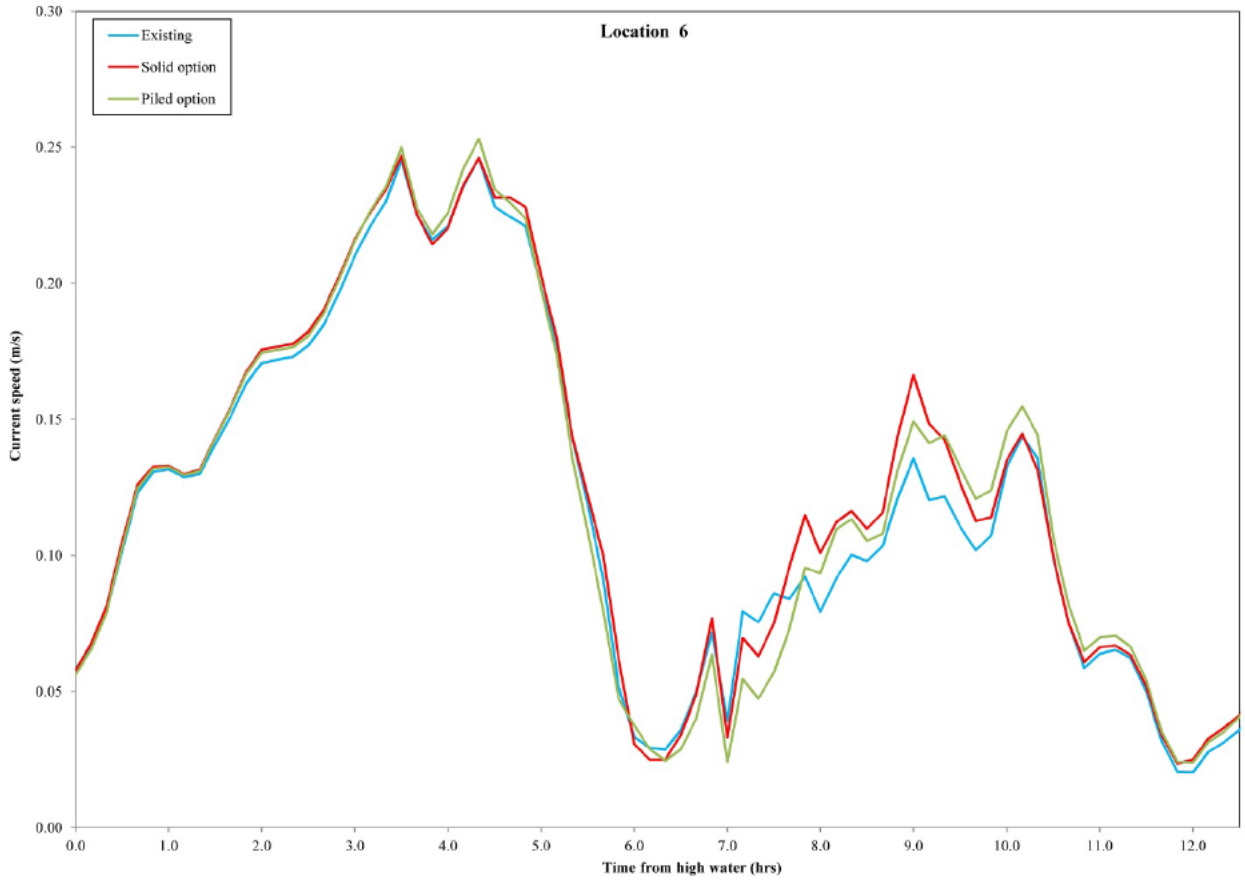

Figure C.27: Time series results at Point 6, spring tide, high river flow

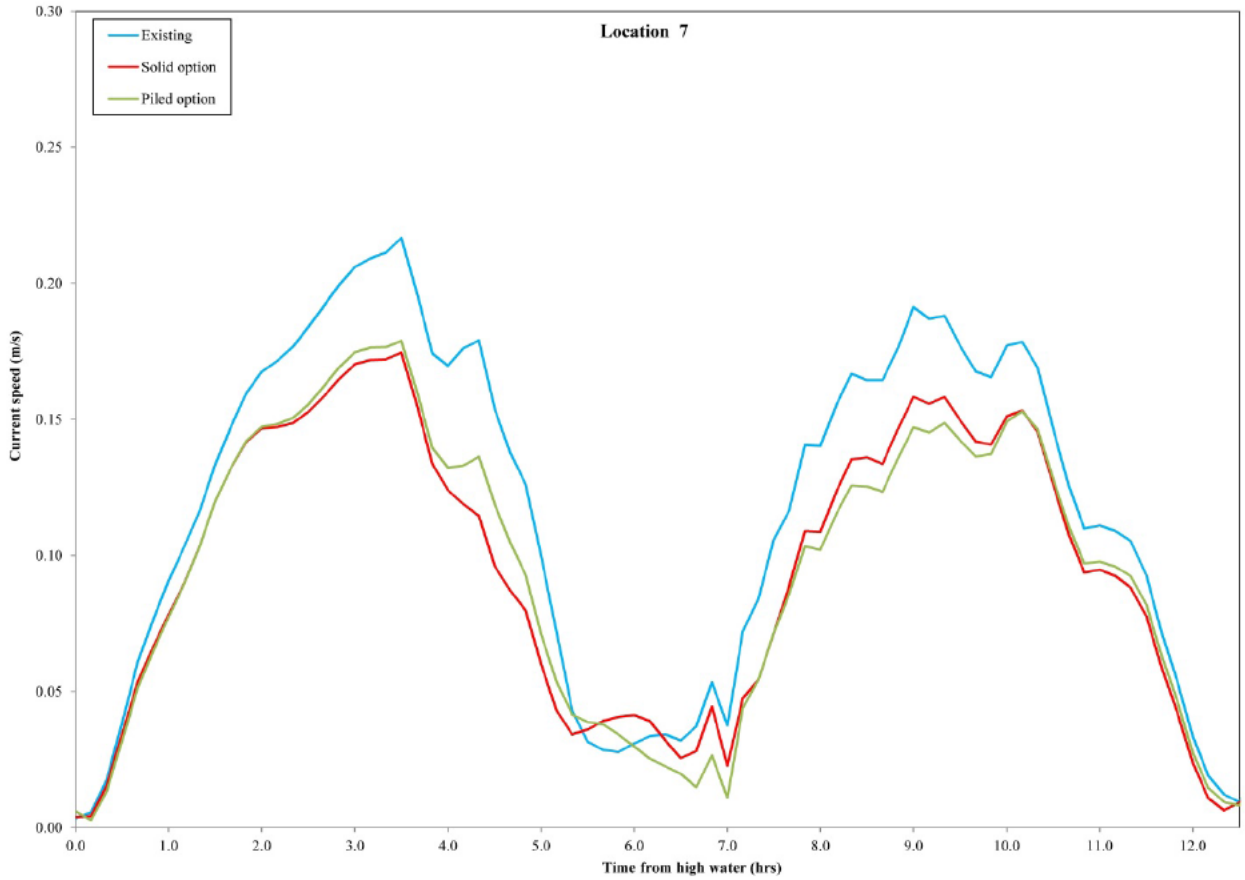

Figure C.28: Time series results at Point 7, spring tide, high river flow

HR Wallingford
Working with water

HR Wallingford is an independent engineering and environmental hydraulics organisation. We deliver practical solutions to the complex water-related challenges faced by our international clients. A dynamic research programme underpins all that we do and keeps us at the leading edge. Our unique mix of know-how, assets and facilities includes state of the art physical modelling laboratories, a full range of numerical modelling tools and, above all, enthusiastic people with world-renowned skills and expertise.

HR Wallingford, Howbery Park, Wallingford, Oxfordshire OX10 8BA, United Kingdom
tel +44 (0)1491 835381 fax +44 (0)1491 832233 email info@hrwallingford.com
www.hrwallingford.com

FS 516431
EMS 558310
OHS 595357